UNIVERSITY OF APPLIED SCIENCES BREMEN

Development of a Nature Inspired Hull Structure for a 46m Sailing Yacht

Master thesis submitted to obtain the academic degree

Master of Engineering

by

David Leidenfrost , B.Eng.

Matr.-Nr.: 241771

Faculty 5: Nature and Technology

Department: Naval Architecture and Ocean Engineering

in cooperation with

Dykstra Naval Architects

Amsterdam

Alfred Wegener Institute

Bremerhaven

First Examiner: Prof. Dipl.-Ing. Olaf Springer

Second Examiner: Prof. Dr.-Ing. Andreas Kraus

Bremen, 27. February 2015

Declaration of Authorship

I, David Leidenfrost, hereby declare that this thesis titled, “Development of a nature inspired hull structure for a 46m sailing yacht", has been composed by me and is based on my own work. Where I have consulted the published work of others, this is always clearly stated. I confirm that I have acknowledged all main sources of help.

Bremen,

Place, Date

Signature

UNIVERSITY OF APPLIED SCIENCES BREMEN

Abstract

Faculty 5: Nature and Technology
Naval Architecture and Ocean Engineering

Master of Engineering

by David Leidenfrost

The encounter with the sailing yacht concept "EXO" raised the question whether it is possible to develop a hull structure inspired by nature that is strong enough to cope with the global loads of a 46m sailing yacht. The concept was developed by Claydon Reeves and Dykstra Naval Architects with the main objective that views below deck match those above by integrating huge glass windows into the hull structure. This is most challenging, as these windows are supposed to be located in an area of the sailing yacht which experiences the highest global loads.

In order to answer this question, the present master thesis project was initiated in a cooperation of Dykstra Naval Architects in Amsterdam and the Bremerhaven based Alfred Wegner Institute. In the framework of this master thesis the hull structure of the "EXO" concept was further developed and evaluated. To enable the integration of huge glass windows and removing major loadings from the glazed areas an unconventional truss structure design was requested with the ability to carry these major global loads acting on the yacht hull. Source of inspiration to achieve this was the beauty and functionality of nature's lightweight designs. Therefore, topology optimizations were implemented to reveal the most advantageous load paths in the yacht hull, ensuring the development of an interwoven truss structure network which is directly related to the forces acting on the yacht.

The evaluation of the concept shows that the developed hull structure with load carrying truss members resembling organic forms is able to cope with the global loads acting on the 46 m sailing yacht "EXO". Furthermore, this master thesis presents a feasible new approach to integrate huge glass windows into a yacht structure.

Acknowledgements

First, I would like to express my sincerest gratitude to Thys Nikkels, managing director of Dykstra Naval Architects for his invaluable support and for giving me the great opportunity to work on this extraordinary sailing yacht concept "EXO". I would particularly like to thank my supervisors Mark Leslie-Miller and Hilbert ten Have for their great support throughout the whole project and for their valuable advices especially regarding to global load calculations and dimensioning of the yacht structure. This thesis would not be possible without their great help and assistance before and during my research. I also want to express my thankfulness to the whole team of Dykstra Naval Architects for all the inspiring meetings and for giving me a valuable knowledge in the field of yacht design.

I am deeply grateful to Dr. Christian Hamm, Head of Department Bionic Lightweight Design at the Alfred Wegener Institute for his constant support and for giving me the unique opportunity to work interdisciplinary by merging yacht design and bionics. My sincere gratitude goes to my supervisor Nils Niebuhr for his great guidance throughout this project. He managed to give me a excellent overview in the field of topology optimizations and his continuous assistance always pushed me forward towards my goals. I want to express my thankfulness to the whole team of the Department Bionic Lightweight Design for giving me valuable knowledge in the field of bionics and lightweight designs and for making my time there very enjoyable.

I would like to offer my special thanks to my supervisor at the University of Applied Sciences Bremen, Prof. Dipl.-Ing. Olaf Springer. He never failed to offer me excellent support throughout my thesis and his knowledge and thinking made me see the challenges of the design and pushed me to improve many aspects of the project.

Special thanks go to Philipp who took the time to read my extensive thesis. Most special thanks go to my parents, Semrin and Christoph Leidenfrost and to my grandfather Johannes Leidenfrost, who made everything I achieved in life possible and for their unconditioned love and support

Contents

List of Figures

List of Tables

Abbreviations

CFD	**C**omputational **F**luid **D**ynamics
FEA	**F**inite **E**lement **A**nalysis
FEM	**F**inite **E**lement **M**ethod
SIMP	**S**olid **I**sotropic **M**icrostructure **P**enalization
SKO	**S**oft **K**ill **O**ption
TO	**T**opology **O**ptimization

1 Introduction

1.1 The 46m Sailing Yacht "EXO"

The London based design office Claydon Reeves initiated the approach in designing a sailing yacht that takes on patterns of nature. In partnership with Dykstra Naval Architects the 46m concept sailing sloop "EXO" was developed. The main objective was to revolutionize the experience of performance cruising by matching the views below deck with those above. As shown in the artist impressions on the following page, huge glass windows allow stunning views of external and underwater environments and illuminate the interior with daylight.

To remove the high loads from the huge glazed areas they found inspiration in nature's exo-skeletal lightweight structures. Consequently the nature inspired carbon chassis displays twisting and turning curves and so does the deck layout and the interior layout; all following the principle of organic forms.

The "EXO" concept with its design specification as stated below is the basis for the presented master thesis.

Length overall	L_{oa}	=	46.00	[m]
Length of waterline	L_{Wl}	=	42.73	[m]
Draft	T_{max}	=	6.50	[m]
Breadth	B_{max}	=	8.88	[m]
Design displacement	Δ_D	=	240	[t]
Hull and rig construction	Carbon composites			
Accommodation	8 Guest and 7/8 crew			

FIGURE 1.1: Artist impressions of "EXO" concept by Claydon Reeves

1.2 Motivation

The encounter of the previously presented sailing yacht concept "EXO" raised the following three questions forming the key drivers of motivation:

- Is it possible to develop a hull structure inspired by nature that is strong enough to cope with the global loads of a 46m sailing yacht?
- What would such a hull structure look like if it followed nature's principles of organic forms while at the same time resisting tension and compressive stresses successfully during cruises at sea?
- How could nature's functionality and efficiency serve as a source of inspiration in terms of developing a hull structure with integrated huge glass windows?

1.3 Approach and Objective

In order to answer these questions the hull structure of the "EXO" concept is further developed within a cooperation of Dykstra Naval Architects in Amsterdam and the Bremerhaven based Alfred Wegner Institute. Source of inspiration for creating such a hull structure is the functionality of nature's lightweight designs. To enable the integration of huge glass windows, which are located in an area subjected to the highest global loads, a truss structure design must be developed. This network of truss members should have the the ability to carry the major global loads imposed on the hull of the 46m sailing yacht and should remove major loadings from the desired glazed areas.

To develop an efficient hull structure with load carrying and stiffness increasing truss members, the major load paths need to be known. For this purpose several topology optimizations are performed in *AltairHyperworks/OptiStruct* with the main objective to arrive at a conceptual load depending structure layout. Prior to this a *Design Suite* is developed. The main task of the *Design Suite* is to create an environment which includes all necessary functions and data to perform the intended topology optimizations. Since results of topology optimizations are highly dependent on the implemented loads, a well-considered load case reflecting the yacht's sailing condition as close as possible is needed.

Load case and load calculations are based on first principles and defined under supervision of Dykstra Naval Architects. According to a worst-case sailing condition critical global loads are calculated and applied to a global FE-Model. This approach is validated with a simple pontoon structure. Furthermore, a design space model is created in *CatiaV5* according to the interior layout of the "EXO" concept, since topology optimizations require a volume, in which the structure layout can evolve.

The topology optimization and the development of the hull structure are supervised by the department of Bionic Lightweight Design of the Alfred Wegener Institute. Since results of topology optimizations act solely as a design proposal, the most promising topology results are refined and abstracted in *CatiaV5*.

The created hull structure is dimensioned on a conceptual level considering a full carbon-composite construction. The dimensioning process is mostly based on first principle calculations and standard engineering methods. For the sake of simplicity and for preliminary evaluations of the concept, the carbon composite structure is simplified and substituted by homogeneous plates with isotropic material properties.

Last but not least, global FE-Simulations are conducted in *AltairHyperworks-OptiStruct* to evaluate the technical feasibility of the structure concept.

2 Theory and Methods

2.1 Forces on a Sailing Yacht

> *"Looking at a sailing yacht, which is under way in steady wind- and sea-state conditions, all forces and moments acting on her hull and rig structure are in equilibrium. While the buoyancy force of the underwater hull balances the yacht weight, aerodynamic forces of the rig must be in balance with the hydrodynamic forces of hull, keel and ruder" [9]*

Apart from the beauty of sailing yachts they exhibit a sophisticated and complex physical system that interacts simultaneously with two fluids (air and water) through the forces of wind and the sea. Hence, the force components of hull, sails, appendages and rigging are closely interconnected and determine the overall performance of a sailing yacht [1]. These force components can be divided in two groups:

- **Static forces:** Weight and buoyancy force are determined by the geometrical characteristics of the hull and are not influenced by the yacht's motion.
- **Dynamic loads:** Aero- and hydrodynamic forces arises for the relative motion between the yacht and the air and and water surrounding it.

For the sake of simplicity, the relationship and equilibrium of forces acting on the yacht are described for a steady-state sailing condition [1].

2.1.1 Righting and Heeling Moment

Figure 2.1 displays the resulting static and dynamic loads on a sailing yacht in steady-state conditions, reflecting sailing in light wind on a calm sea.

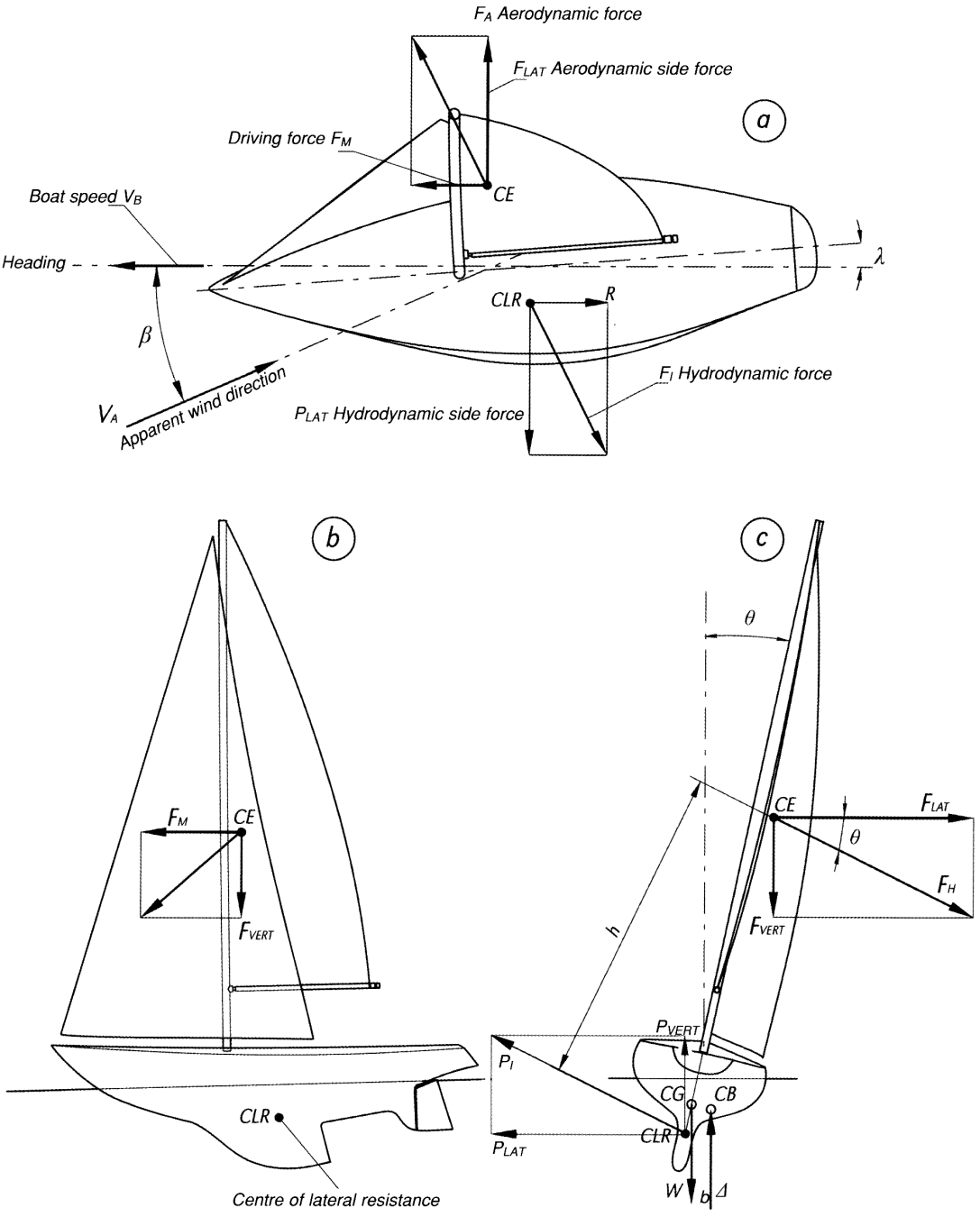

FIGURE 2.1: Forces on a sailing yacht [1]

While sailing through the water a resistance (R) is developed. This resistance force is under equilibrium conditions balanced by the driving force from the sail

(F_M). These forces are small components generated by the corresponding aerodynamic (F_A) and hydrodynamic forces (F_I). Unfortunately they cannot be created without at the same time obtaining an aerodynamic side force (F_{LAT}) which is balanced by the hydrodynamic side force (P_{LAT}) [2]. As shown in figure 2.1 (B) the aerodynamic side force does not only push only the yacht sideways, but also inclines it to leeward by its heeling force component (F_H). The heeling force (F_H) stays always at the right angle to the mast and is balanced by the hydrodynamic lift (P_I). Due to the fact that both forces are separated by the distance (h) they generate a heeling moment HM [1]:

$$HM = F_H \cdot h \tag{2.1}$$

In heeling condition the center of buoyancy (CB) moves outward due to the hull shape and a distance (b) is generated between the two force lines of weight (W) and buoyancy (displacement Δ) [1].The righting moment is given by the following formula and counteracts the yacht's heeling moment :

$$HM = RM = \Delta \cdot b \tag{2.2}$$

Obviously, to fulfil the static equilibrium of a floating object (Archimedes' principle) the buoyancy force must be equal to the weight of the displaced water (= weight of yacht) [2].

A commonly agreed severe heeling angle is $\phi = 30$ degrees, since it corresponds to a reasonable high wind strength, with the sails still generating high forces and the yacht making favourable speed. Sailing at higher heeling angles slows the yacht down due to higher resistance and corresponding smaller aerodynamic forces caused by flat trimmed sails and an unfavourable angle of attack (β) of the sails [2] [1].

2.1.2 Loads on Hull Structure

The hull structure of sailing yachts must be able to cope with all the loads induced by the previously described dynamic and static forces. The loads on the hull structure as visualized in figure 2.2 can be divided in two groups:

- **Global loads**, mainly induced by rig loads and wave bending moments, affect the hull structure as a whole and bend the hull girder.
- **Local loads** try to deform plating and stiffeners. They are induced by hydrostatic pressures and dynamic loads (slamming) imposed by the sea, waves and by attachment points of rig components, keel, rudder, winches, sheet blocks etc. High local loads can also derive from severe conditions like running aground [2].

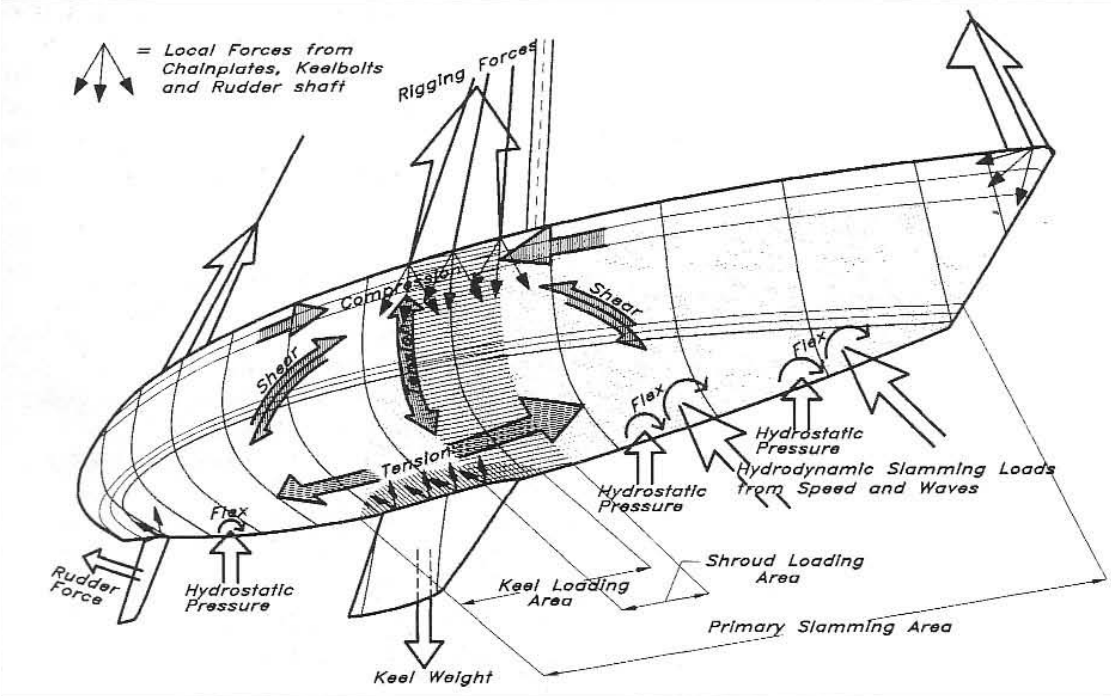

FIGURE 2.2: Loads on hull structure [2]

As visualized in figures 2.2 & 2.3, tension loads in headstay and backstay and the compression force of the mast bend the hull girder and put the deck into compression and the hull bottom into tension. The longitudinal bending moment caused by the rig loads has its maximum at the position of the mast base [2].

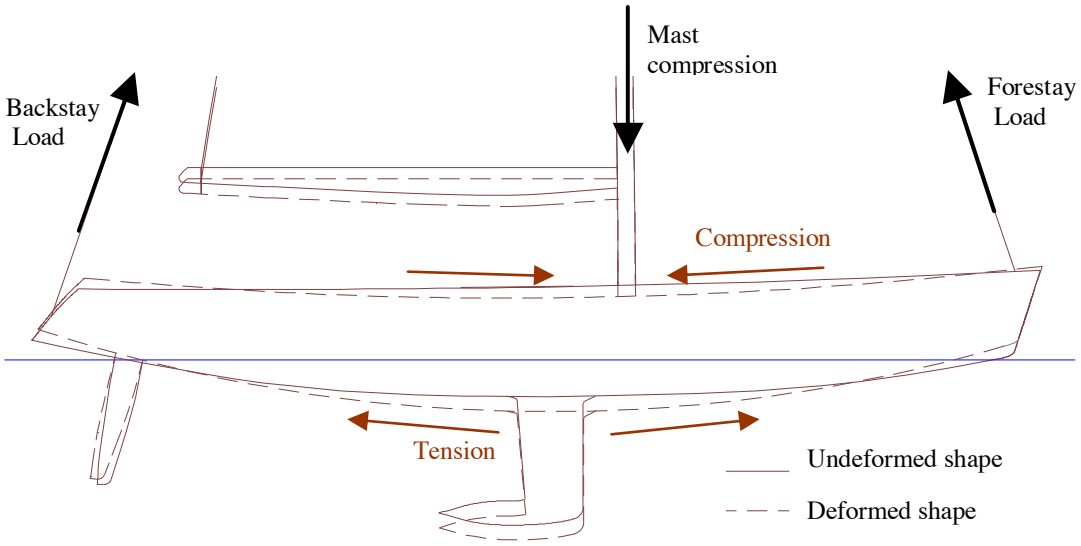

FIGURE 2.3: Rig bending moment [3]

This effect, where the deck is subjected to compression and the hull bottom to tension loads, is increased in case of a sagging condition, where the wave through is amidships with its crest at bow and stern (figure 2.4).

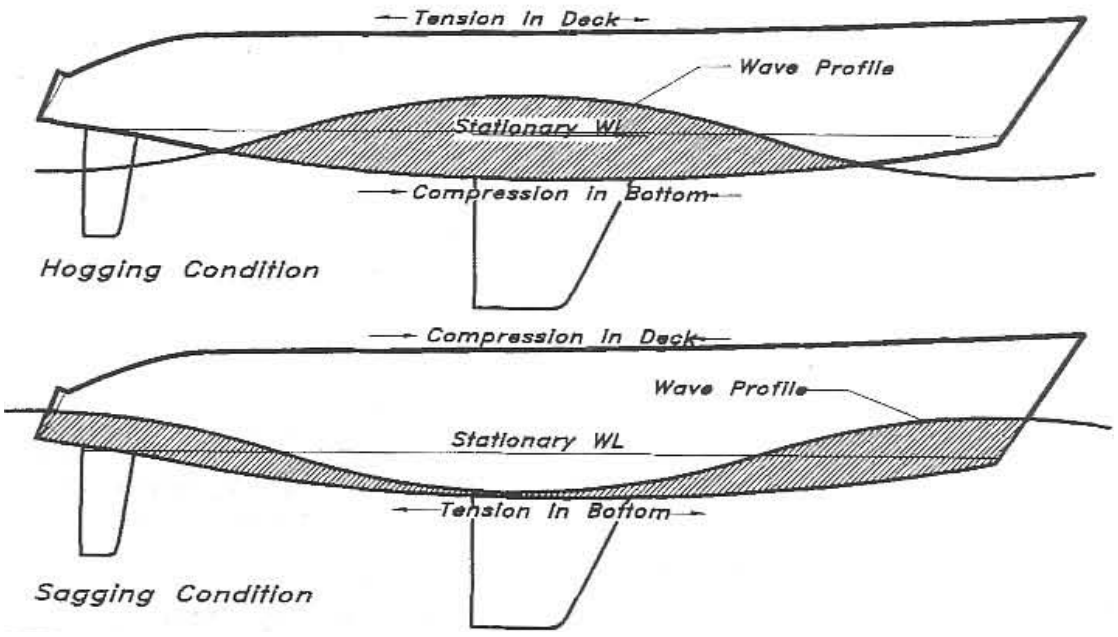

FIGURE 2.4: Hogging and sagging condition [2]

Especially in case of sailing yachts over 30 meters, where the wavelength approaches hull length, the wave bending moment (sagging conditon) can have a

significant contribution on the overall longitudinal bending moment. In conclusion, the "rig-sagging" condition is the most severe one for sailing yachts, where the highest global loads are derived [3] [2].

2.2 Topology Optimization

In the field of structural design, optimizations are inevitable to find a optimum solution for predefined objectives, e.g. minimizing mass or stress or maximising stiffness. In short, structural optimizations have in common finding the optimum structure lay-out. As shown in figure 2.5 three methods of optimization are displayed. Size optimization has the objective to find the optimal thickness distribution of a predefined plate or truss structure design. Shape optimization can be seen as an extension of size optimization, since due to extra freedoms the shape of the predefined layout is optimized within a given design domain, still the topology stays unchanged. Topology optimization extends size and shape optimization and allows the determination of features such as the number, location and shape of holes and the connectivity of the design domain [4].

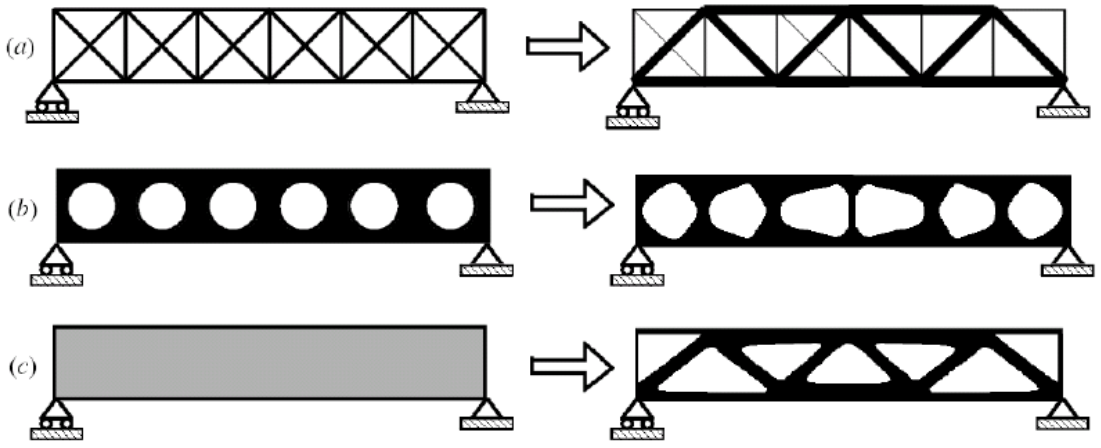

FIGURE 2.5: a) Sizing- b) shape- c) topology optimization [4]

Topology optimisations (TO) are a mathematical approach that generate an optimized material distribution for a set of loads and constraints within a given design domain, which can be an area or a volume [10]. They are the most widely used type of structure optimization. Especially for concept developments they are conducted to find the most advantageous material distribution inside an available

design domain with regard to design constraints and objectives. In other words topology optimizations reveal the optimum load paths between loading and supporting points. Their results act mostly as a source of inspiration and need to be interpreted to come up with first design lay-outs.

In most cases topology optimizations are performed in conjunction with the finite element method, since the typical approach is to discretise the design domain in a number of finite elements and to assign full material, partial material or lack of material to each element. Within an iterative scheme the optimal material distribution converges inside the domain [11]. Following two topology optimization methods are presented.

2.2.1 SKO Method

The Soft Kill Option SKO, was developed 20 years ago at the Karlsruhe Institute of Technology, where the lightweight principle of the bone growth was adapted. Inspiration was the biological mineralization process of living bone, which is stress-controlled. In high stressed areas bone cells (osteoblasts) ensure that more material is accumulated. To the contrary in weakly loaded areas material is taken away. As visualized in figure 2.6 this process lead to a structure where little beams (trabeculae) are oriented along the main stress directions [5].

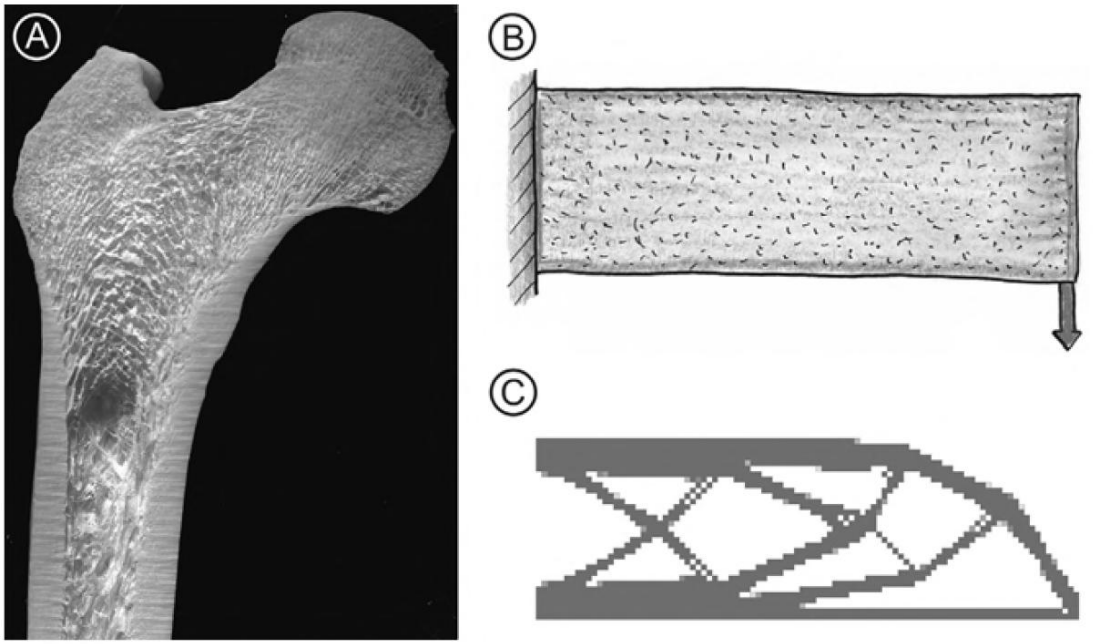

FIGURE 2.6: a) Human bone, b) maximum design space for SKO, c) Lightweight desing of SKO [5]

The first step in this method is to obtain the stress distribution. According to low stress areas material is made softer ("killed") and in high stressed areas the Young's modulus is increased. With the new material properties the stress distribution is recomputed. This iterative process converges when the separation of the weak and strong material is sharp. The aim of the method is to find the layout that gives a uniform stress distribution [5].

2.2.2 SIMP Method

The most implemented method in commercial software is the SIMP method (Solid Isotropic Microstructure with Penalization). In comparison to SKO, this time the material density is used as a design variable and the aim is to find a stiff structure for a certain target volume/mass.

Hence, the design domain is divided into a grid of n elements (solid isotropic microstructures) where each element has a fractional material density, varying continuously between 0 and 1 (void and solid). The stiffness of the material is assumed to be linearly dependent on the density. The objective function is to minimize strain energy (compliance). Strain energy represents a global measurement of the structure's displacements with regard to certain boundary conditions. The lower the strain energy the higher the stiffness of the structure. Accordingly, this method searches for a material density distribution inside the design domain that minimizes strain energy for a target structure volume [11] [10].

In general, the optimized solution based on the density method involves large areas of intermediate densities in the design domain. Therefore, this method with Penalization "penalizes" intermediate densities and encourage in this way the development of elements which are either 0 or 1 (void or solid), leading to favourable topology optimization results. The equation below presents the penalization technique:

$$\underline{K}_{(\rho)} = \rho^p \cdot K \tag{2.3}$$

where $\underline{K}$ represents the penalized and K the real stiffness matrix of an element; ρ is the density and p the penalization factor which is always $p > 1$ [10].

3 Development of Design Suite

"[...] applying just enough amount of material at every single spot of the structure; deleting the lines where unnecessary and using them only where the structure demands them, usually ends up in organic forms. This approach has a great potential to achieve stunning beauty if the designer can be ungenerous enough in using his ingredients just like the nature does in her designs."

– *Mete Mordağ, Industrial designer*

3.1 Introduction

Since the objective of this present master thesis is to develop a nature-inspired hull structure, first nature's principles of design must be understood. How we explain it to ourselves, her principles of design are based on a very pragmatic approach, claiming for maximum strength with a minimum amount of material. This approach reflects the guiding principle of any lightweight structure found in nature or in technical systems. However, lightweight designs are definitely not a development of the modern age since over million years of evolution nature developed a marvellous diversity of lightweight designs and there are numerous reasons for their origin. To mention only two reasonable examples; being lighter in weight makes it possible to run faster and prevents from being eaten by a predator or it enables flying and thus exploring new areas of land and so on [5]. Last but not least the endless struggle of survival has brought nature's philosophy of design to perfection resulting in efficient and breathtaking designs with beautiful organic forms. For reasonable structures and load cases the main load paths, where

most of the material should be added, can be imagined and assumed by *"simply following the forces"*; so usually the more experienced the designer or engineer the better the result will be. However, considering complex load cases and structures, like in case of the 46m sailing yacht "EXO", this method is challenging.

Nowadays, besides relying on one's experience and intuition for finding an optimal structure layout according to certain design requirements, numerical methods are available. Topology optimisation, as described in detail in section 2.2, is a mathematical approach that generates an optimized material distribution for a set of loads and constraints within a given design space [10]. Some topology optimizations methods are based on lightweight principles found in nature, like in case of the Soft Kill Option SKO, developed 20 years ago at the Karlsruhe Institute of Technology, where the lightweight principle of bone growth was adapted [5].

Hence, in the framework of this concept study topology optimizations are implemented with the main objective to arrive at a conceptual load depending structure layout of the yacht hull. It should be noted, that the results of the topology optimizations act solely as a design proposal and still need to be refined, abstracted and dimensioned before a final evaluation of the structure concept can be performed.

3.1.1 Task of Design Suite

The main task of the design suite is to create an environment which includes all necessary functions and data for performing the intended topology optimizations. Topology optimizations require a design space defining a model volume where the structure layout may evolve. Results are highly dependent on predefined loads and model constraints. Hence the following six points are thoroughly investigated and constitute the design suite:

- **Definition of a load case**
- **Definition of load model**
- **Validation of load model**
- **Load calculations**
- **Definition of design space**
- **Definition FE-Model**

3.2 Definition of Load Case

In case of sailing yachts defining design driving loads is most challenging as yachts are constantly exposed to a huge variety of loads depending on sea state, wind conditions, sailed courses and their own weight distribution.

There are several possibilities to determine these loads. The most common approach in maritime industry is to apply rules for classification and construction of ships. The main purpose of classification societies is to define technical minimum standards for construction and operation of ships and to evaluate whether existing technical systems are complying to them or not. It is common practice to use classifications rules as a safe guideline to dimension ship constructions. For this concept study however classifications standards are not a viable basis for calculating global loads since they do not mirror the actual forces acting on the hull in sailing condition.

Considering latest state of the art technology it is possible to simulate a yachts sailing condition within global finite element analysis (FEA) linked to computational fluid dynamics (CFD) for computation of hydrodynamic and static wave pressures or aerodynamic sail loads. Yet, such a simulation would be exaggerated for this concept study.

Hence, solution-orientated a worst-case sailing condition is defined. The corresponding loads are calculated and applied to a global FE-Model with a simplified approach, presented in the following section 3.2.1.

3.2.1 The Quasi-Static Load Case

According to section 2.1 and with regard to a worst-case condition, critical global loads are reached at a heeling angle of 30 degrees during beating into the wind and being locked in wave sagging condition. The rig loads induce a huge longitudinal bending moment into the hull where the deck is in compression and the bottom in tension. This effect is increased in case of a sagging condition, where the wave through is amidships with its crest at bow and stern (sagging) and the wavelength approaches hull length. Thus, the load case consists out of two load groups: wave induced and rig induced global loads.

Since the main objective of this present thesis is to develop the primary structure of the hull with respect to global loads, local and dynamic loads are completely neglected. This includes for example loads due to rudder side-forces, slamming or keel groundings (as presented in section 2.1.2). They can be absorbed by secondary structures and additional reinforcements.

The quasi-static load case is defined as followed:

- **Steady state sailing condition**
- **Heel angle of yacht: 30 degrees**
- **Wave direction: head sea**
- **Wave shape: approximated as sinusoidal wave**
- **Wave length: equal to hull waterline length**
- **Maximum wave height: below the wave breaking limit**

With regard to section 2.1 all calculated forces and resulting moments of the predefined load case need to be in balance in order to represent a yacht sailing in steady-state conditions.

3.3 Load Model for Global FE-Analysis

Due to the fact that the complete hull structure of the 46m sailing yacht "EXO" needs to be developed and evaluated an implementation of a global finite element model (FE-Model) is inevitable. However, considering the time frame of this master thesis a simplified method o determine and apply global loads to the FE-Model is required. In order to receive convenient results from the topology optimizations this simplified method should not distort (or at least as little as possible) the loads.

A common engineering method is the beam theory, often utilized for estimation of global structure behaviours or fast dimensioning of constructions. This method simplifies the complex structure as a beam with a certain cross section and thus only global behaviours (e.g. deformations) of the structure can be estimated.

Hence, to take local as well as global structure behaviours into account the following load model is presented:

A global FE-Model coupled with adapted principles of the beam theory for calculating and applying loads

In case of the sailing yacht locked in a sagging wave the hull structure is exposed to loads derived from its own weight and from its pressure distribution of the underwater body. Since dynamic loads are neglected only hydrostatic pressures are taken into account. The hydrostatic pressures or so called buoyancy distribution has to be in balance with the weight distribution according to Archimedes' principle. Weight and buoyancy loads are calculated and applied as described below:

- The hull is divided into 20 equal sections and for the corresponding cross sections weight and buoyancy loads are separately calculated.
- Each cross section load is distributed to the global FE-Model corresponding to its hull section.
- For this purpose RBE3 elements are utilized; beam elements which transfer loads without inducing additional stiffness to the FE-Model
- For proper boundary conditions of the FE-Model calculated cross section loads need to be distributed the way they act on the real hull in sailing condition.
- Weight forces are applied to the whole area of each section, since the whole yacht is exposed to the same gravity.
- Buoyancy forces are only applied to areas representing the wetted hull of each section, since hydrostatic pressures act only on the underwater body.

This method, visualized in section 3.7, leads to favourable results and hardly distorts the overall structure behaviour of the yacht, as the following validation of the load model shows. In relation to rig loads no special considerations are necessary. For development of the hull structure only resulting rig forces at the hull attachment points are design driving. Complex aerodynamic sail forces are of minor interest. Calculations of rig loads are based on standard methods applied in yacht design, as they lead to satisfactory results. The force components of the calculated rig loads are applied to the FE-Model at their designated hull attachment points (chain plates and mast base), as described in section 3.7.

3.4 Validation of Load Model

To validate the design suite of chapter 3 the assumptions of simplifying and applying global loads to a global FE-Model are evaluated through a floating pontoon structure which is exposed to a triangular shaped wave. For this purpose loads acting on the pontoon structure are solely derived from its buoyancy distribution in the triangle wave and from its own weight; no heeling and no further loads are considered.

3.4.1 Overview of Validation

Three FE-Simulations are performed and presented in this section to assess the quality of the load model:

The 1^{st} simulation is aimed to reflect reality as close as possible by applying hydrostatic pressures to the wetted hull area and gravity to the FE-Model. Depending on weight of the pontoon and hydrostatic pressure distribution (=buoyancy distribution) the FE-Model finds its own equilibrium of forces and displays the deformation of the structure.

The 2^{nd} simulation is based on the principles of beam theory where buoyancy and weight loads acting on the structure are applied over a designated amount of cross sections. The theory is a proven method for preliminary estimations or fast dimensioning. At the same time local structure behaviours/deformations are widely neglected or misinterpreted, especially in conjunction with complex loading cases.

The 3^{rd} simulation reflects the assumptions of the new load model devised in this thesis. Similar to the 2^{nd} simulation all loads acting on the structure are still applied over a designated amount of cross sections. However, in order to take local deformations into account as well and to reach better results regarding the overall structure behaviour, weight forces are applied to the whole area of each section and buoyancy forces only to areas representing the wetted hull of each section.

3.4.2 The FE-Model A - Pontoon

The pontoon has the following main particulars listed in table 3.1.

Length over all	L_{oa}	=	42700	[mm]
Breadth	B	=	8800	[mm]
Depth	D	=	5000	[mm]
Design draft	T_d	=	1500	[mm]
Draft at wave crest	T_{Wc}	=	3000	[mm]
Skin thickness	t_{Skin}	=	250	[mm]
Displacement	Δ	=	578	[t]
Density of sea water	ρ_{sea}	=	1025	$[kg/m^3]$
Gravity	g	=	9.81	$[m/s^2]$

TABLE 3.1: Main particulars of pontoon

For ensuring a uniform weight distribution the FE-Model has an equal skin thickness t_{skin} and the bulkheads at both ends are replaced by elements (RBE2) with an infinite stiffness, highlighted in yellow in figure 3.1. The modelled and analysed quasi-static load case represents a triangle wave with its peak at half length of the pontoon. Thus, the load case correlates to a hogging condition without heeling.

The FE-Modell is generated out of solid elements and since this model should only identify the relative influence of different ways of applying global loads a fictitious material with mechanical properties as listed in table 3.2 is used. Though, it is important to note that the materials density arises from the constraint that the structure volume multiplied by its density is equal to the displacement of the pontoon (detailed calculation, see appendix A).

Young's modulus $[N/mm2]$	Poisson's ratio [-]	Density [t/mm3]
10000	0.3	2.035E-09

TABLE 3.2: Mechanical properties for solid elements

3.4.3 Boundary Conditions - Pontoon

Only half of the pontoon needs to be modelled, because of the symmetrical weight and buoyancy distribution. The transverse symmetry plane is located at half length of the pontoon. Because solid elements have no rotational freedom [10] only

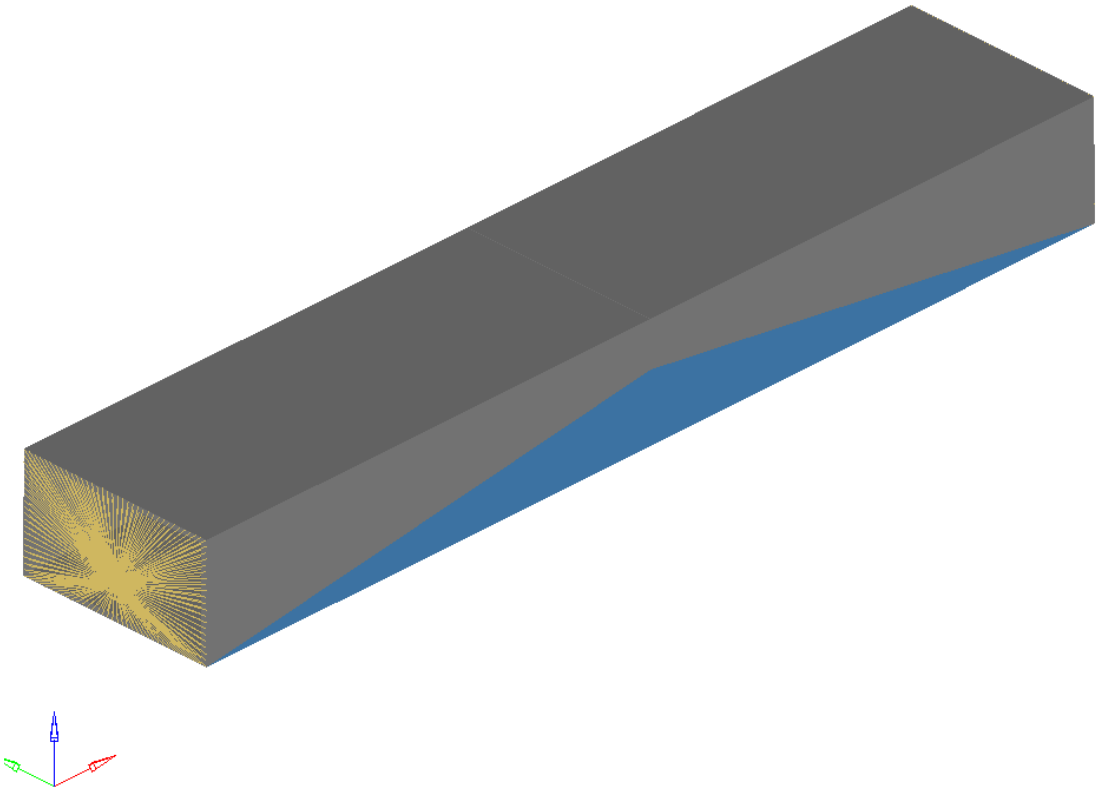

FIGURE 3.1: FE-Model of pontoon

their nodes in the plane of symmetry need to be restricted against longitudinal translation (DOF=1) for complying with the symmetry condition, as shown in figure 3.2 (left). The rigid elements (RBE2) connect all solid nodes in the plane of the bulkhead at the end of the pontoon and coincide in one master point at the level of the design draft T_d. For this RBE2 master point translational and rotational degrees of freedom are constrained as listed in table 3.3 and shown in figure 3.2 (right):

Axial direction	**Translation 1, 2, 3**	**Rotation 4, 5, 6**
x	-	0
y	0	-
z	0	0

TABLE 3.3: Degrees of freedom - RBE2 master point

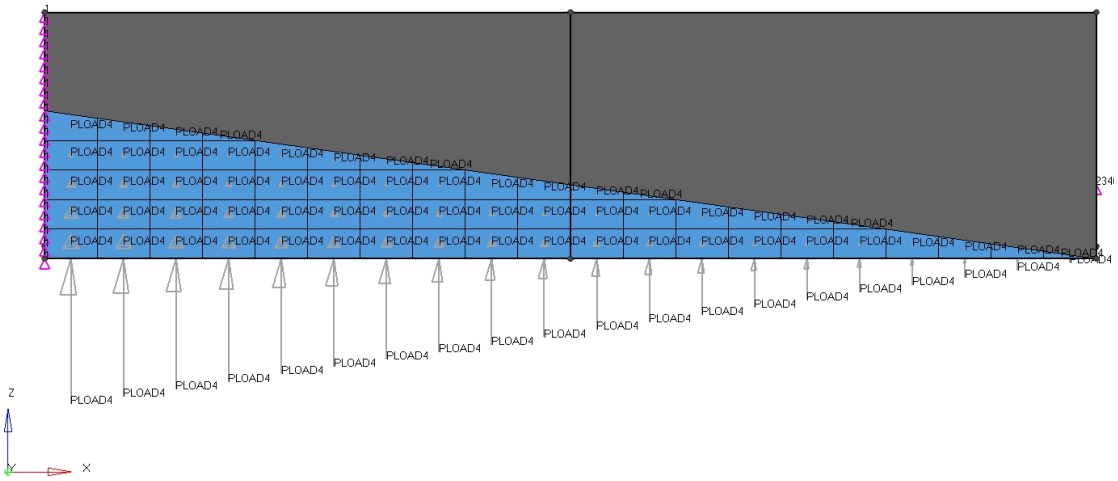

FIGURE 3.2: Boundary condition of FE-Model

In figure 3.2 hydrostatic pressures of side and bottom elements are visualized as well. Manually calculated hydrostatic pressures are applied as pressure loads to each membrane element. The membrane elements (blue, in figure 3.2) have no bending, coupling or shear stiffness [10] and have the sole purpose of defining the wetted hull area and distributing applied pressure loads to the solid elements. The membrane elements are glued to the solid elements over a auto-contact condition. Calculation of hydrostatic pressures are attached in appendix A. To take the weight distribution of the pontoon into account a gravity load of g = 9.81 m/s^2 is defined for the whole model space.

3.4.4 Result of 1^{st} Simulation - Pressures & Gravity

As described in section 3.1.1 only quality of deformations of the structure is of major importance and should be as undistorted as possible. Hence, only displacements of the pontoon structure are investigated and compared to those of simulation 2 and 3.

In figure 3.3 displacements of the whole pontoon structure in a triangle wave are displayed.

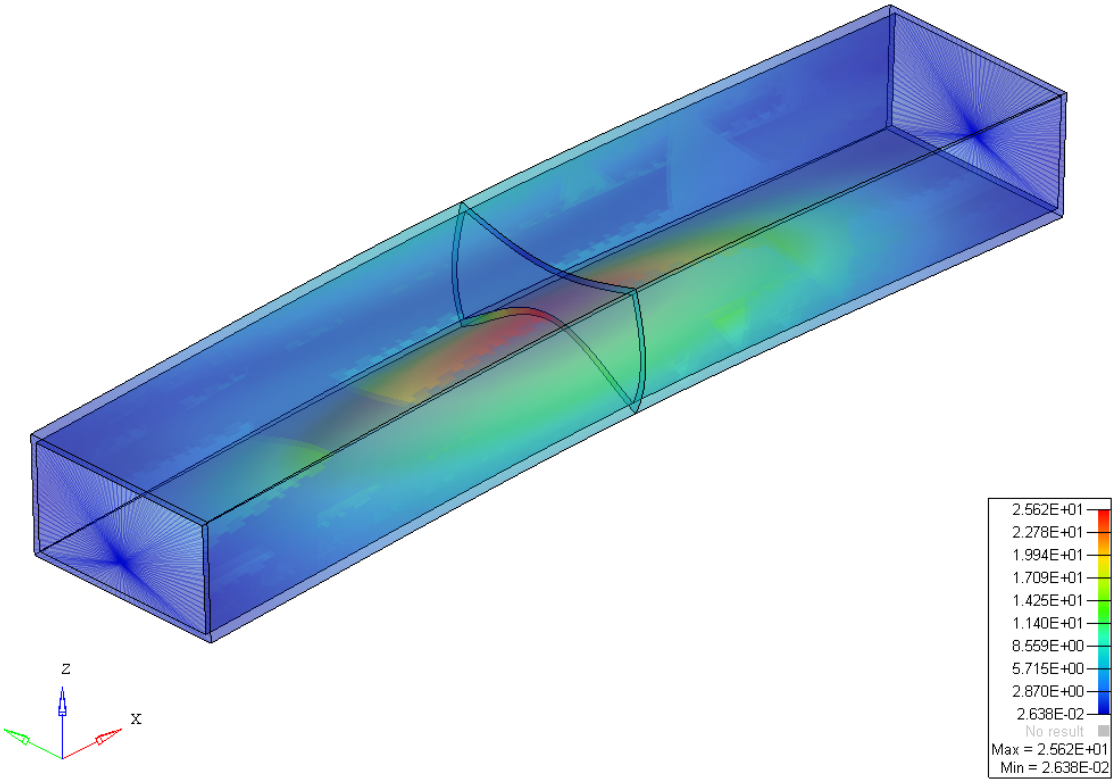

FIGURE 3.3: Displacements of pontoon - Hydrostatic pressure & gravity

In table 3.4 the displacements at points of major interest are evaluated. Four points are selected at half length, two at the pontoon edges (deck and bottom level) and two in the center plane (deck and bottom level). Because the side walls of the pontoon have a major bending stiffness in comparison to deck and bottom panels the two points at the pontoon edges mirror global deformations and likewise the two points at the center plane local deformations. Furthermore table 3.4 lists two sub-load cases stating deformations in case the pontoon is only exposed to weight forces or buoyancy forces.

Load case	**Local displacement of panels in [mm]**		**Global displacement of edges in [mm]**	
	Deck	Bottom	Deck	Bottom
Gravity	27	27	24	24
Pressure	-27	-53	-31	-30
Pressure & Gravity	0	-26	-7	-6

TABLE 3.4: Displacements at points of interest

Since the results of the 1^{st} simulation are seen as a benchmark they are validated with a rough manual calculation, attached in appendix A.2. In table 3.5 results of the FE-Analysis and of the manual calculations are set against each other:

Comparison	**Global displacement at L/2 of edges in [mm]**			
	Deck	DEV	Bottom	DEV
FE-Model	-7	17%	-6	0%
Manual calculation	-6		-6	

TABLE 3.5: Comparison of hand calculation and FE-Results

As shown in the table there is no deviation greater than 20%; therefore it is reasonable to assume the 1^{st} simulation as a valid benchmark to check results of simulation 2 and 3.

3.4.5 FE-Model B for 2^{nd} Simulation

FE-Model B for the 2^{nd} simulation is identical to the description in section 3.4.2, aside from the changed boundary condition regarding loads applied to the pontoon structure. Since the 2^{nd} simulation is based on the principles of the beam theory the structure is divided into 12 sections over its length. Due to the symmetry condition the resulting section loads consisting of buoyancy and weight forces are calculated and applied at 6 sections to the pontoon. Calculation of the section loads are listed in appendix A.

Instead of gravity and pressure loads to the wetted hull area 6 master points are defined in the center plane at the level of the design draft T_d. Each master point defines the center of each section and resulting section loads are calculated for these positions. For transferring the load from each master point to the pontoon structure RBE3 elements are utilized. RBE3's transfer loads without inducing additional stiffness to the system [10].

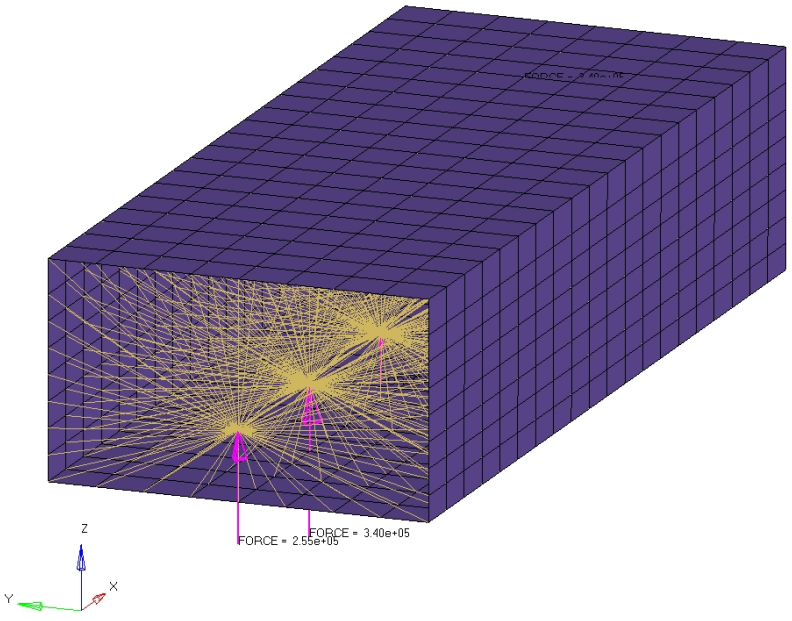

FIGURE 3.4: Application of RBE3's for distributing section loads

As illustrated in the figure 3.4 each master point is connected over RBE3 elements to the outer faces of the solid elements belonging to each section. For this purpose the Faces-Method is used to extract the utmost nodes of the solids representing the pontoon skin [10].

3.4.6 Results of 2^{nd} Simulation - Principles of Beam Theory

The results of the 2^{nd} simulation with the adapted FE-Model B are shown in figure 3.5. The same figure also includes displacements of the benchmark FE-Model A of the 1^{st} simulation. At first sight the disadvantage of the beam theory concerning local structure deformations becomes obvious.

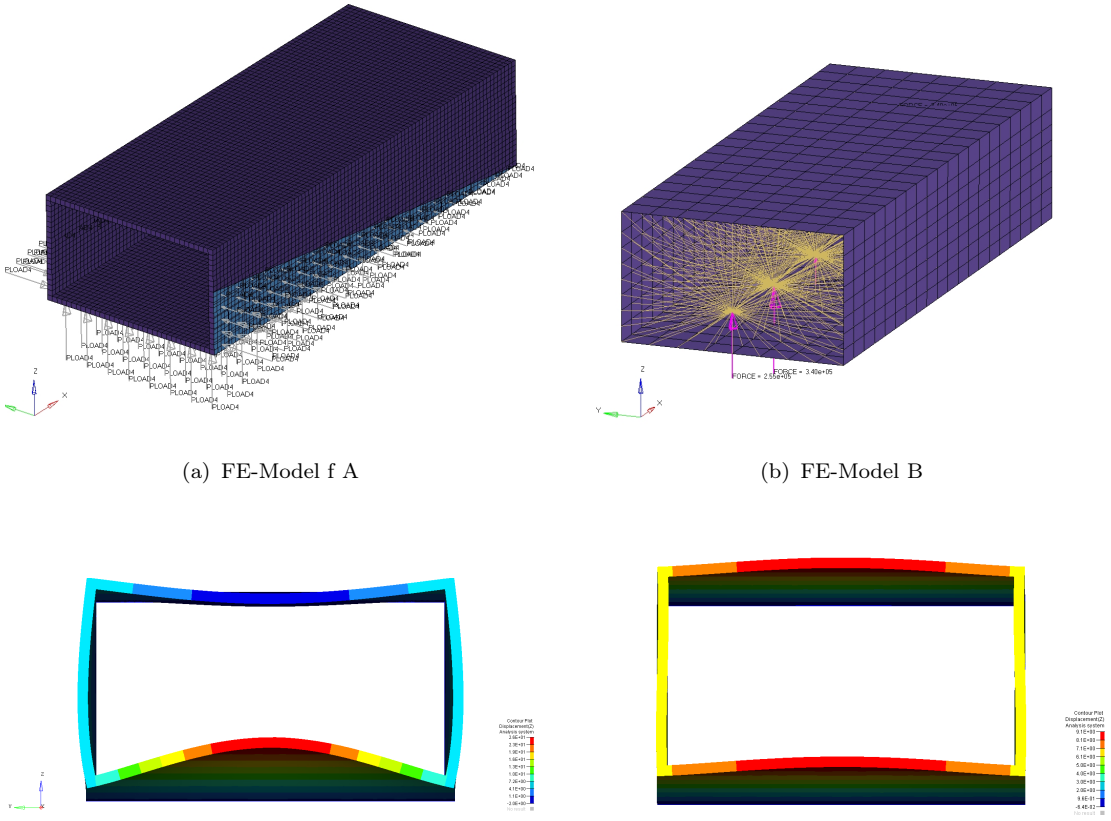

(a) FE-Model f A

(b) FE-Model B

FIGURE 3.5: Displacements at L/2 of FE-Model A and B - Cross section view

Since the resulting section loads are equally distributed over the whole cross sections the buoyancy force, which actually acts only at the wetted hull area and thus mainly on the bottom panels, deforms the deck panels as well. Table 3.6 clarifies the obvious results of simulation 1 and 2:

Load case	**Local displacement at L/2 of panels in [mm]**				**Global displacement at L/2 of edges in [mm]**			
	Deck	DEV	Bottom	DEV	Deck	DEV	Bottom	DEV
Weight_RBE3 Gravity	27 27	0%	27 27	0%	24 24	0%	24 24	0%
Buoyancy_RBE3 Pressure	-37 -27	37%	-37 -53	-30%	-31 -31	0%	-31 -30	3%
Section loads_RBE3 Pressure&Gravity	-10 0	100%	-10 -26	-62%	-7 -7	0%	-7 -6	17%

TABLE 3.6: Displacements of FE-Model A and B - at points of interest

Looking only at global structure behaviours, FE-Model B based on the principles of beam theory leads to satisfying results with a maximum deviation of 17% to the benchmark FE-Model A. However, in terms of local displacements deviations

up to 100% are reached. Furthermore the sub-load cases in table 3.6 show that distribution of weight forces over the whole section leads to suitable results, because the gravity is acting equally over the whole cross section. The same cannot be said looking at the buoyancy forces.

3.4.7 FE-Model C for 3^{rd} Simulation

The FE-Model C for the 3^{rd} simulation is identical to the description of Model B, aside from a tiny change in terms of applying the section loads to the pontoon structure, which has a huge impact on the following results. Since the 3^{rd} simulation should reflect the approach of the new load model and as learned from the results of the previous 2^{nd} simulation section loads are applied as following:

- **Weight loads:** to the whole area of each section
- **Buoyancy loads:** only to the wetted hull areas of each section

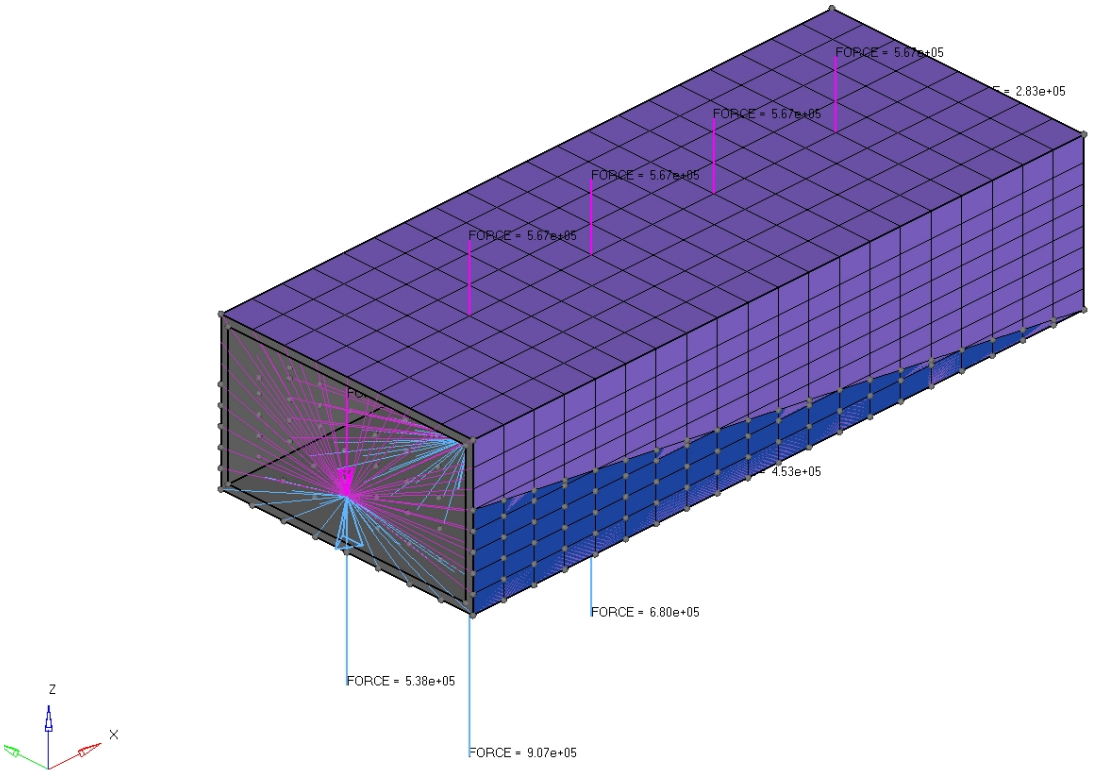

FIGURE 3.6: FE-Model C: Distribution of section loads

This approach of distributing the section loads to the pontoon structure is illustrated in figure 3.6, where weight forces and their RBE3 elements are highlighted in blue and buoyancy force and their RBE3 elements in purple.

3.4.8 Results of 3^{rd} Simulation - Method of load model

Figure 3.7 shows the displacements of the FE-Model A and C. Compared to the 2^{nd} simulation and the 3^{rd} simulation results are outstanding; there's hardly a difference to be seen when looking at local as well as global deformations of model A and B.

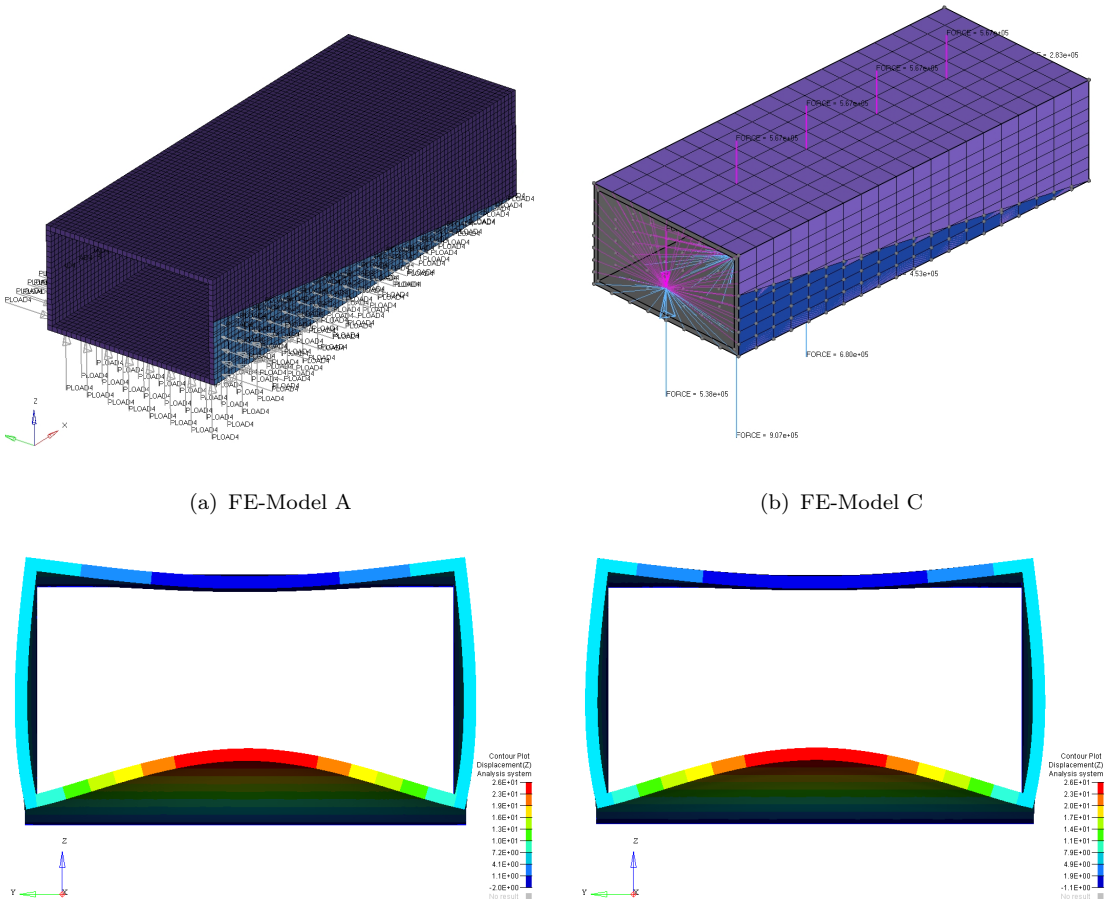

(a) FE-Model A

(b) FE-Model C

FIGURE 3.7: Displacements at L/2 of FE-Model A and C - Cross section view

Evaluating deformations at the four points of interest, as listed in table 3.7, only a maximum deviation of 4% between FE-Model C and the benchmark FE-Model A can be determined. Regarding global structure behaviours, there are no deviations to be noted.

Load case	**Local displacement at L/2 of plates in [mm]**				**Global displacement at L/2 of edges in [mm]**			
	Deck	DEV	Bottom	DEV	Deck	DEV	Bottom	DEV
Gravity_RBE3 **Gravity**	27 27	0%	27 27	0%	24 24	0%	24 24	0%
Pressure_RBE3 **Pressure**	-26 -27	-4%	-54 -53	2%	-31 -31	0%	-30 -30	0%
All_loads_RBE3 **Pressure&Gravity**	0 0	0%	-27 -26	4%	-7 -7	0%	-6 -6	0%

TABLE 3.7: Displacements of FE-Model A and C - at points of interest

3.4.9 Conclusion of Validation

The results of the 3^{rd} simulation in section 3.4.8 show that the approach of the load model is suitable for simplifying and implementing weight and buoyancy loads to a pontoon structure. Summarized, in case no distortion of the overall structure behaviour is desired, global loads need to be applied over a designated amount of cross sections, considering that weight loads are distributed over the whole area of each section and buoyancy loads only to areas representing the wetted hull of each section.

Since this approach leads to very satisfying results on the pontoon structure the method of the load model is assessed as suitable for its application on the hull structure of the 46m sailing yacht "EXO".

3.5 Calculation of Global Loads

Section 3.5 gives a brief insight how the global loads are calculated. Complete load calculations with detailed explanations can be found in appendix B.

For the 46m sailing yacht "EXO" with the main particulars as listed in table 3.8 the global loads are calculated according to the load case definition in section 3.2.1.

Length overall	L_{oa}	=	46000	[mm]
Length waterline	L_{wl}	=	42725	[mm]
Draft of canoe body	T_c	=	1600	[mm]
Draft max	T_{max}	=	6500	[mm]
Breadth max	B_{max}	=	8880	[mm]
Depth	D	=	4740	[mm]
Displacement	Δ	=	250000	[kg]
	∇	=	243.902	$[m^3]$
Longitudinal center of gravity	LCG	=	23176	[mm]
Vertical center of gravity	VCG	=	0	[mm]
Keel weight	G_K	=	50400	[kg]
LCG of keel	LCG_K	=	21261	[mm]
VCG of keel	VCG_K	=	-5158	[mm]

TABLE 3.8: Main particulars (HASC) of 46m sailing yacht "EXO"

To reflect a more realistic loading condition of the yacht during sailing all values in the table above are according to the "*Half-Average-Sailing Condition*" (HASC = tanks 50% filled) with a displacement of $\Delta = 250$ tons, slightly bigger than the design displacement of $\Delta_D = 240$ tons.

Furthermore, since the load case mirrors a steady-state sailing condition all calculated loads must yield to the quasi-static load case where all forces and moments are in equilibrium:

$$\Sigma F_{(x)} = 0 \quad \Sigma F_{(y)} = 0 \quad \Sigma F_{(z)} = 0 \tag{3.1}$$

$$\Sigma M_{(x)} = 0 \quad \Sigma M_{(y)} = 0 \quad \Sigma M_{(z)} = 0 \tag{3.2}$$

For an easier data exchange and a reasonable FE-Model setup the yacht, although 30 degrees heeled, is modelled throughout the whole project in upright position with a 30 degrees rotated water surface.

Last but not least it is very important to note that **no safety factors** are considered with regard to the global load calculations!

3.5.1 Hydrostatic Data

First, the hydrostatic data of the underwater hull must be evaluated to calculate the global wave induced loads. According to the load case description the hydrostatic data of the yacht is evaluated for a sagging condition in a sinusoidal wave with a wave length λ equal to the yacht's waterline length L_{Wl} and a maximum wave height of $H_{1/100}$=3.427 [m]. In this steady-state sailing condition the yacht is due to its sail forces heeled up to $\phi = 30$ degrees and a trim angle of zero is assumed. Detailed calculations and explanations to the wave data in appendix B.2.

Displacement	Δ	=	250000	[kg]
	∇	=	243.902	[m^3]
Longitudinal CoG	LCG	=	23.176	[m]
Longitudinal CoB	LCB	=	23.176	[m]
Wave length	λ	=	42.725	[m]
Maximum wave hight	$H_{1/100}$	=	3.427	[m]
Heeling	ϕ	=	30	[°]
Trim	β	=	0	[°]

TABLE 3.9: Input data for hydrostatic calculations

As the available software Rhinoceros-ORCA3D can only evaluate a yacht's hydrostatic data for a flat water surface an own evaluation tool is set up in Catia V5. The 3D-Model used for the evaluation is the same one as later described in section 3.6. According to the values in the table above a water surface, based on a sinus curve, is generated which divides the hull and defines the underwater body, as illustrated in figure 3.8. The data points of the sinus curve are determined by the following equation with an oscillation amplitude of half the maximum wave height:

$$z_{(x)} = \frac{H_{1/100}}{2} \cdot \sin(\frac{2 \cdot \Pi \cdot x}{\lambda}) \tag{3.3}$$

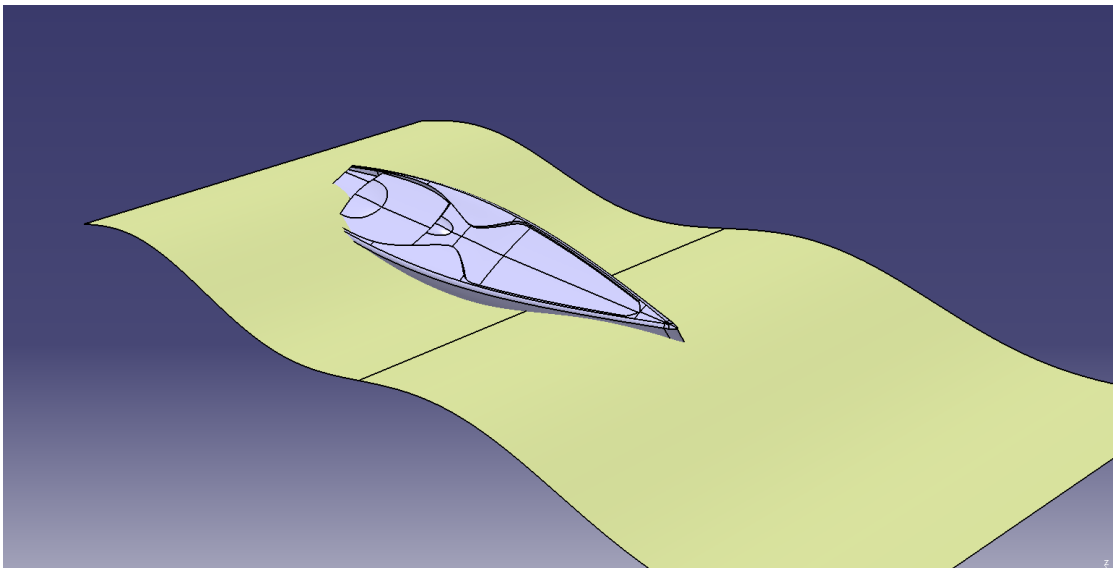

FIGURE 3.8: Load case visualized in CatiaV5

In figure 3.9 the underwater hull of the 46m sailing yacht "EXO" is displayed in upright position (grey) and in heeled condition (yellow). Furthermore, parameters necessary for adjustment of the hydrostatic data in CatiaV5 are visible. The hydrostatic data of the hull in upright position acts as a reference, since the displacement (Volume) and the longitudinal center of buoyancy LCB (in Catia labelled as CGx) must be equal in both conditions. At a trim of zero the longitudinal center of buoyancy LCB of both conditions must comply with the longitudinal center of gravity LCG as well.

The longitudinal and vertical position of the wave surface is adjusted until displacement and longitudinal center of buoyancy of the heeled condition and the upright position are the same.

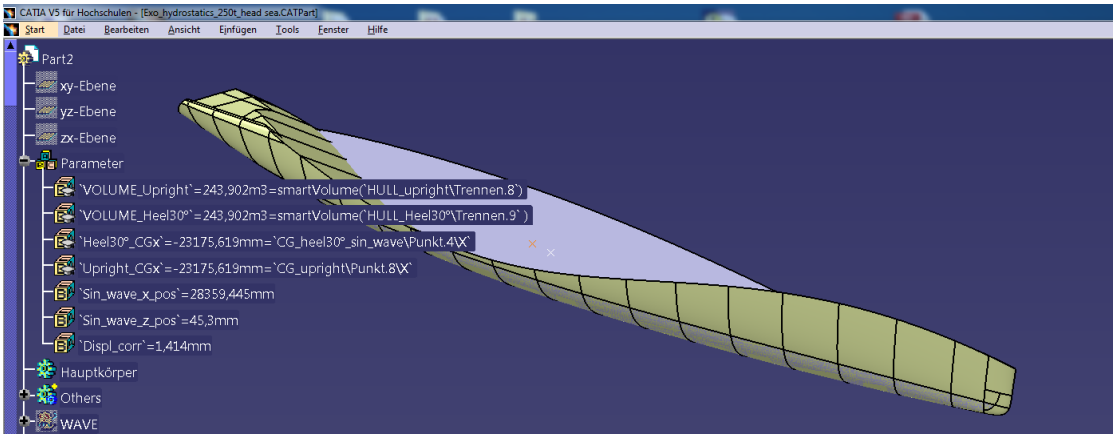

FIGURE 3.9: Underwater body in upright (grey) and heeled condition (yellow)

According to the load model in section 3.3 the underwater hull at 30 degrees of heel (yellow) is divided into 20 equal volume sections along its entire length. Each section's buoyancy and corresponding center of buoyancy in longitudinal, transverse and vertical position are analysed. The CatiaV5 Export-file displaying the hydrostatic data is attached in appendix B.2.1.

3.5.2 Wave and Weight Induced Loads

According to the description of the load model in section 3.3 the hull is divided into 20 equal sections along its length and thus the wave and weight induced loads acting on the hull structure are approximated at 20 loading points (master points). Each master point represents the longitudinal center of each section where the calculated section load acts. All master points are along the whole length in transverse and vertical alignment with the origin and thus likewise with the vertical center of gravity of the yacht VCG = 0. The load model counts in total 21 master points. One of them does not represent a hull section but the loading point of the keel with its longitudinal center of gravity LCG_K, as stated in table B.1.

Basis for the load calculation is a given weight distribution of the 46m sailing yacht "EXO" and its prior determined buoyancy distribution in a sinusoidal wave at a heeling angle of $\phi = 30$ degrees, displayed in figure 3.10.

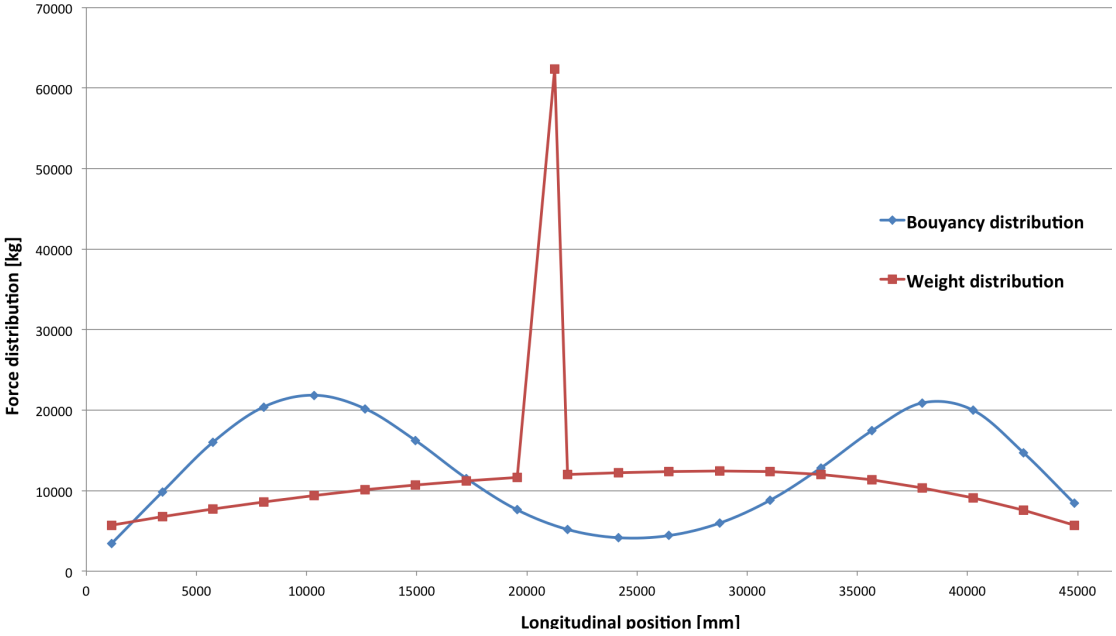

FIGURE 3.10: Weight and buoyancy distribution along 21 master points

Since the whole weight of the bulb keel is assigned to one master point the weight distribution displays an exaggerated peak. However, in the FE-Model this highly concentrated load is distributed across a larger designated area, where the keel is actually attached to the hull (section 3.7).

Diagram 3.11 illustrates the basic principle load calculations are based upon. At each section heel angle dependent transverse and vertical force components for the given weight and buoyancy distribution are calculated. Force components of the weight distribution (Fg_y & Fg_z) act at the center of gravity (CG) and force components of the buoyancy distribution (Fb_y & Fb_z) act at the shifted center of buoyancy (CB'). Due to heeling and hull shape characteristics the buoyancy center of the hull moves outward and generates a transverse and vertical lever arm towards its origin (CB'_y & CB'_z). The lever arms vary along the 20 hull sections but are available from the previously executed hydrostatic analysis.

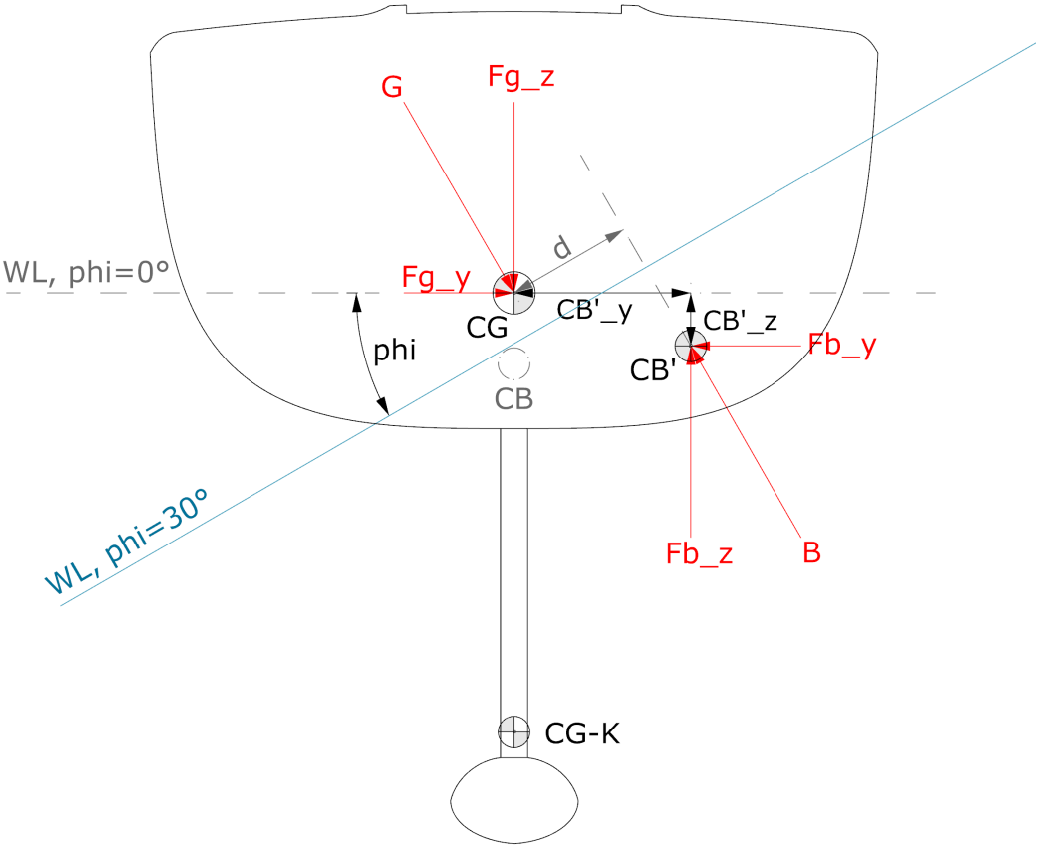

FIGURE 3.11: Diagram of righting arms and force components

The righting moment of a heeled yacht is depending on the distance d between the force lines of the center of gravity CG and the center of buoyancy CB' as shown in

figure 3.11 ($RM = d \cdot \Delta$). Since the yacht's vertical center of gravity VCG is zero and in alignment with the origin of the coordinate system, only the righting arm d measured from the buoyancy force line to the origin is needed to determine the righting moment, as shown in diagram 3.11. This distance d is unknown, but the transverse and vertical lever arms (CB'_y & CB'_z) for each section are available from the hydrostatic analysis and their corresponding buoyancy force components from the spreadsheet calculations.

$$RM_{(x)} = B_{(x)} \cdot d_{(x)} = Fby_{(x)} \cdot CB'z_{(x)} + Fbz_{(x)} \cdot CB'y_{(x)} \tag{3.4}$$

Due to each section's outward moving center of buoyancy, every single hull section contributes its specific amount to the total righting moment:

$$RM = \Sigma RM_{(x)} = 2\,638\,817\,\mathrm{Nm} \tag{3.5}$$

It should be noted that the previous explanations only give an idea of the principle on which the the load calculations are based upon. In fact the spreadsheet is more complex as various adjustments are made. For complete load calculations with detailed explanations see appendix B.

3.5.3 Rig Loads

Rig load calculations are conducted according to GL - Rules for Classification & Construction Part 4, *Chapter 2 - Design and Construction of Large Modern Yacht Rigs* [12]. These rules are based on standard methods found in yacht design literature and yield to convenient results. As only resulting rig forces at hull attachment points determine the development of the hull structure, complex aerodynamic sail forces are of minor interest.

The following paragraph gives a rough overview of the design principles on which the load calculations are based.

Instead of calculating sail forces, resulting heeling moment and rig loads for a certain wind speed, the transverse sailing forces (side force) are determined through the righting moment of the yacht. This is possible because the hull's righting moment and the heeling moment induced by the sail forces are in balance at a

steady-state sailing condition. A commonly agreed on heeling angle is 30 degrees, as it corresponds to a reasonable high wind strength with sails still generating high loads and the yacht making good speed through the water. More heel in reality means a slower boat due to higher resistance with corresponding smaller aerodynamic forces caused by flat trimmed sails and an unfavourable angle of attack of the sails [2] [1].

Hence, basis for all rig loads are the transverse sailing forces, which are determined from the previously calculated righting moment of the yacht at 30 degrees of heel in a sinusoidal wave. Figure 3.12 shows all calculated rig components that induce high tension or compression forces into the hull structure.

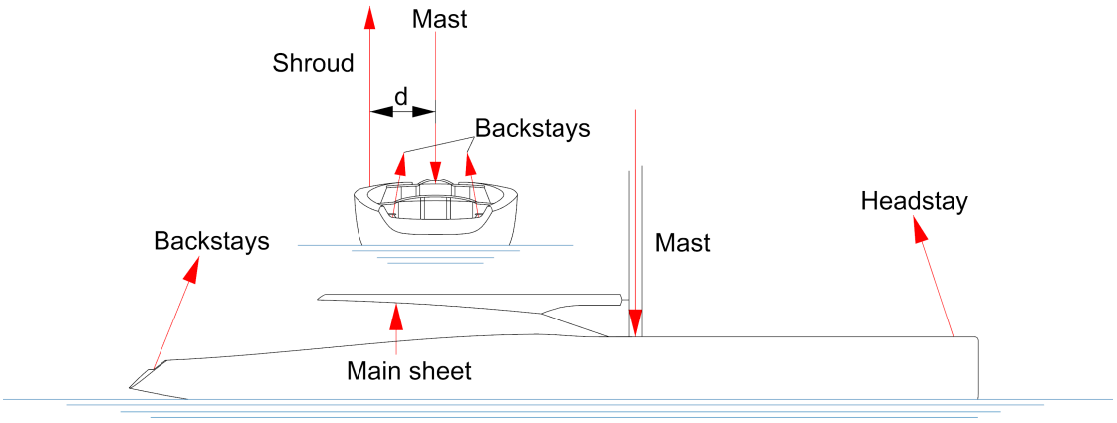

FIGURE 3.12: Diagram of highly loaded rig components

Some of the tension loads in the rig (e.g. headstay) are determined by using the *catenary formula*, where the transverse sail force is distributed along a sail edge (leech, foot or luff) and a certain sag (camber) for the sail edge is taken into account.

On the contrary the shroud tension load (V1) is determined by the classical *Skene's Method* [7]. *Skene's Method* is based on the equilibrium of hydrostatic righting moment of the yacht to the heeling moment due to sail forces. During steady-state sailing condition the mast is in compression and the windward shrouds in tension. Hence, the heeling moment (=RM) can be approximated to equal the vertical chain plate load times the horizontal distance (d) between the mast and the chain plate of the shroud, as illustrated below:

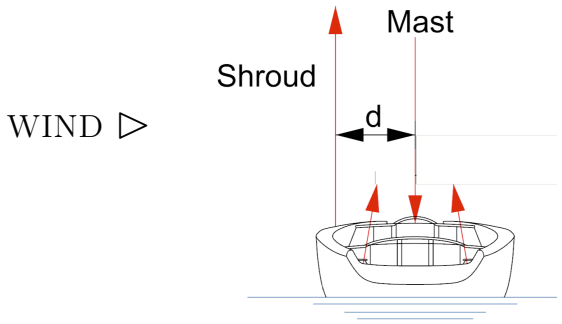

$$F_{V1} = \frac{RM_{30^\circ}}{d}$$

Since backstays, headstays, shrouds and even the mainsheet (through the boom and mainsail) are attached to the mast at a certain point, their vertical force components are transferred to the mast and add up to an overall mast compression force.

For complete rig load calculations and detailed explanations see appendix B.

3.5.4 Summary of Loads

In the following tables all calculated forces and moments that are applied to the FE-Model are listed.

Table 3.10 displays all wave and weight induced loads. It should be noted that not only weight force components are applied at the master points but buoyancy force components as well, since influence of the actual outward shifted loading point (CB') is taken into account via each section's righting moment. Master points 1-20 correspond to the 20 hull sections, master point 9a represents the loading point of the keel at its longitudinal center of gravity.

		Weight loads		**Buoyancy loads**		**Righting moment**
Master points	**x-pos. [mm]**	**Fg_y$_{(x)}$ [N]**	**Fg_z$_{(x)}$ [N]**	**Fb_y$_{(x)}$ [N]**	**Fb_z$_{(x)}$ [N]**	**Mx$_{(x)}$ = RM$_{(x)}$ [Nmm]**
1	1150	28051	48586	-16910	-29289	-6.98E+06
2	3450	33232	57560	-48270	-83606	-2.10E+07
3	5750	37967	65760	-78582	-136108	-3.49E+07
4	8050	42292	73253	-100045	-173283	-4.51E+07
5	10350	46210	80038	-107194	-185665	-5.17E+07
6	12650	49638	85976	-98999	-171471	-5.71E+07
7	14950	52576	91064	-79557	-137797	-6.13E+07
8	17250	55105	95444	-56586	-98010	-6.00E+07
9	19550	57225	99117	-37444	-64854	-5.16E+07
9a	21261	247212	428184			-1.28E+09
10	21850	58938	102083	-25420	-44028	-4.20E+07
11	24150	60080	104062	-20417	-35364	-3.79E+07
12	26450	60813	105331	-21734	-37645	-4.32E+07
13	28750	61137	105892	-29305	-50758	-5.96E+07
14	31050	60692	105121	-43313	-75020	-8.70E+07
15	33350	58923	102057	-63001	-109121	-1.22E+08
16	35650	55544	96205	-85485	-148064	-1.58E+08
17	37950	50845	88066	-102523	-177576	-1.75E+08
18	40250	44677	77382	-98089	-169895	-1.38E+08
19	42550	37043	64161	-72084	-124854	-7.59E+07
20	44850	28051	48586	-41292	-71520	-3.59E+07
Summation		1226250	2123927	-1226250	-2123927	**-2.64E+09**

TABLE 3.10: Summary of global loads - wave induced

In table 3.11 all rig induced loads are listed - all acting at their designated hull attachment points. It should be noted that the listed heeling moment is only a result of applied rig loads and thus not implemented in the FE-Model.

	Rig loads			**Heeling moment**
Rig component	**Fx [N]**	**Fy [N]**	**Fz [N]**	**Mx = HM [Nmm]**
Main sheet			147643	0.00E+00
Head stay	131154		393805	0.00E+00
Shroud V1			742701	2.64E+09
Backstay Ps	-65577	6815	97703	-2.38E+08
Backstay Sb	-65577	-6815	97703	2.38E+08
Mast comp.			-1479555	0.00E+00
Summation:	0	0	0	**2.64E+09**

TABLE 3.11: Summary of global loads - rig induced

According the quasi-static load case reflecting a steady-state sailing condition all calculated forces and resulting moments are in equilibrium. This equilibrium is validated and listed in detail in table B.7 & B.10 in appendix B.

In short the summation of all forces in transverse and vertical direction is zero and so are the moments around the transverse and vertical axes. Obviously the summation of moments around the longitudinal axis add up to the righting moment RM, which is in balance with the heeling moment induced by the sail forces.

3.6 Creation of Design Space

For performing topology optimizations design and non-design spaces must be defined. Starting point for the design space definition is a given *Rhinoceros* 3D-Model of the 46m sailing yacht "EXO". Based on this model a simplified surface model was created in CatiaV5. The CatiaV5 model ensures a closed surface definition which is essential because it constitutes the foundation for hydrostatic analysis, topology optimizations, hull structure visualizations and for final FE-Simulations.

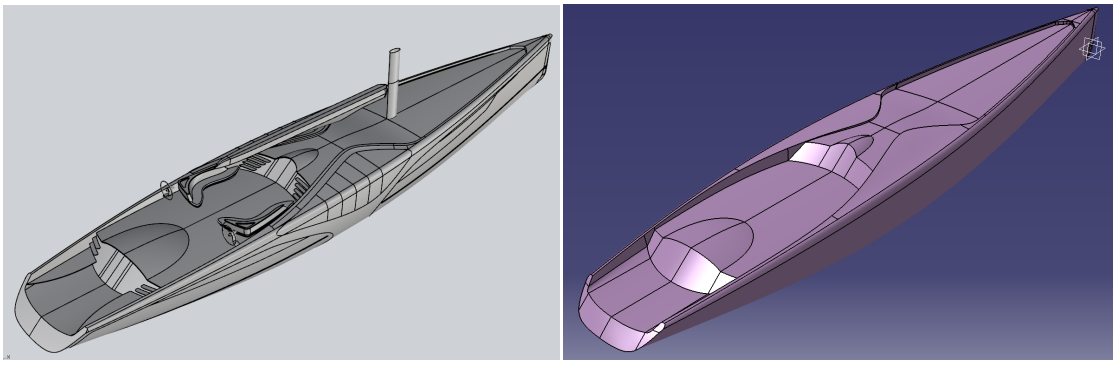

FIGURE 3.13: "EXO" 3D-Model - Rhinoceros (left), CatiaV5 (right)

The design space defines the model volume in which the weight distribution is optimized or respectively the structure layout can evolve. Non-design spaces are voids - volumes which are subtracted from the design space in areas where no structure is desired.

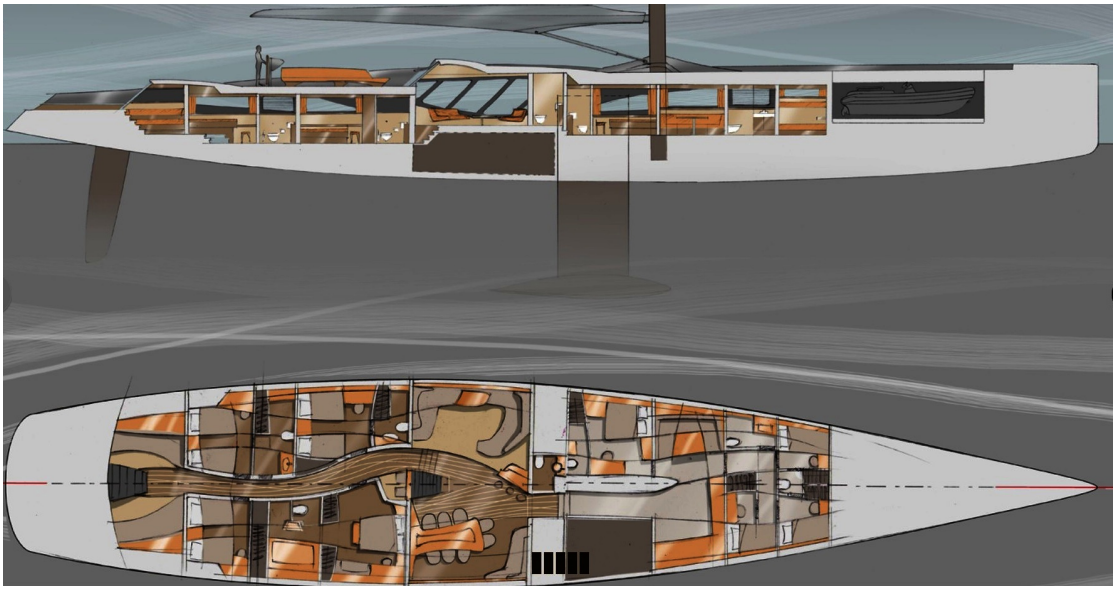

FIGURE 3.14: Interior layout of 46m sailing yacht "EXO"

In figure 3.14 the interior layout of the 46m sailing yacht "EXO" is visualized. Together with *Dykstra Naval Architects* non-design spaces are determined corresponding to this interior layout.

Non-design spaces are corresponding to areas as stated below (bow to stern):

- Tender garage, crew accommodation, lifting keel box,
- Saloon, engine room (below tween deck),
- Guest accommodation and aft pavilion

To create the design space a closed volume is created based on the simplified surface model. From this volume the above stated non-design spaces are subtracted resulting in the desired design space definition, as displayed in figure 3.15.

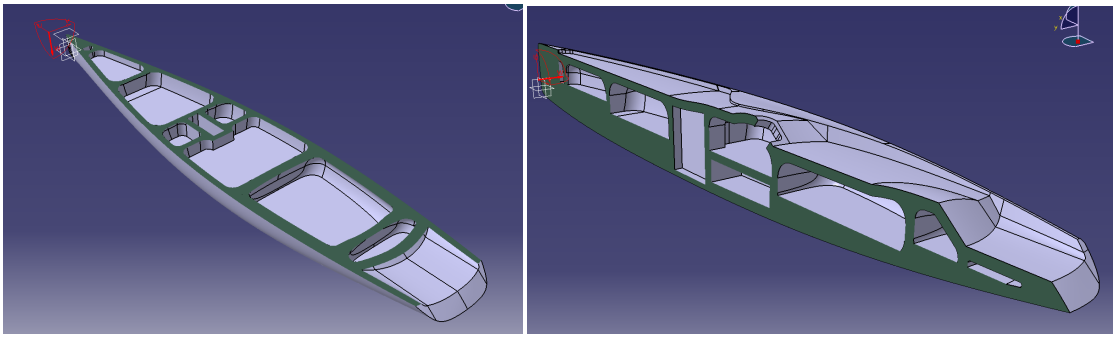

FIGURE 3.15: CatiaV5-Model: Design space for topology optimization

As visible in the figure above the whole area below tween deck, except for engine room and keel box, is assigned to the design space. This is possible since the area below tween deck is mainly designated to fuel, fresh and grey water tanks and would not interfere with the hull structure. Due to subtraction of separated non-design spaces the collision bulkhead and two main bulkheads at the keel box together with four other bulkheads are formed and assigned to the design space. In the whole 3D-Model, which defines the design space, a distance of at least 500 mm between outer and inner skin is maintained for structure evolvement.

3.7 Implementation of FE-Model

In the framework of this master thesis all topology optimizations and finite element analyses are performed with the software package *HyperWorks* from *Altair-Engineering*:

- **HyperMesh**, **HyperView** and **HyperGraph** for pre- and post-processing.
- **OptiStruct** as the solver for linear static FE-Simulations and topology optimizations (SIMP method).

3.7.1 Description and Boundary Conditions of FE-Model

According to the load model description in section 3.3 the previously calculated global loads need to be applied to a predefined design space. First, the design space created in Catia V5 is auto-meshed with solid elements (Tetra) of an average size of 280mm, as visualized in figure 3.16. The meshed design space counts 754214 solid elements, which have all the same E-Modulus of E = 210000 N/mm^2 and a Poisson's ratio of ν = 0,3.

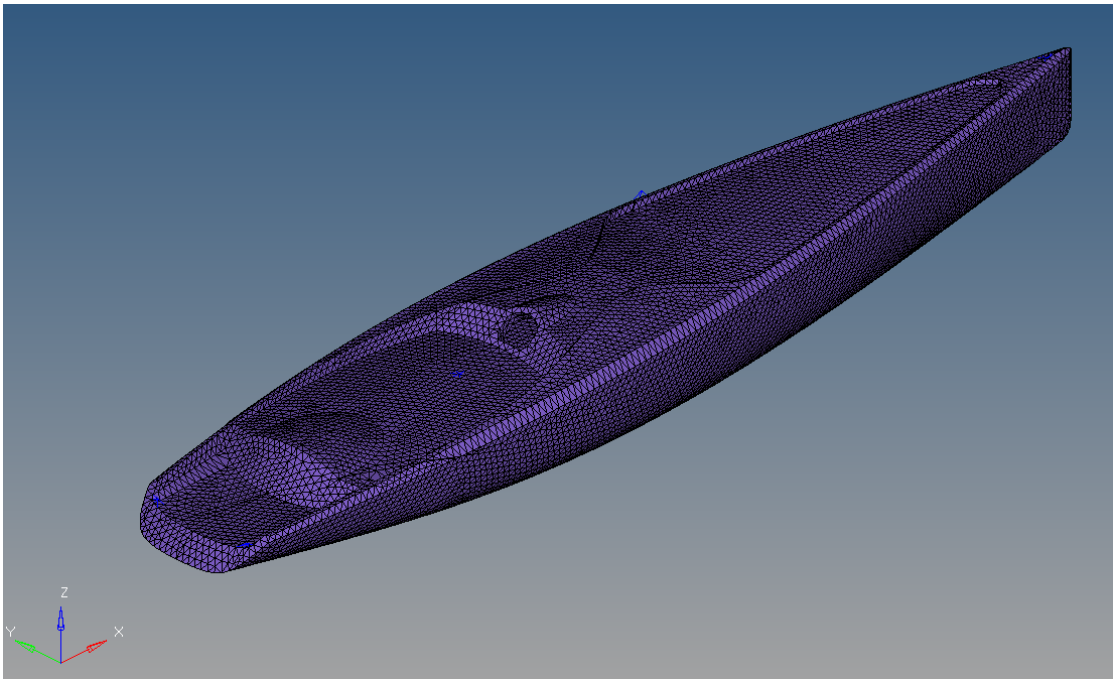

FIGURE 3.16: Meshed design space of 46m sailing yacht "EXO"

Subsequently, buoyancy and weight loads are applied to the meshed design space. For the load application 21 master points, defining the loading point of each section load, are created. Originating from these master points 41 RBE3 elements are created for distribution of calculated section loads to their corresponding hull sections. Within each section the RBE3 element should transfer the applied load only to the outer faces of the solid elements. For this purpose the *Faces-Method* is used to extract the utmost faces (nodes) of the solid elements.

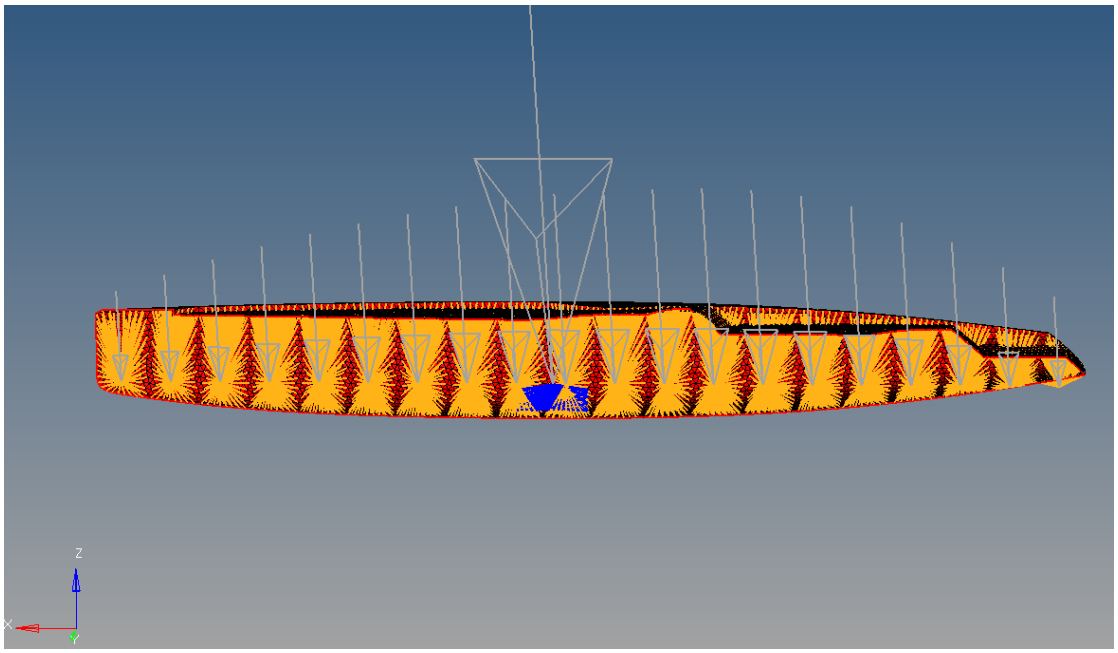

FIGURE 3.17: Distribution of weight forces

In figure 3.17 20 RBE3's (orange) distribute the weight loads to the whole area of the corresponding 20 hull sections and one RBE3 (blue) distributes the high loads from the bulb keel to the lifting keel box; likewise this blue highlighted element transfers the bulb keel induced righting moment to the lifting keel foundation. The RBE3 element of the keel only connects the inner solid faces of the lifting keel box, where the keel is actually clamped in its lowered position (area between hull bottom and approx. 1000 mm above). The grey arrows represent the yacht's weight distribution and are scaled according to their load (see also figure 3.10).

Likewise 20 RBE3's (blue) in figure 3.18 distribute the calculated buoyancy force components and righting moments of each hull section to the FE-Model. Yet, according to the load model in section 3.3 the RBE3's only connect the outer solid faces defining the wetted area of the corresponding 20 hull sections (illustrated

through the shape of the sinusoidal wave). The grey arrows represent the yacht's buoyancy distribution and are scaled according to their load (see also figure 3.10).

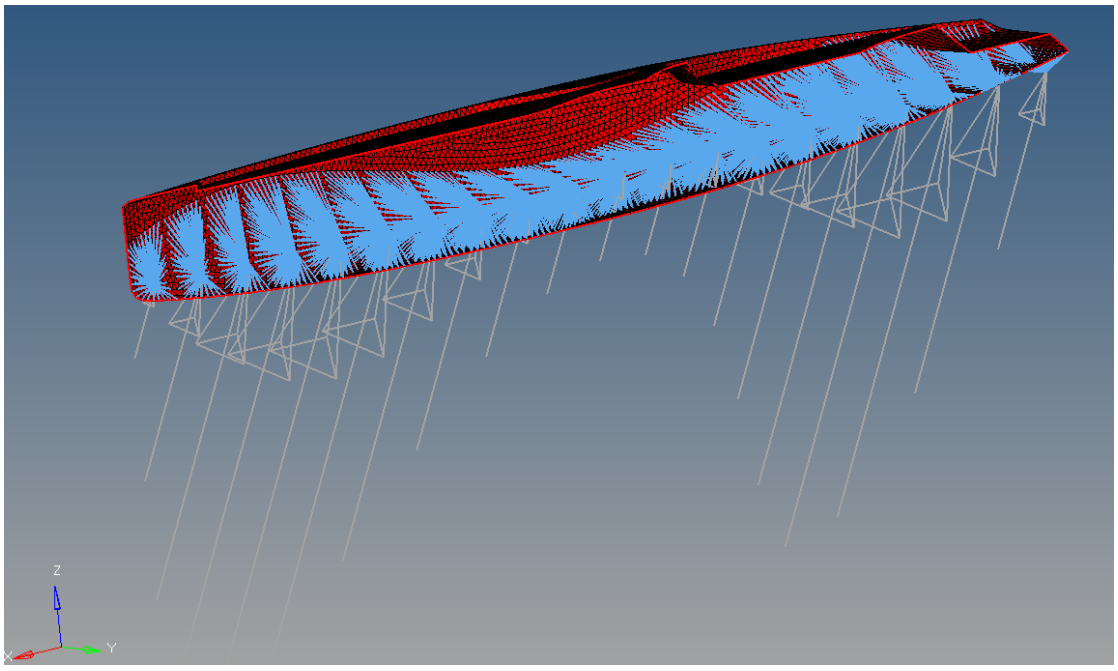

FIGURE 3.18: Distribution of buoyancy forces

The force components of the calculated rig loads are applied at their designated hull attachment points as visualized in figure 3.19.

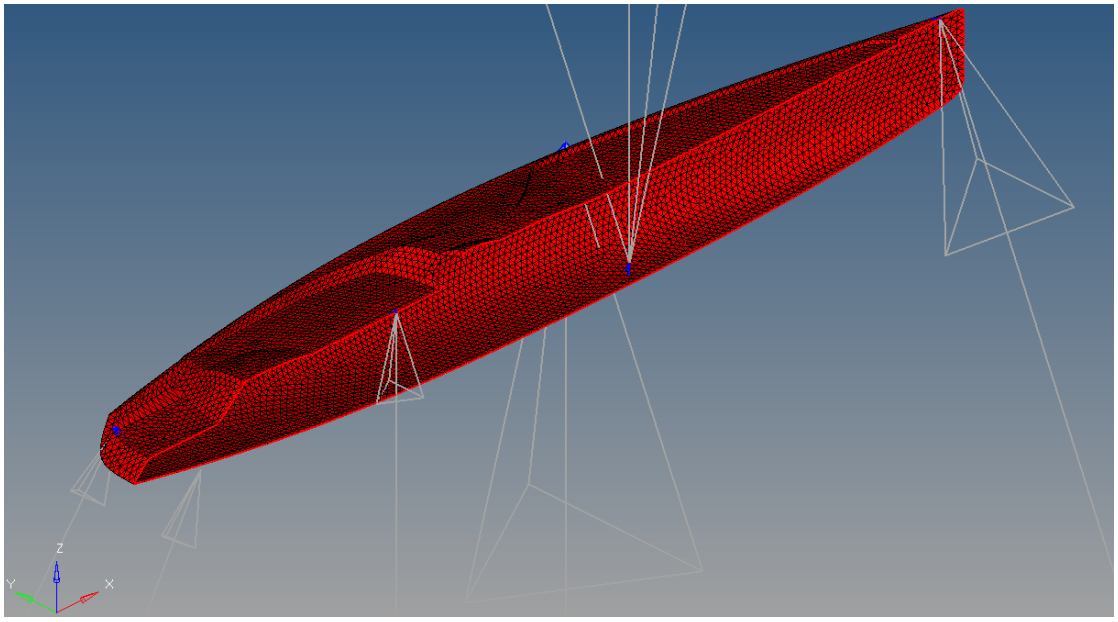

FIGURE 3.19: Application of rig loads

As rig components induce very high point loads and to avoid strong local deformations of the hull structure substantial local reinforcements distribute them to larger areas. Hence, these reinforcements are remodelled in this FE-Model by RBE2 elements transferring the high rig loads to more solid faces. RBE2's are infinite stiff (rigid) elements for transferring loads. Furthermore, their application avoids unrealistic hot spots in FE-Simulations.

Due to the fact that all calculated forces and moments are in balance, reflecting a steady-state sailing condition, the FE-Model needs to be constrained only at one random node to enable computations and maintain convergence.

3.7.2 Validation of Global Loads and FE-Model

Before first topology optimizations will be executed a linear static analysis is performed to detect inconsistencies in the FE-Model setup. The main focus lies on single point constraints (SPC). Since all calculated forces and moments are in balance reaction forces and moments at the solely constrained node should be approx. zero.

Extracted SPC results of the output-file show that all reaction forces and moments converge to zero. The reaction moment around the longitudinal axis shows the largest deviations with a magnitude of 1E+04 Nmm. However, taking into account an applied righting moment (RM = Mx) in the magnitude of 1E+09 Nmm this deviation correlates to a general distortion of results by 0,001% which is well negligible.

```
Residual energy ratio for static load case        1 = -5.040926E-10
-------------------------------------------------------------------------
 Label     x-force    y-force    z-force   x-moment   y-moment   z-moment
-------------------------------------------------------------------------
Sum-App.  6.000E-02  1.610E-01 -1.600E-01  3.422E+04 -1.445E+01  8.169E+03
Sum-SPCF -6.049E-02 -1.612E-01  1.603E-01 -3.422E+04  2.396E+01 -8.170E+03
-------------------------------------------------------------------------
Notes: 1. All applied and SPC forces are transferred to
          the origin of the basic coordinate system,
          so that the applied and SPC loads can match.
```

In addition, the longitudinal bending moment can be extracted with HyperGraph, as shown in the figure 3.20. The total longitudinal bending moment (TB) is the sum of the rig bending moment (RB) induced by the applied rig loads and the wave bending moment (WB) derived from applied buoyancy and weight loads.

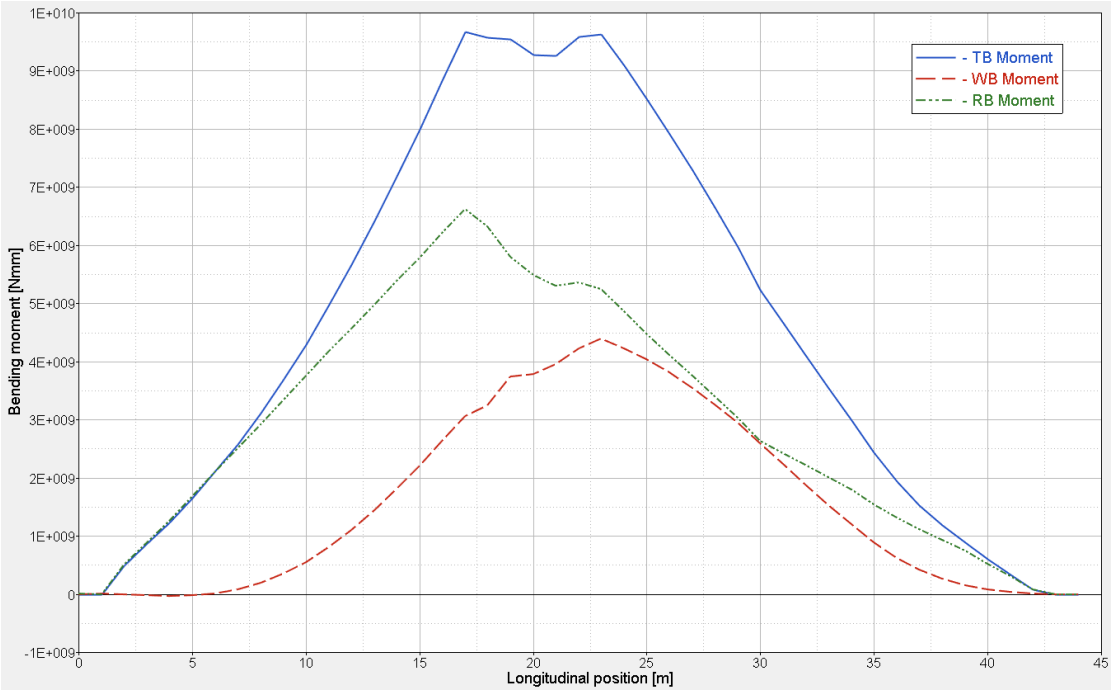

FIGURE 3.20: Longitudinal bending moments induced by global loads

The maximum total longitudinal bending moment adds up to approx. 9500 kNm (see figure 3.20). Its magnitude is convenient for the yacht's length of 46 meters, as the maximum total bending moment of a 36 m sailing yacht by *Dykstra Naval Architects* for instance is up to 6200 kNm [13]. A rig induced bending moment of approx. 6700 kNm is appropriate according to figure 3.21 from a publication about *"Design and Building of Composite Sailing Super Yachts"*. The maximum longitudinal bending moment induced by rig loads for 46m Sloops statistically runs up to 7000 kNm [3].

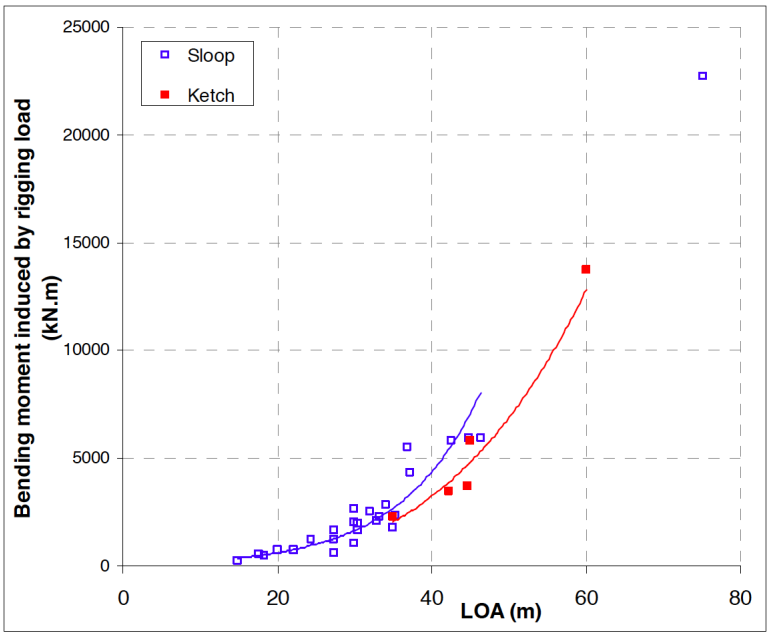

FIGURE 3.21: Bending moment versus Loa [3]

Summarized, the distribution of the total longitudinal bending moment along the hull length correlates to the global loads the hull structure has to cope with in a worst-case sailing condition (as defined in section 3.2.1).

4 Creation of Hull Structure

In this chapter the hull structure of the 46m sailing yacht "EXO" is created, inspired by nature's principles of design. To develop the final hull structure four topology optimizations, based on the SIMP method are performed. In the ambit of this concept study these topology optimizations are conducted with the main objective to obtain a load dependent structure layout of the yacht hull. All necessary data and functions for their application are provided by the design suite as presented in the previous chapter 3.

Results of the presented topology optimizations act as a source of inspiration and are then refined and abstracted during the creation process of the hull structure. For a final evaluation the developed structure concept is dimensioned preliminarily.

4.1 Topology Optimizations - SIMP Method

Depending on the defined design space, type of applied loads and objective of topology optimization several parameters need to be set.

Following parameters are defined:

- **Design objective:** ***Minimize compliance***

  This objective function reflects the principle of lightweight designs where a maximum of stiffens with a minimum amount of material is claimed. To maximize stiffness, displacements need to be minimized, which is equal to minimizing compliance (strain energy) [10].

- **Design constraint:** ***Volume fraction, upper boundary = 0,1 or 0,3***

  This fraction defines the volume ratio of optimized structure to original design space. An upper boundary of e.g. 0,3 means, that the optimized volume can count may be up to maximum 30% of the design space volume [10].

- **Geometric constraints:**

a ***Symmetry constraint = midship plane***

In case of the present load case definition, forces are not applied symmetrically with regard to the yacht's center plane and would in this manner lead to diverging structure layouts on port- and starboard side. The defined symmetry plane claims a symmetric result of the topology optimization with respect to the yacht's midship plane.

b ***Draw direction constraint = z-axis***

This constraint defines the direction in which material with high density should be accumulated.

The presented topology optimizations are conducted on a workstation with 16 processing cores and with the parameters stated above; volume fraction and draw direction vary.

4.1.1 Result of 1^{st} Topology Optimization

Figure 4.1 shows the result of the first topology optimization (TO) performed with the design data as summarized below:

Design space	solid (Tetra)
Average element size	280 $[mm]$
Number of elements	754214
Volume fraction	0.3
Draw direction	no

In figure 4.1 the initial design space (as defined in section 3.6) is visualized as well to emphasize the clear result.

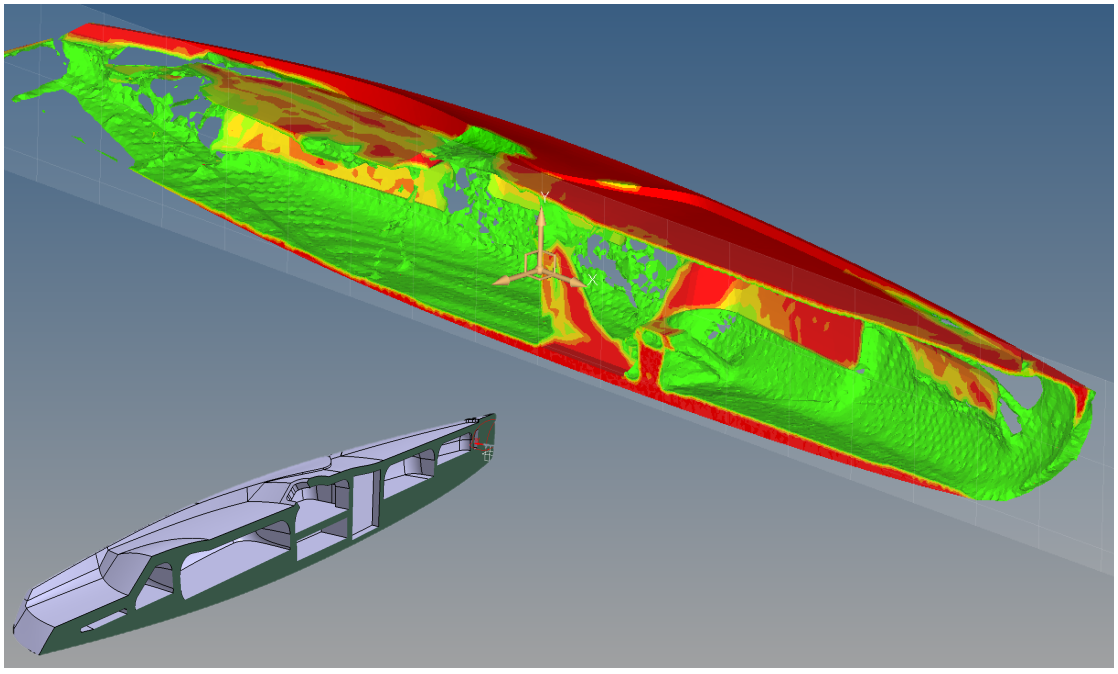

FIGURE 4.1: Initial design space & result of 1^{st} TO

During the optimization process most of the generously provided design space volume is scraped out and accumulated close to hull skin and main deck. This is a very plausible distribution, since only material far away from the yacht's neutral faces increases global stiffness of the structure effectively. Furthermore, the optimized distribution shows that material is also placed around the keel lifting box and the main bulkhead; areas which are obviously subjected to high loads from mast and keel.

4.1.2 Results of 2^{nd} Topology Optimization

To refine material distribution and to reveal main load paths of the yacht structure the draw direction constraint is activated and the volume fraction is reduced as stated below:

Design space	solid (Tetra)
Average element size	280 $[mm]$
Number of elements	754214
Volume fraction	0.1
Draw direction	z-axis

The result is a layout more similar to a truss structure where material of high density is accumulated along the main load paths. Figure 4.2 shows that outgoing from the load center (4), where substantial keel and mast loads are acting, truss members are carved out along the main load paths running to the rig attachment points. The load paths coincide with the chain plates of the headstay (1), backstays (2) and shrouds (3). Furthermore, two diagonal load paths form a cross at the chain plate of the main sheet (5).

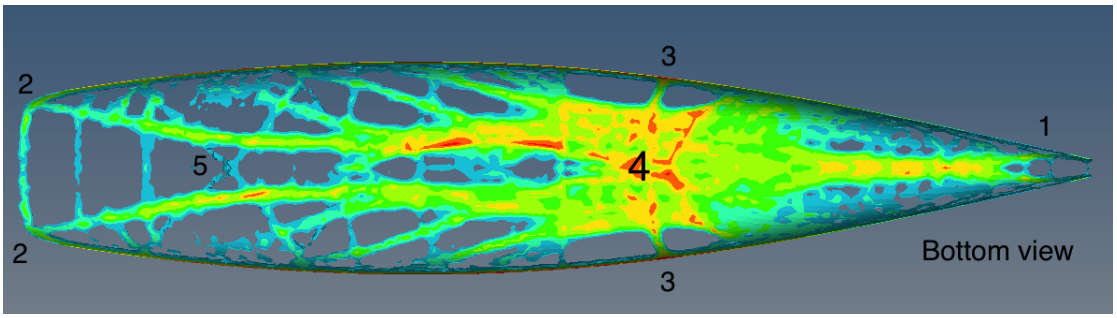

FIGURE 4.2: Result of 2^{nd} TO - labelled loading points

These are very plausible results, since still only material far away from the yacht's neutral faces is placed and mainly accumulated along the main load paths to distribute high rig loads smoothly into the yacht structure.

Figure 4.3 shows that like in the 1^{st} TO the distributed material forms two main bulkheads and additional reinforcements for distributing high loads from mast and keel smoothly into the hull structure.

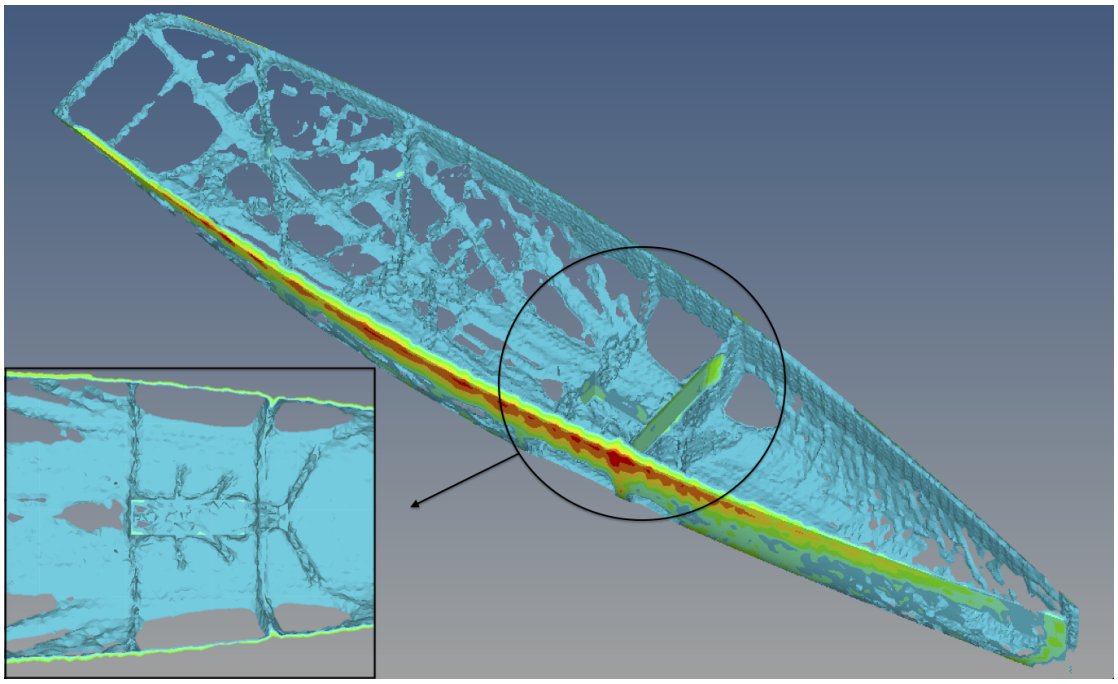

FIGURE 4.3: Result of 2^{nd} TO - Material distribution at main bulkheads

From the first two topology optimizations the conclusion has been derived, that for further refinements of results a surface model is more suitable, since material is only distributed along the hull skin, main deck and the two main bulkheads with the lifting keel box in-between.

4.1.3 Results of 3^{rd} Topology Optimization

Prior to the 3^{rd} TO a new design space is created, describing hull skin, main deck and the two main bulkheads with the lifting keel box in-between as surfaces. With regard to the implementation of the FE-Model boundary conditions are unchanged (as described in section 3.7). But in contrast to the initial FE-Model the design space is defined by surfaces, which are auto-meshed with shell elements (Tria, quad) of an average size of 100 mm. Additionally, a shell thickness of 500 mm is applied to all elements to provide a volume for which material distribution can be optimized. Furthermore, RBE3 & RBE2 elements are updated and connected to corresponding nodes of the generated shell elements.

Design space	shell (Tria/quad)
Average element size	100 $[mm]$
Number of elements	101534
Volume fraction	0.3
Draw direction	no

In figure 4.4 and 4.5 the results of the 3^{rd} TO are displayed. Similar to the results of the 2^{nd} TO material of high density is accumulated along the same main load paths running to the rig attachment points. Yet, this time more intermediate load paths are obtained forming a network of interwoven truss members.

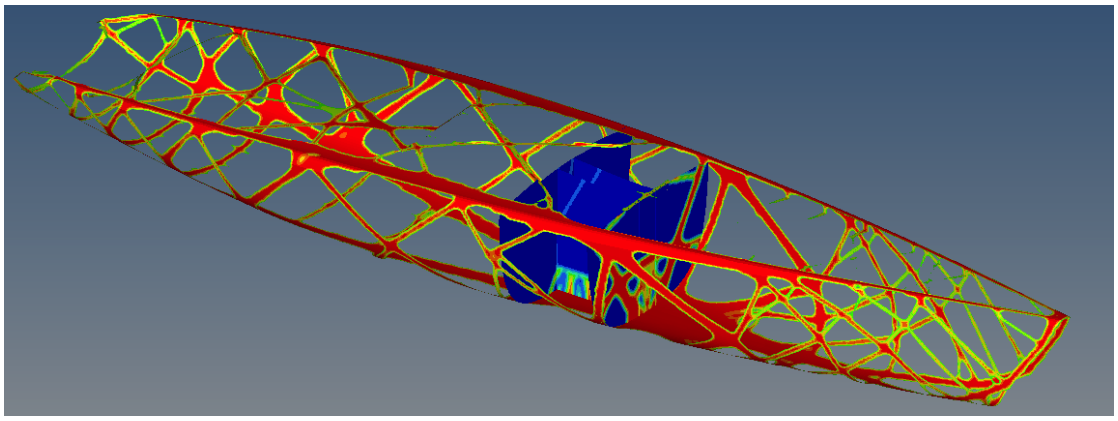

FIGURE 4.4: Result of 3^{rd} TO - perspective

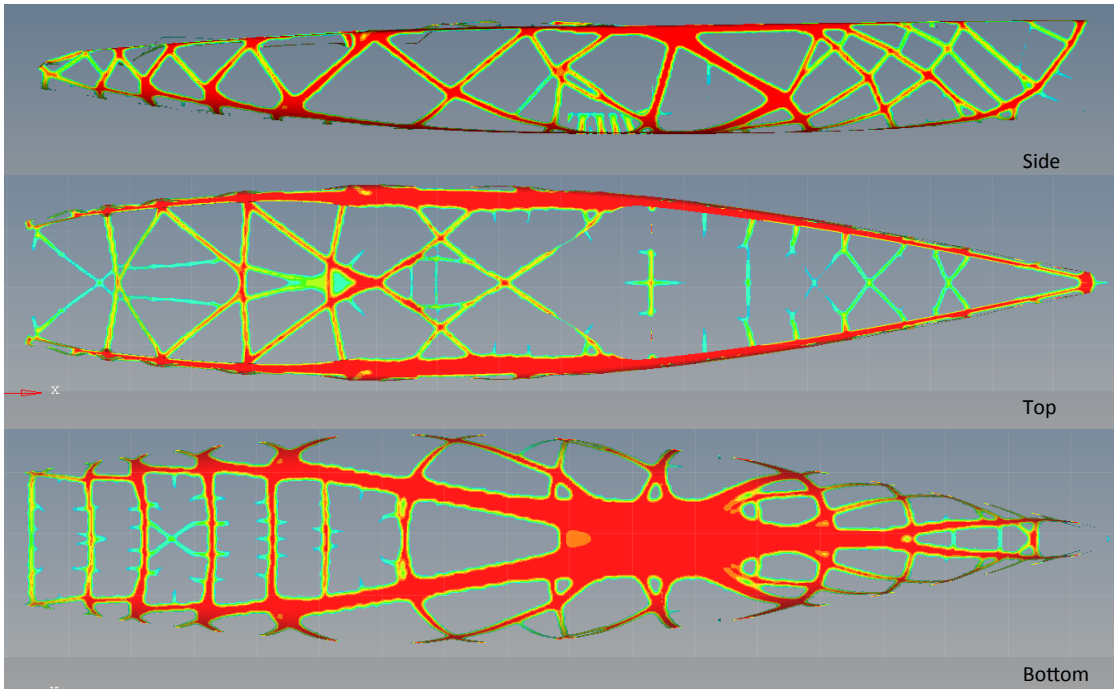

FIGURE 4.5: Result of 3^{rd} TO - side, top & bottom view

Like in case of the 2^{nd} TO, convenient results are obtained. But this time finer, interwoven truss members are generated - reminding of organic forms. Hence, the results of the 3^{rd} TO act as a design proposal for creating the truss structure of hull, deck, main bulkheads and keel box structure.

4.1.4 Results of 4^{th} Topology Optimization

Nevertheless, a 4^{th} TO is conducted to visualize load paths in structure components like tween deck, bulkheads (except main bulkhead) and lifting keel box. These structure components do not contribute enormously to the longitudinal stiffness, since they partly or completely disappear in the 1^{st} & 2^{nd} TO. Though they are requested to comply with important sub-divisions (collision, engine room bulkhead, et cetera) of the designer's interior layout (figure 3.14). Apart from this fact they increase the overall transverse stiffness of the yacht structure.

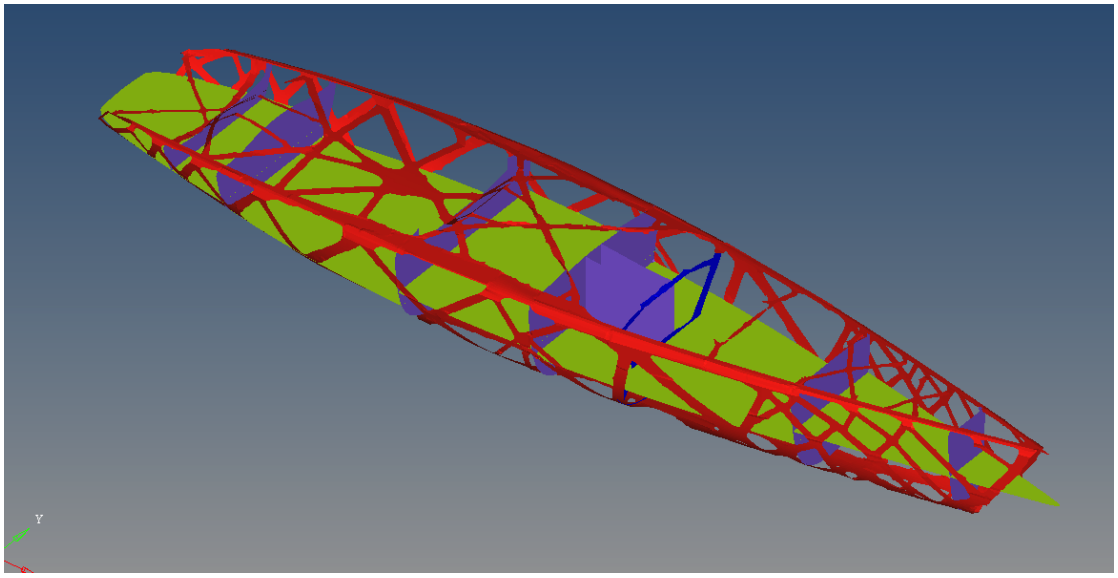

FIGURE 4.6: Design space (green, violet) & non-design space (red, blue)

Figure 4.6 visualizes the set-up for the final topology optimization. Since the truss structure of these components should later on coincide with the ones of hull and deck, the result of the 3^{rd} TO is exported as a surface. This surface is meshed with shell elements as described in section 4.1.3 and RBE3 & RBE2 elements are updated respectively. It should be mentioned, that for this topology optimization the imported structure layout of the 3^{rd} TO represents a non-design space, because only inner structure components (except main bulkhead) need to be optimized.

Design space	shell (Tria/quad)
Non-design space	shell (Tria/quad)
Average element size	100 $[mm]$
Number of elements	75731
Volume fraction	0.3
Draw direction	no

In figure 4.7 the load paths of inner structure components are visualized. Material is mainly distributed along load paths which coincide with hull and main deck members.

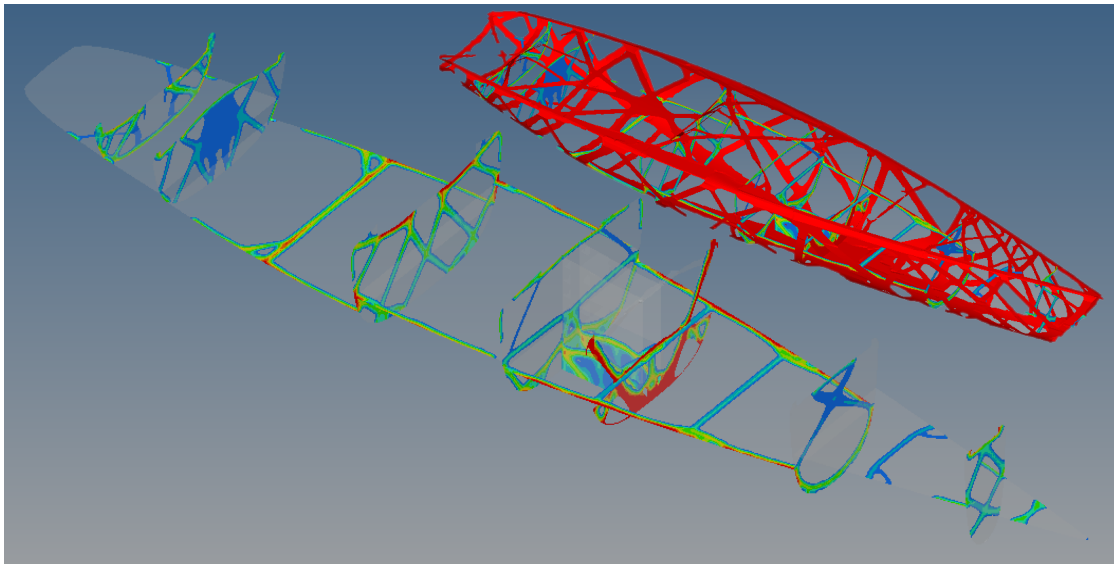

FIGURE 4.7: Result of 4^{th} TO

The results of the 4^{th} TO act solely as a design proposal to create the truss structure of lifting keel box and bulkheads; apart from the main bulkhead. Since no substantial results are attained with respect to the tweendeck, this structure component is neglected in further steps of the present concept study.

4.2 Refinement and Abstraction of TO Results

From the topology optimizations results a load dependent structure layout is obtained. Due to the objective function of the performed topology optimizations, the material is optimized within the design space with respect to maximise stiffness. The optimized material distribution reveals efficient load paths which act as guidelines to create the actual truss members of the yacht's hull structure. Furthermore, with respect to the objective of this thesis, to develop a nature inspired hull structure, the revealed load paths already reflect organic forms. Yet, these results present a preliminary design layout to create a consistent hull structure of the 46m sailing yacht "EXO". They are therefore defined and abstracted as described in this section.

To refine the topology results obtained load paths are exported as surfaces and overlaid with the "EXO" 3D-Model in CatiaV5. The load paths are then traced with spline curves in Catia V5. These splines smooth out and refine the exported topology results. Along these spline curves half cylinders are extruded representing truss members of the hull structure. In order to obtain an overall consistent hull structure, several truss members are added and/or adjusted.

As these steps of refinement and abstraction are more of a creative process, they are presented visually on the following pages.

4.2.1 Hull Structure

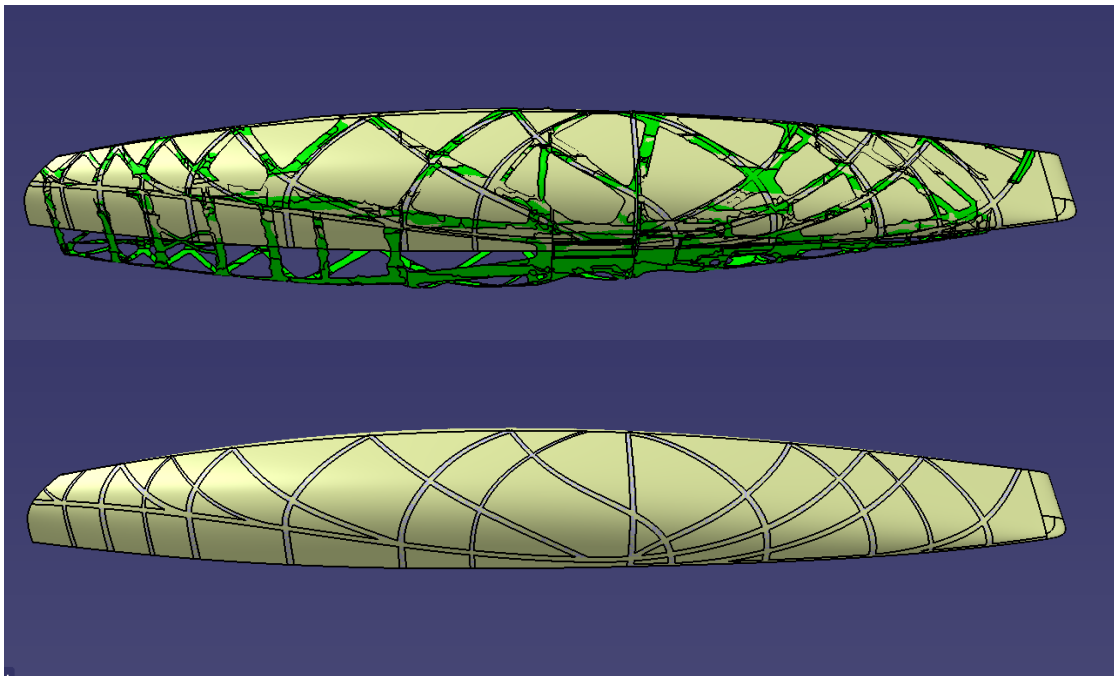

FIGURE 4.8: Refinement of 3^{rd} TO results (green)

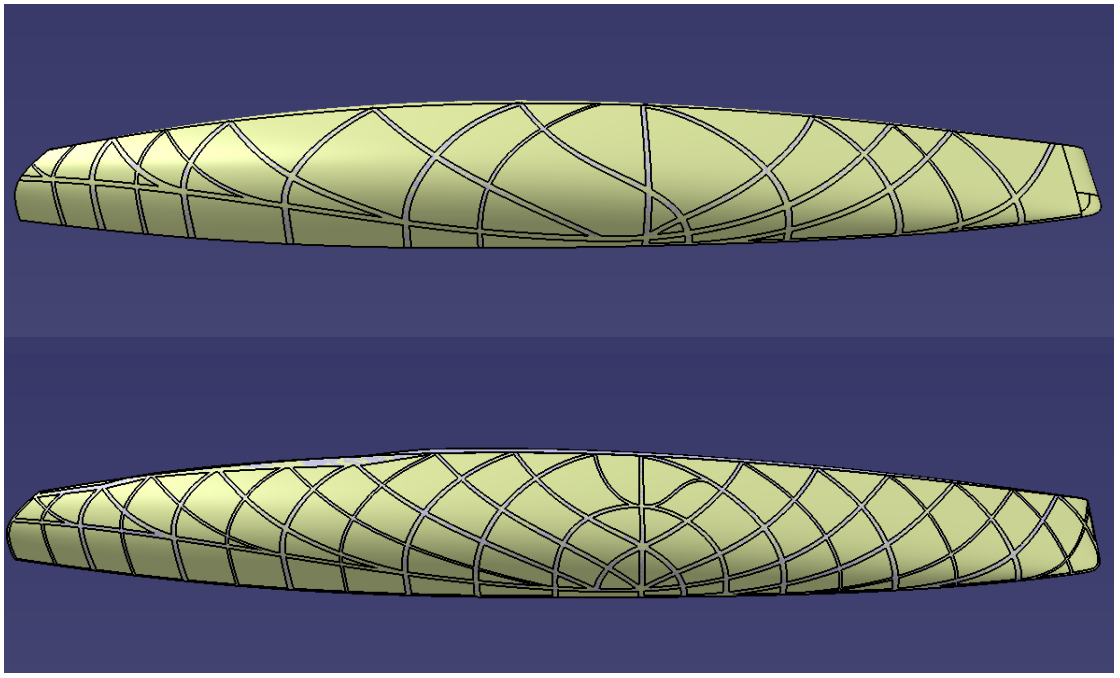

FIGURE 4.9: Abstraction of refined truss structure

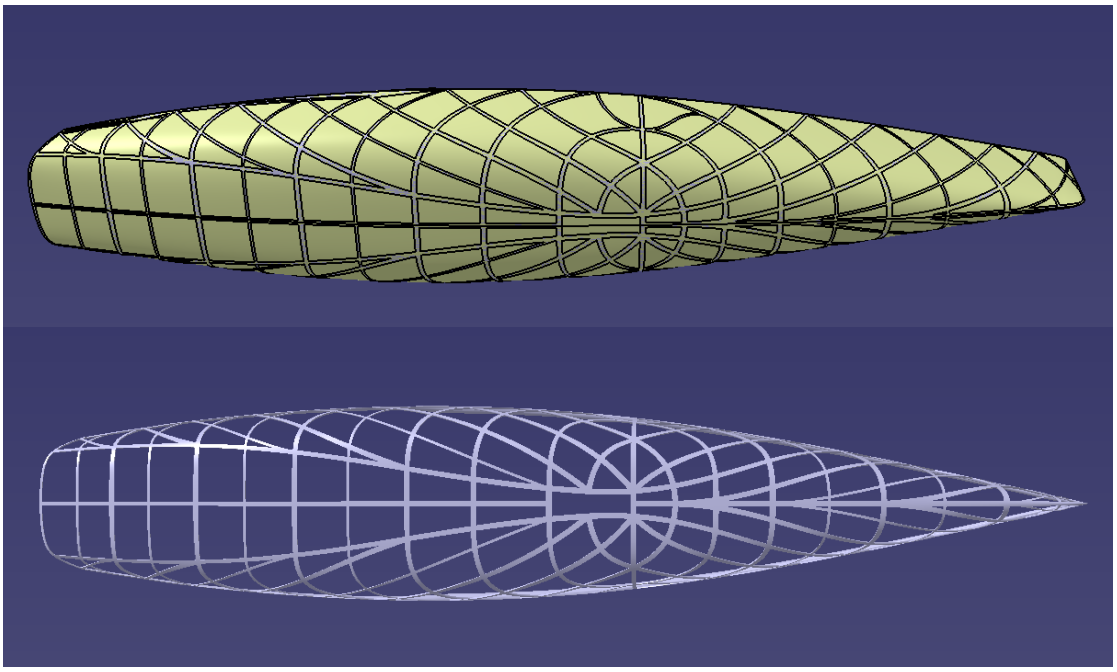

FIGURE 4.10: Abstracted hull structure

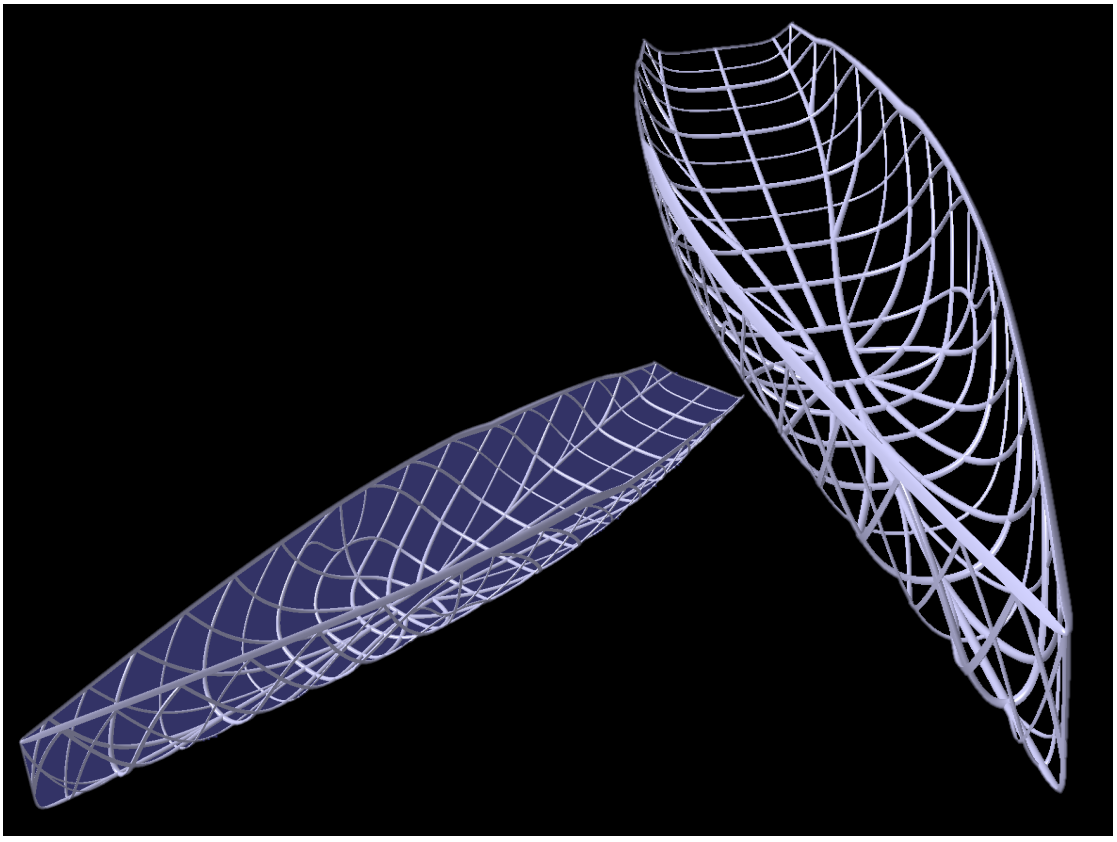

FIGURE 4.11: Visualization of hull structure

4.2.2 Deck Structure

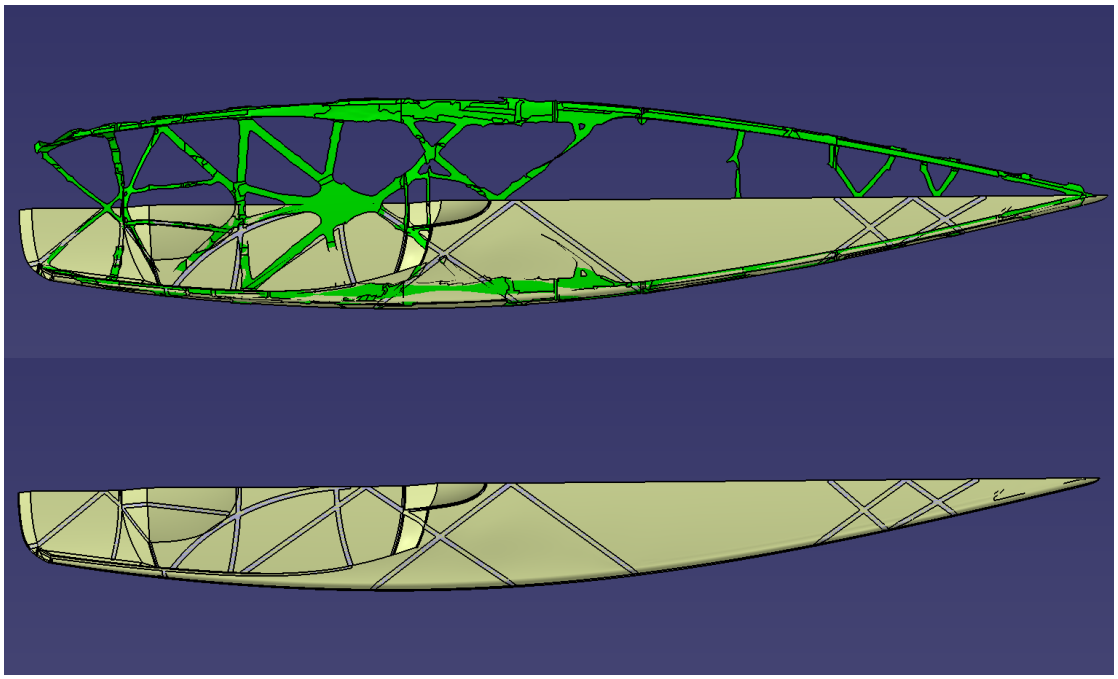

FIGURE 4.12: Refinement of 3^{rd} TO results (green)

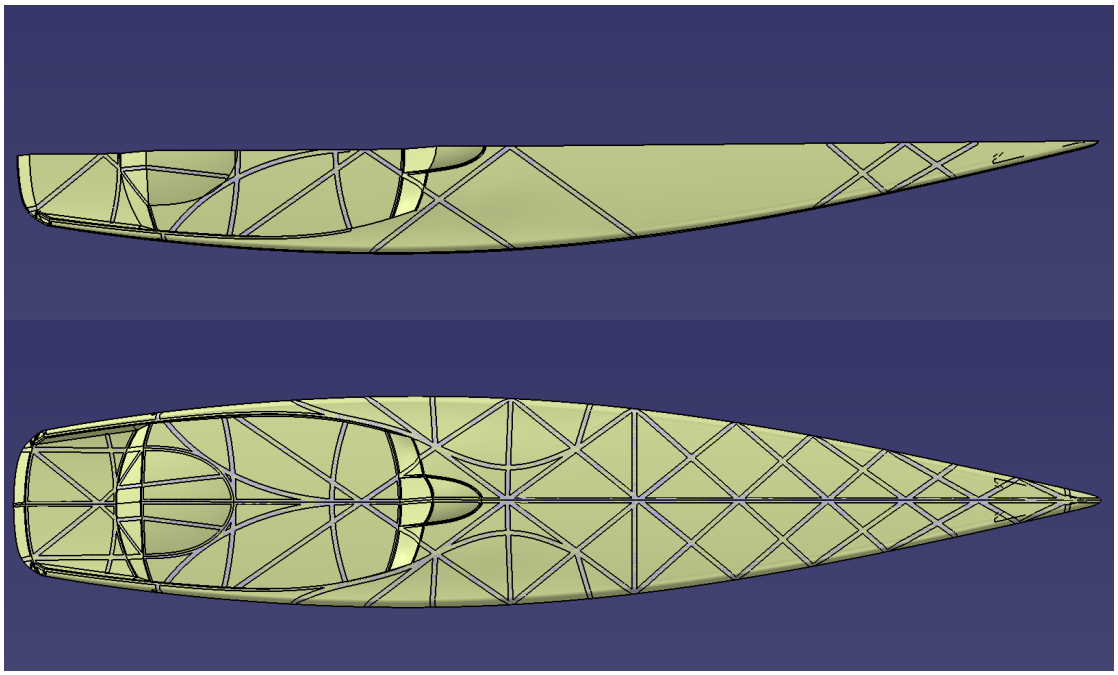

FIGURE 4.13: Abstraction of refined truss structure

4.2.3 Structure of Bulkheads

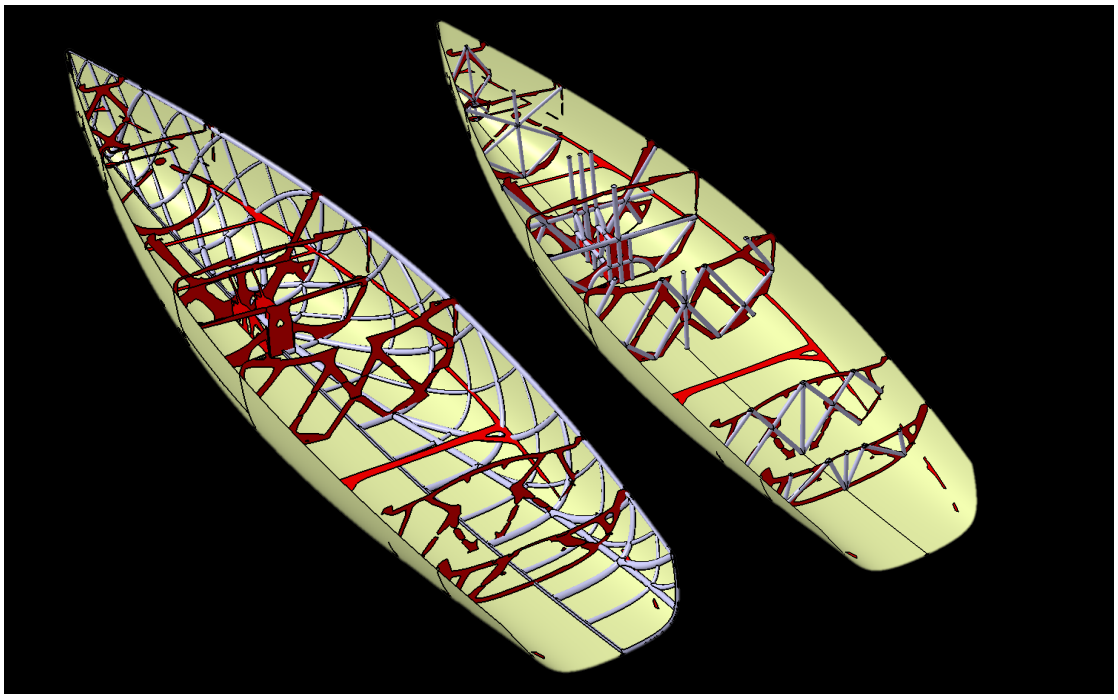

FIGURE 4.14: Refinement and abstraction of 4^{th} TO results (red)

4.2.4 Structure of Mast and Keel Foundation

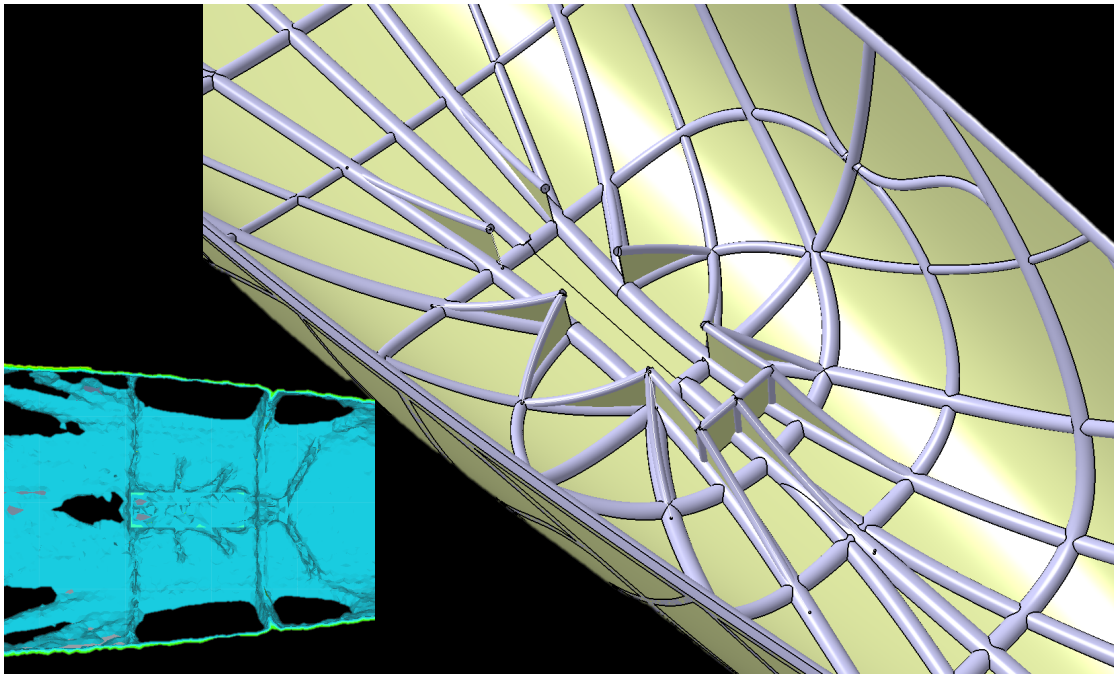

FIGURE 4.15: Abstraction of 2^{nd} TO results

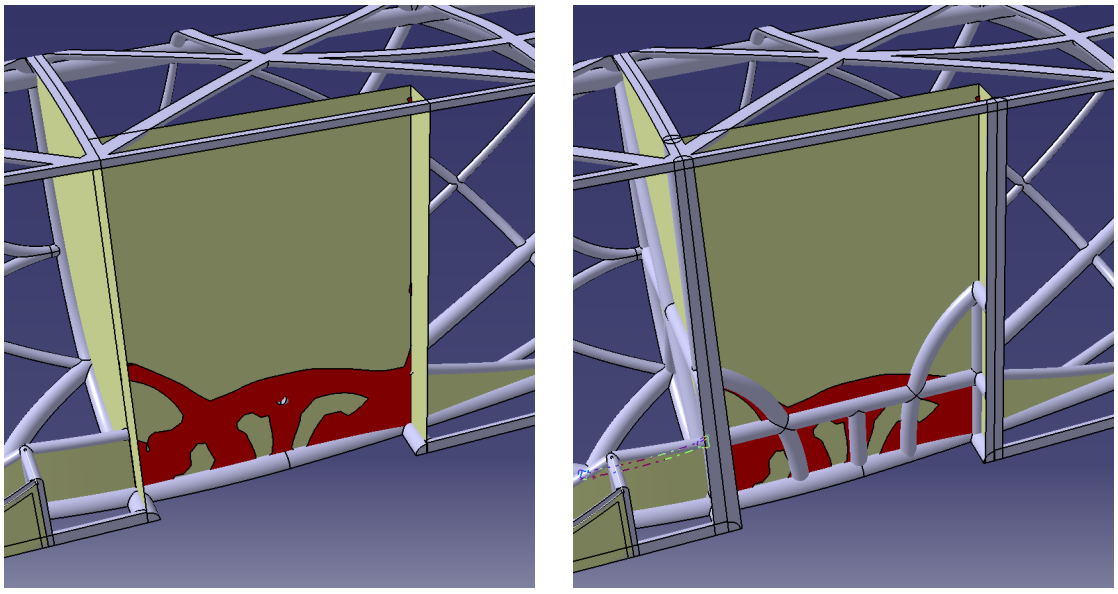

FIGURE 4.16: Refinement and abstraction of 4^{th} TO results (red)

4.2.5 Visualization of Yacht Structure

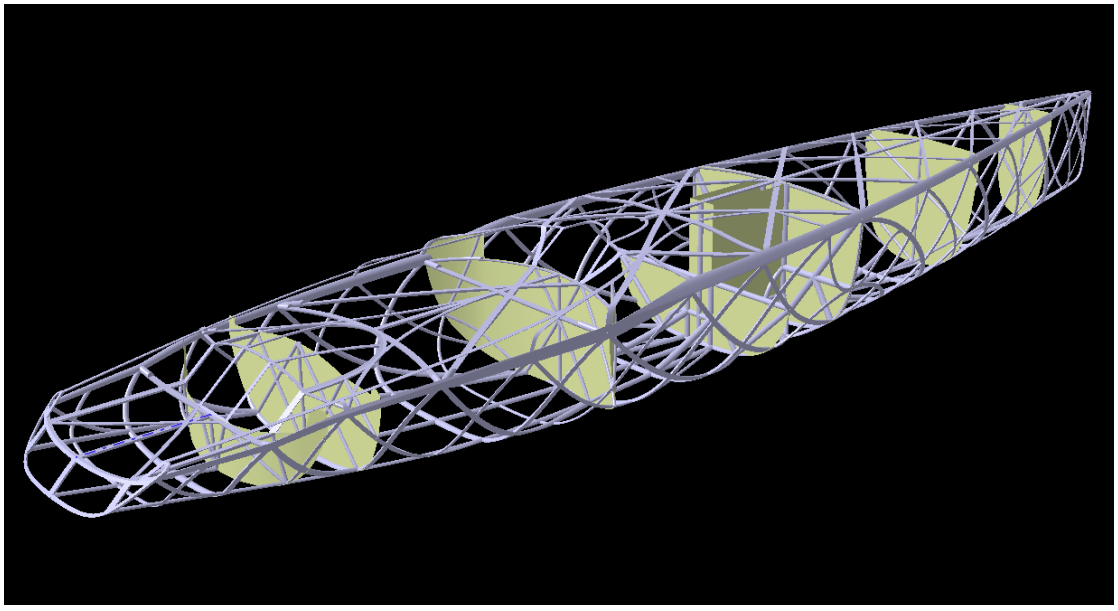

FIGURE 4.17: All structure components - transparent main deck & hull skin

4.3 Dimensioning of Hull Structure

To evaluate the technical feasibility of this unconventional hull structure final FE-Simulations are performed to simulate the yachts behaviour in sailing condition. For this purpose the structure of the 46m sailing yacht "EXO" is dimensioned on a conceptual level considering a full carbon-composite construction.

Section 4.3 gives only a short summary of the structure components and calculation principles. Complete calculations, dimensions of structure components and detailed explanations with regard to design constraints, design stresses, material properties and so on can be found in appendix C.

4.3.1 Dimensioning Process and Principles

Due to the fact that the developed hull structure is not similar to any conventional hull construction, the application of rules and standards from classifications societies is limited to preliminary dimensioning. Hence, dimensions are mostly based on first principle calculations and standard engineering methods. Occasionally, rules and standards from classifications societies are applied in parts and act only as first indications.

Three major steps are constitute the dimensioning process:

- **Dimensions of sandwich panels**

  In the framework of this concept study dynamic loads (e.g. slamming) are neglected and bottom panels are dimensioned with respect to their hydrostatic pressure loads. The required moment of inertia is only calculated for one bottom panel, which has the largest unsupported span in the hull structure. Its dimensions are defining a guideline for all other sandwich panel dimensions of the yacht structure.

- **Dimensions of truss members**

  In view of the objective to create a hull with load carrying and stiffness increasing truss members, hull and deck panels are solely dimensioned to withstand hydrostatic pressures, any additional stiffness to cope with global loads derives from the truss members. In several iterations truss member

dimensions and their laminate thicknesses are varied until the cross section of the yacht complies with the required section modulus. It derives from defined design constraints considering allowable hull bending and design stresses with a **safety factor of 2**.

Maximal hull deflection L/200	230 mm
Maximal stress - tension σ_{dt}	122 N/mm^2
Maximal stress - compression σ_{dc}	75 N/mm^2

TABLE 4.1: Design constraints

- **Isotropic E-Moduli of homogeneous plates**

  The final FE-Simulations are performed with a surface (shell) model and the highly anisotropic composite materials are simplified as isotropic for a preliminary evaluation of this concept. Hence, the structural properties of the sandwich panels and truss members need to be substituted by a homogeneous plate with an isotropic E-Modulus. These isotropic E-moduli are approximated by claiming that the stiffness for sandwich laminate and homogeneous plate are the same.

4.3.2 Homogenized Properties of Structure Components

As a result of the dimensioning process for each surface group, the input values for the FE-Model are known. A surface group includes structure components with the same dimensions and composite lay-up and thus with the same isotropic E-Moduli and total thickness, as listed in table 4.2. Detailed dimensions with mechanical properties and laminate layups can be found in appendix C, section C.6.

Surface groups	**Typ**	**Area** $[m^2]$	**Thickness** $[mm]$	E_{iso} $[Mpa]$	**Laminate weight** $[kg/m^2]$	**Area weight** [kg]
Hull	panels	428.4	40	3729	12.45	5334
Large truss members	1st members	86.3	246	1380	41.09	3547
Small truss members	3rd members	18.2	156	2124	32.09	583
Edge beam		30.8	258	1541	44.97	1384
Deck	panels	270.0	39	3024	9.26	2501
Medium truss members	2nd members	38.1	205	1486	33.9	1292
Small truss members	3rd members	19.7	155	1936	28.9	569
Bulkheads	panels	155.3	39	3024	9.26	1438
Large truss members	1st members	8.6	245	1258	37.9	326
Medium truss members	2nd members	8.3	205	1486	33.9	282
Small truss members	3rd members	12.1	155	1936	28.9	351
Mast&keel foundation	panels	12.5	39	3024	9.26	116
Small truss members	3rd members	4.3	155	1936	28.9	124
	Total area	**1093**			**Total weight**	**17847**

TABLE 4.2: Homogenized properties of structure components and weight

With the calculated laminate weight and the surface area of each component group the total weight of the composite hull structure is estimated. Though it should be noted, that this value can only be seen as a rough indication, as it doesn't include any structure reinforcements, full laminates, adhesive films between cores and laminates, core bonds, gel coat and so on.

5 Evaluation of Hull Structure

5.1 Adaption of FE-Model for Final Simulation

Prior to conduction of final FE-Simulations the FE-Model as described in section 3.7 needs to be adapted.

First the surfaces (in CatiaV5), defining truss members and panels of hull, deck, bulkheads and mast&keel foundatio need to be extracted and imported to the FE-Model. Surfaces of structure components with the same dimensions and composite lay-ups form a surface group, each visualized in a different colour in figure 5.1.

All surfaces are auto-meshed with shell elements (tria, quad) of an average size of 50 mm. 479330 Elements are generated. RBE3 & RBE2 elements are updated and connected to the corresponding nodes of the generated shell elements.

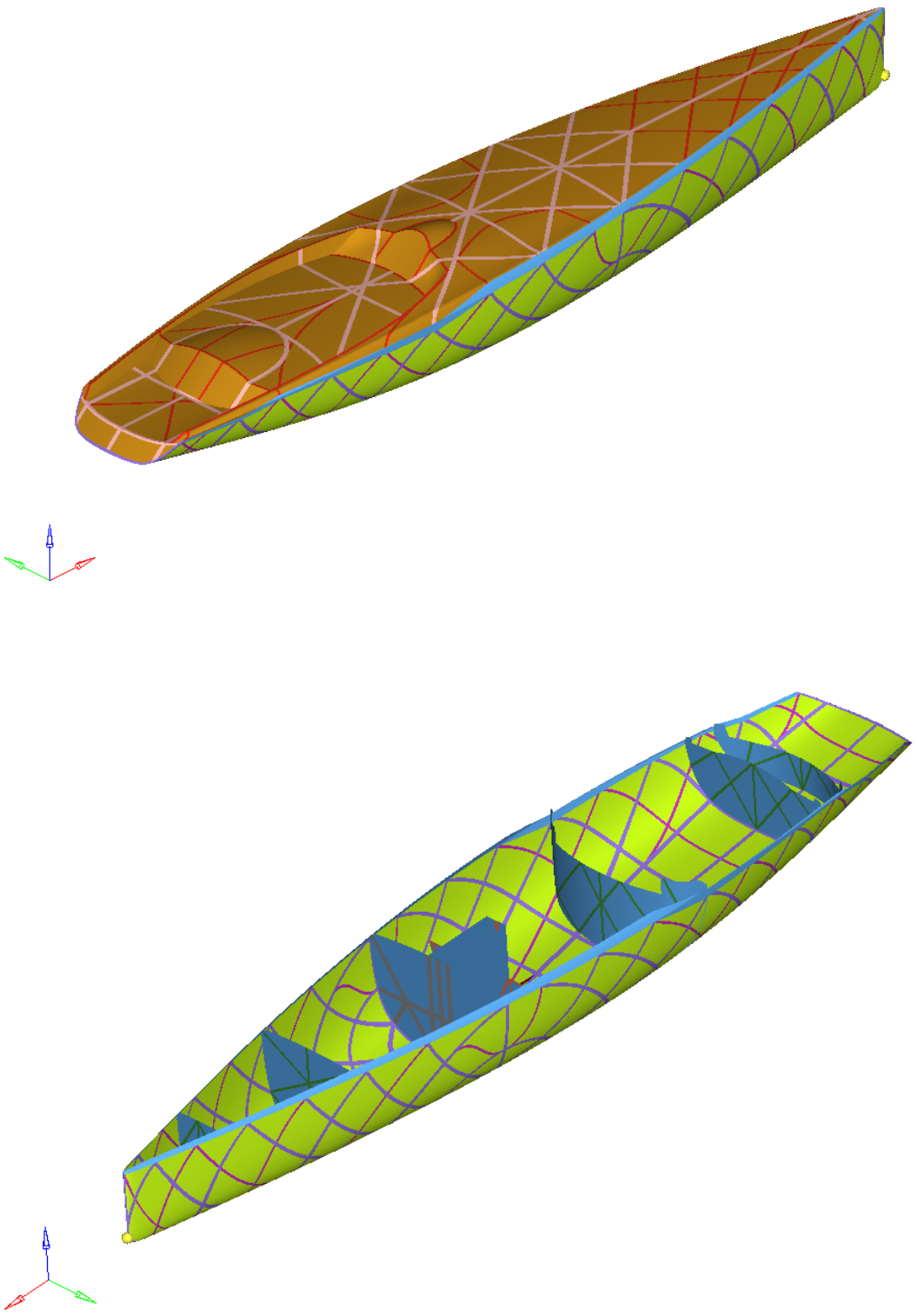

FIGURE 5.1: Surface groups of same structure components

With regard to the implementation of the FE-Model (as described in section 3.7) boundary conditions stay unchanged, except for the RBE3 elements distributing mast and keel loads to the structure. These two RBE3 elements are replaced by RBE2 elements. This is necessary as only composite materials are defined and local reinforcements - like keel box and mast base foundation - not taken into account. Since these foundations are made out of steel, laminated into the hull structure and adequately dimensioned to cope with high local keel and mast loads, they are substituted by RBE2 elements (infinite stiffness).

Shell thickness and isotropic E-Modulus of each surface group are implemented as previously calculated and listed in table 4.2. The Poission's ratio stays unchanged with $\nu = 0.3$.

5.2 1^{st} Simulation - Yacht without Saloon Windows

Results of the first simulation show that global hull bending reaches a total of 181 mm at approximately half length of the hull. Furthermore, structure deformation are noticeable at the main sheet chain plate (1) and at the aft bottom panels (2), as visualized in figure 5.2. The relative displacements add up to 73 mm at the main sheet chain plate (1) and 46 mm at the bottom panels (2). These results indicate that in these areas further refinements are necessary, considering additional reinforcements, other materials or increased structure dimensions.

5.2.1 Results of 1^{st} Simulation - Displacements

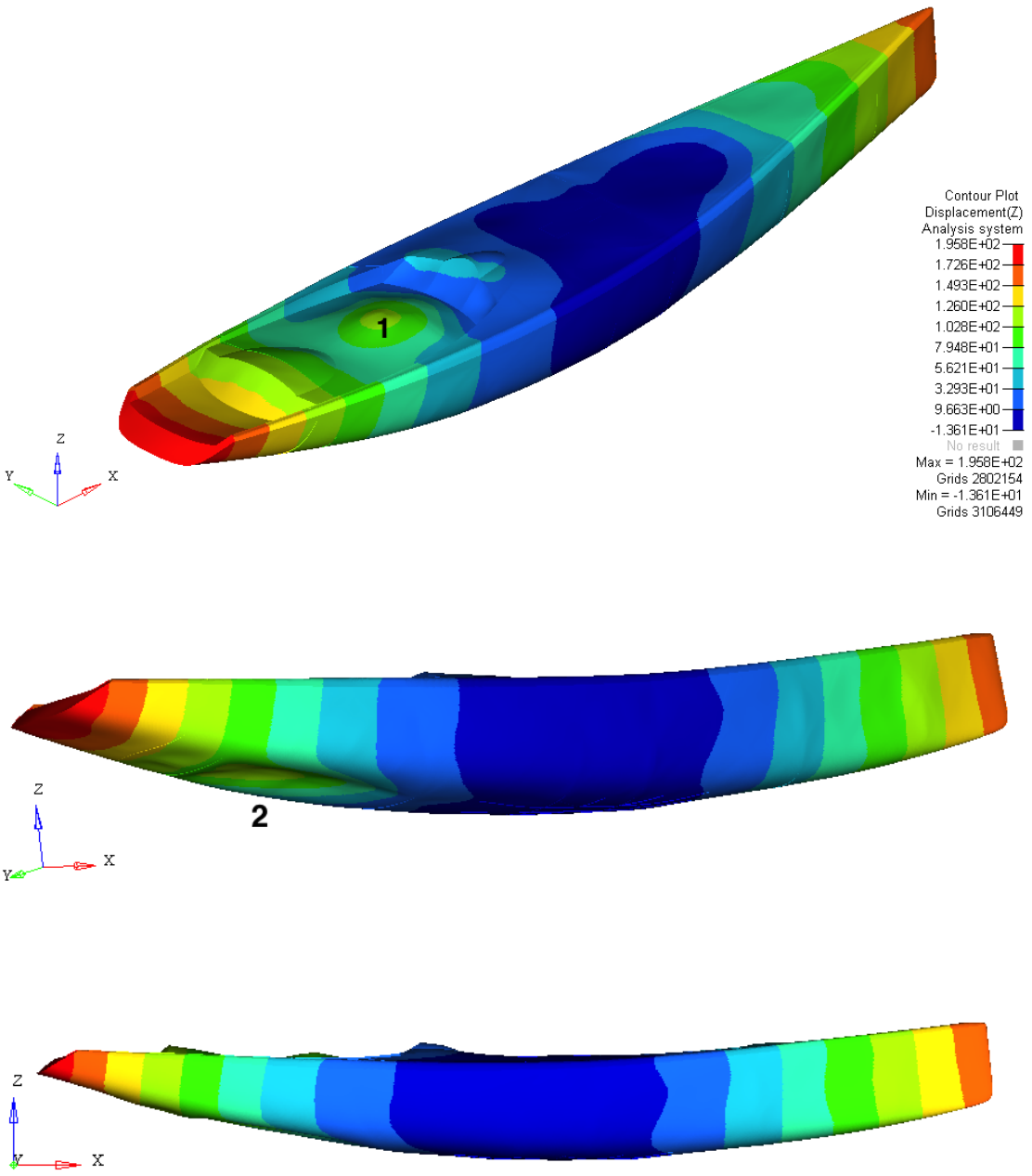

FIGURE 5.2: Displacements of hull structure

Displacements at [mm]		**Global hull bending** [mm]
Bow	166	**181**
Stern	196	

TABLE 5.1: 1^{st} Simulation - global hull bending

5.2.2 Results of 1^{st} Simulation - Stresses

As a final point, the resulting stresses in the hull structure should be discussed. As mentioned in section 4.3, the carbon composite structure with anisotropic material properties is simplified and all sandwich panels and truss members are substituted by homogeneous plates with isotropic E-Moduli. With regard to this simplification (more detailed information can be found in appendix C, section C.4&C.5) the FE-Model exhibits sudden jumps in stiffness at the transition between each truss member and sandwich panel - making an interrupted stress distribution inevitable.

Hence, the following figure can only give a rough idea of the actual stress distribution on the hull structure and has to be viewed critically.

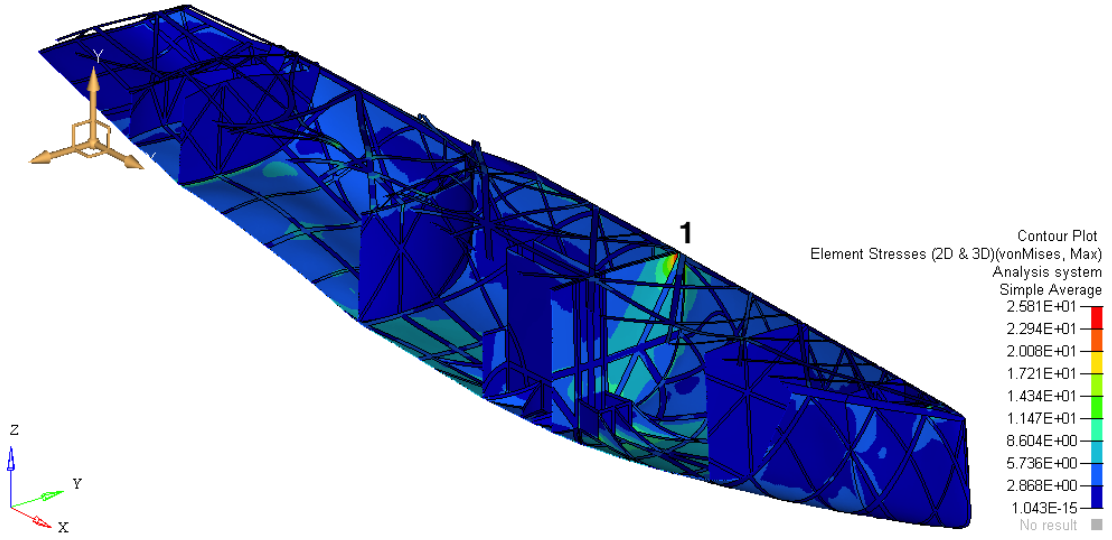

FIGURE 5.3: Von Mises stresses on hull structure

Figure 5.3 displays Von Mises stresses on the hull structure (deck panels transparent and clipping plane). High loads of keel and mast are appropriately distributed into the hull structure without causing any hot spots. On the contrary, the highly loaded windward shroud (1) causes a hot spot in the main bulkhead panel with a Von Mises stress of $\sigma_v = 26N/mm^2$. This value represents the maximum stress in the hull structure.

Although these results must be viewed critically, highly stressed areas of the hull structure are detected for further refinements and optimizations, which are not carried out within the ambit of this thesis.

5.3 2^{nd} Simulation - Yacht with Saloon Windows

To asses the influence of EXO's saloon windows with regard to the overall structure behaviour, a second simulation is conducted. From a conservative point of view it is assumed that these glazed areas are not load carrying and are simply modelled by removing desired deck and hull panels, as visualized in figure 5.4. These cut outs follow the load depending truss members and by doing so they do not interrupt any major load paths. The defined saloon windows on port and starboard side have a glazed area of 63 m^2. The second simulation is performed with the same structure dimensions, material properties and boundary conditions as described in section 5.1; only that RBE3 elements are updated in the areas of the hull structure cut outs.

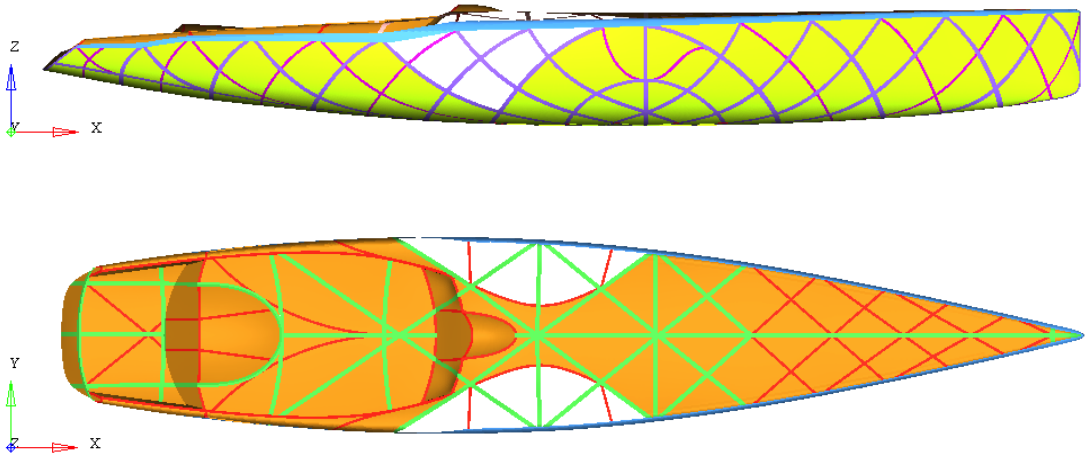

FIGURE 5.4: Conceptual saloon window layout

5.3.1 Results of 2^{nd} Simulation - Displacements

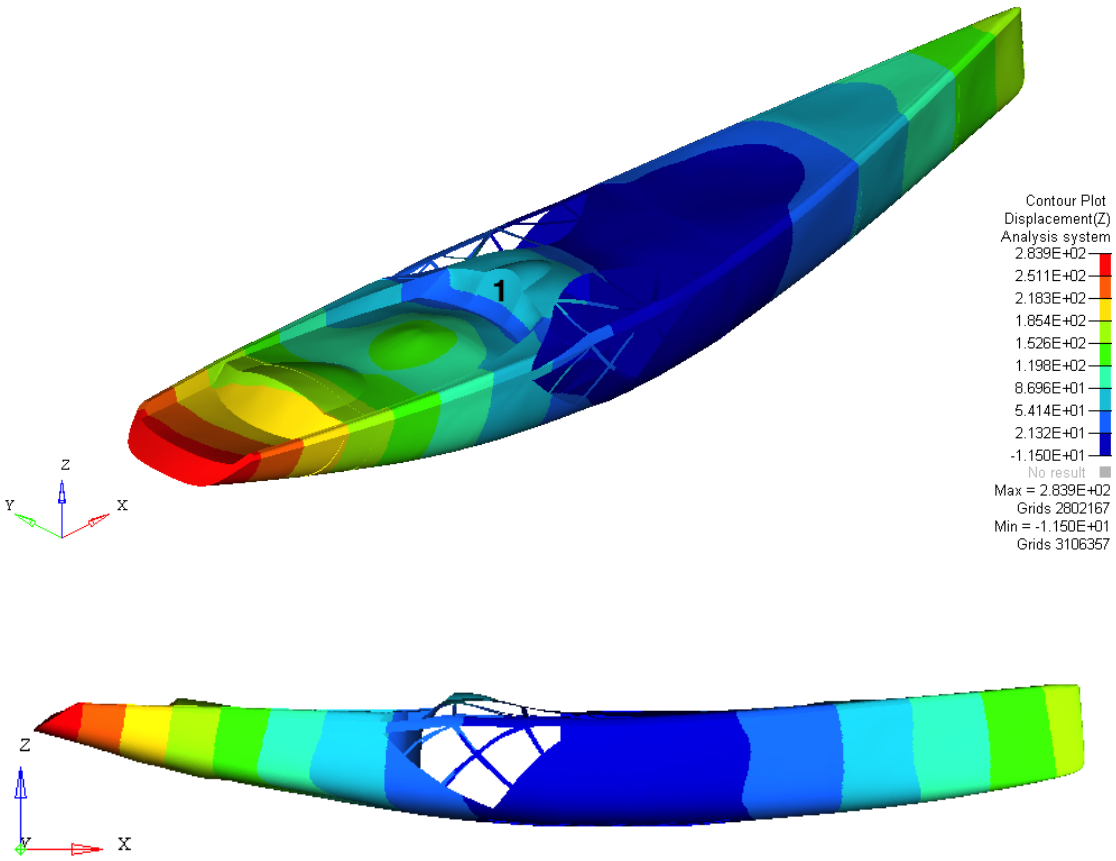

FIGURE 5.5: Displacements of hull structure with saloon windows

Displacement at mm		**Global hull bending** mm
bow	172	**228**
stern	284	

TABLE 5.2: 2^{nd} Simulation - global hull bending

According to figure 5.5 in the second simulation a global hull bending of 228 mm is reached at half length of the hull. Besides the unchanged displacements at the mainsheet chain plate and aft bottom panels, increased structure deformations are noticeable at the main entrance (1).

5.3.2 Results of 2^{nd} Simulation - Stresses

With regard to the first simulation and as shown in figure 5.6 the distribution of Von Mises stresses on the hull structure hardly changed with a maximum of $\sigma_v = 26N/mm^2$ at the windward shroud chain plate (1).

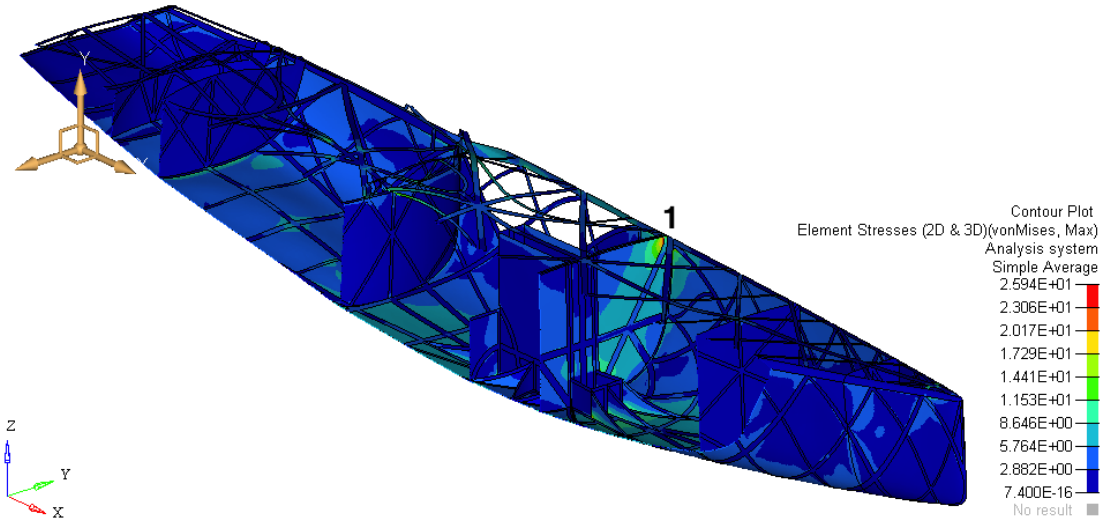

FIGURE 5.6: Von Mises stresses on hull structure with saloon windows

5.4 Plausibility Check of Final FE-Analysis

For a rough validation of obtained FEA-Results, the global hull bending can be estimated with a simplified model related to the beam theory. The yacht's hull is considered as a beam freely supported at both ends with a defined cross section according to the yacht's main section. Subjected to a force derived from the maximal longitudinal bending moment, the beam's deflection can be calculated as presented in appendix C, section C.5.

The results of hand calculation and FE-Simulation (table 5.3) deviate from each other up to 53%, which seems to be a lot at the first sight. However, with regard to the major simplification that the beam's cross section was assumed to be equal along the whole length of the yacht, which is obviously not the case in consideration of the 46m sailing yacht "EXO", the FE-Results are assessed as reasonable.

Comparison	**Global deflection of hull girder**	
	Deflection at L/2	Deviation
Hand calculations Beam theory	118 [mm]	53%
1^{st}FE-Simulation	181 [mm]	

TABLE 5.3: Comparison of beam theory and FE-Results

5.5 Technical Feasibility of Structure Concept

To asses the technical feasibility of this structure concept some reference data is necessary to benchmark the results of the final simulation. In order to reveal and confirm advantages and disadvantages of the developed structure concept, data from a conventional structure layout for the 46m sailing yacht "EXO" has to be available. Then a third finite element simulation could be conducted where the conventionally constructed hull (carbon-composite construction, but without an interwoven network of load carrying and stiffness increasing truss members) is exposed to global loads derived from the same load case. Due to the absence of this information, the present concept can only be assessed by validating the results with regard to own defined design requirements. These design constraints were defined to come up with preliminary dimensions of structure components, as presented in table 4.1 and in appendix C. From a designer's perspective it is crucial to ensure that sailing yachts are adequately rigid, since excessive hull bending leads to loss in sailing performance and distortion of the designed hull lines. Thus, apart from local reinforcements due to load/stress concentrations, the design of a sailing yacht is rather driven by stiffness than strength [3].

Since the Design Suite is developed to implement a global FE-Model which reflects the overall structure behaviour close to reality, the maximum allowable hull deflection is considered as a benchmark value. Due to the fact that the carbon composite structure is simplified with an isotropic material, the stress distribution is viewed critically and thus of minor importance for the evaluation of the concept.

The yacht adequately dimensioned with regard to a maximum allowable hull deflection of L/200 = 230 mm reaches in the first simulation a maximum of 181 mm. It should be highlighted that the maximum stress of $\sigma_v = 26\ N/mm^2$ induced by tension load of the shroud is far below the design limit of $\sigma_{dt} = 122\ N/mm^2$. In general it can be said, that the developed concept presents - in terms of design constraints - a stiff hull structure where truss members following the major load paths distribute the high rig, mast and keel loads smoothly into the hull.

Furthermore, the second simulation shows that the objective to develop a hull structure with load carrying and stiffness increasing truss members is fulfilled. In the second simulation several hull and deck panels were removed; these cutouts represent non-load carrying saloon windows. As a result, hull bending reaches a maximum of 228 mm. Although an area of 63 square meters is removed at

half length of the hull and structure dimensions stay unchanged (no additional reinforcements are added), the overall hull bends only 26% more than in the first simulations. This result is achieved due to the fact that the window layout does not interrupt any major load paths of the structure. This is in case of this concept crucial, since this truss-structure network has the responsibility to carry the global loads acting on the yacht hull and the panels in-between are dimensioned to withstand a hydrostatic pressures at the most.

It should be mentioned that in the ambit of this thesis, the hull structure is dimensioned on a conceptual level where superior carbon-composites are simplified as isotropic materials. If this structure concept were to be dimensioned from carbon composites without any abstractions of material properties in the FE-Model, an even better overall structure performance could be expected.

In view of manufacturing, this concept study presents a rather labour intensive carbon composite structure due to the complex interwoven network of truss members. Apart from that, the load depending structure layout inspired by natures principles of design and its beautiful organic forms is assessed as a technical feasible concept according to the results of the present thesis.

6 Conclusion

With regard to the three questions stated in chapter 1, the following answers can be given:

First, the results clearly show, that it is possible to develop a hull structure inspired by nature strong enough to cope with global loads of a 46m sailing yacht. This is due to the fact that similar to any lightweight design found in nature, maximal strength with a minimum amount of material was claimed regarding the design process of the hull structure. This already answers the last question, how nature's functionality and efficiency can serve as a source of inspiration. Like in nature material is only applied where the structure demands it, leading to beautiful lightweight designs. The load carrying and stiffness increasing truss members of the hull follow the most advantageous load paths derived from the performed topology optimizations. This load dependent layout can be seen as a guideline where most of the material should be added to the hull structure. After refining and abstracting the structure layout, it is only a matter of adequate dimensions to ensure that the yacht is able to cope with global loads in regard to predefined design constraints.

In view of the second question, what such a nature inspired hull structure might look like, the structure concept of the yacht's hull is visualized in figure 4.11. The hull structure presents twisting and turning curves radiating from the load center around the mast and keel area towards the rig attachment points at the bow and stern.

The evaluation of the concept shows that the developed hull structure with load carrying truss members resembling organic forms is able to cope with the global loads acting on the 46 m sailing yacht "EXO". In addition, this master thesis presents a feasible new approach to integrate huge glass windows into a yacht structure.

A Pontoon in Triangular Wave

A.1 Load Calculations for FE-Models A, B and C

All load calculations are performed in an Excel-Spreadsheet *"Quasi-static load case"/Pontoon* (on CD-ROM). The main particulars of the pontoon and all necessary data for following load calculations are listed in the table A.1.

Length over all	L_{oa}	42700	[mm]
Breadth	B	8800	[mm]
Depth	D	5000	[mm]
Draft at wave crest	T_{Wc}	3000	[mm]
Skin thickness	t_s	250	[mm]
Displacement	Δ	578	[t]
Volume	∇	564	$[m^3]$
Density of sea water	ρ_{sea}	1025	$[kg/m^3]$
Gravity	g	9.81	$[m/s^2]$

TABLE A.1: Main particulars of pontoon

On the following pages the different applied loads on FE-Models A,B and C are listed and briefly explained.

A 3D-model of the pontoon in *Rhinoceros* with the main particulars as stated in table A.1 serves as a basis for the load calculations.

A.1.1 Calculation of Hydrostatic Pressures for FE-Model A

In figure A.1 the membrane elements of the 3D-Model in *Rhinoceros* are visualized, representing the wetted hull area in a triangle wave.

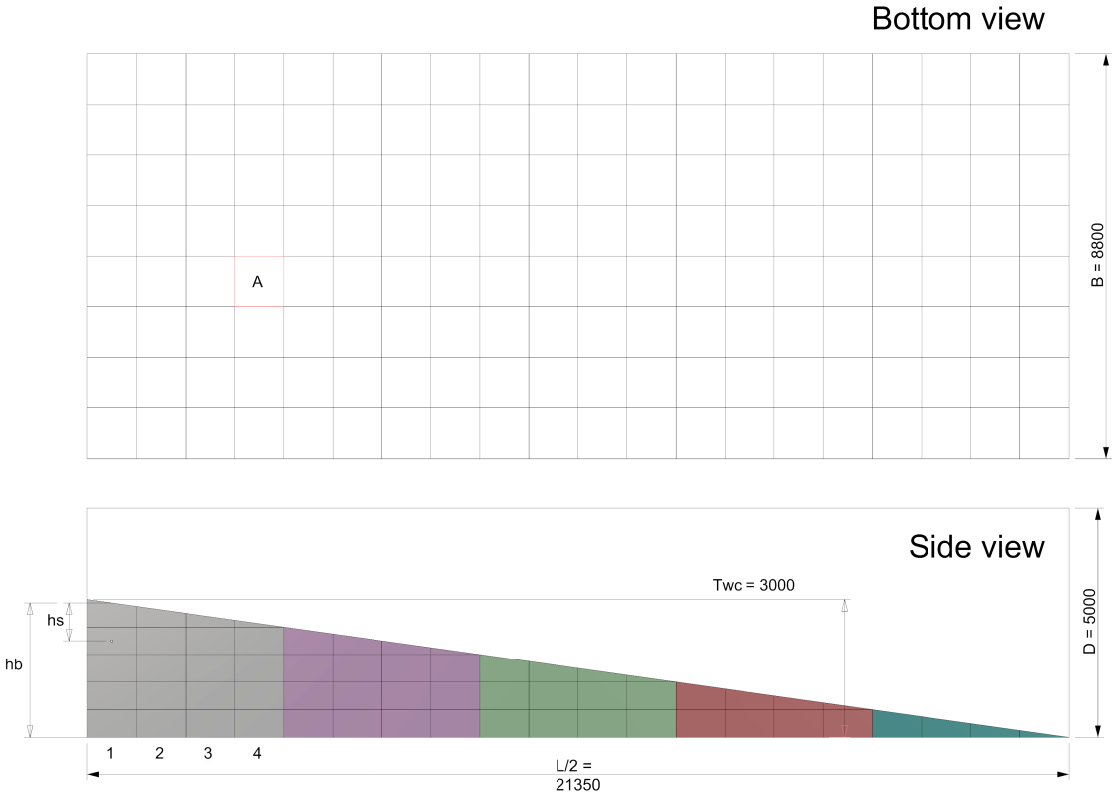

FIGURE A.1: Membrane elements representing wetted hull area in triangle wave

The hydrostatic pressures of the side elements in table A.2 are calculated with the following equation:

$$P_s = \rho_{sea} \cdot g \cdot h_s \tag{A.1}$$

The distance h_s is measured from the water surface to the center of each side element, as shown in figure A.1.

The listed hydrostatic pressures of the side elements in table A.2 are the values for the grey columns in figure A.1. Due to the isogrid and the triangular shaped wave these hydrostatic pressures are also valid for the side elements in the purple, green, red and blue highlighted columns. As an example, the hydrostatic pressures in the first row of table A.2 also apply to the elements of the blue columns in figure A.1.

1		2		3		4	
hs $[mm]$	Ps $[N/mm^2]$	hs [mm]	Ps $[N/mm^2]$	hs [mm]	Ps $[N/mm^2]$	hs [mm]	Ps $[N/mm^2]$
264	0.0027	190	0.0019	117	0.0012	50	0.0005
825	0.0083	675	0.0068	525	0.0053	375	0.0038
1425	0.0143	1275	0.0128	1125	0.0113	975	0.0098
2025	0.0204	1875	0.0189	1725	0.0173	1575	0.0158
2625	0.0264	2475	0.0249	2325	0.0234	2175	0.0219

TABLE A.2: Hydrostatic pressure of side elements

The hydrostatic pressures of the bottom elements in table A.3 are calculated with the following equation:

$$P_{b_{(x)}} = \rho_{sea} \cdot g \cdot h_{b_{(x)}} \tag{A.2}$$

The distance h_b, as shown in figure A.1, is measured from the water surface to each bottom element at the stated x- position.

In case of the pontoon structure only hydrostatic pressures of the bottom elements are responsible for the received buoyancy force. Since 8 bottom elements over the whole breadth B have the same hydrostatic pressure, the following equation gives the buoyancy force of each bottom stripe:

$$F_{b_{(x)}} = A_{Elm} \cdot 8 \cdot P_{b_{(x)}} \tag{A.3}$$

The summation of all forces is equal to the buoyancy force of half the pontoon:

$$\Delta = \frac{2 \cdot \Sigma F_{b_{(x)}}}{g} = \frac{2 \cdot 2\,833\,871\,\mathrm{N}}{9.81\,\mathrm{m/s^2}} = 578\,\mathrm{t} \tag{A.4}$$

According to equation above the hydrostatic pressures applied to FE-Model A are correct.

x-pos. [mm]	$h_{b_{(x)}}$ [mm]	$P_{b_{(x)}}$ [N/mm2]	Aelm [N/mm2]	$F_{b_{(x)}}$ [N]
21350	2925	0.0294	1174250	276293
20283	2775	0.0279	1174250	262124
19215	2625	0.0264	1174250	247955
18148	2475	0.0249	1174250	233786
17080	2325	0.0234	1174250	219617
16013	2175	0.0219	1174250	205448
14945	2025	0.0204	1174250	191280
13878	1875	0.0189	1174250	177111
12810	1725	0.0173	1174250	162942
11743	1575	0.0158	1174250	148773
10675	1425	0.0143	1174250	134604
9608	1275	0.0128	1174250	120435
8540	1125	0.0113	1174250	106267
7473	975	0.0098	1174250	92098
6405	825	0.0083	1174250	77929
5338	675	0.0068	1174250	63760
4270	525	0.0053	1174250	49591
3203	375	0.0038	1174250	35422
2135	225	0.0023	1174250	21253
1068	76	0.0008	1174250	7184
			$\Sigma\ F_{b_{(x)}}$	**2833871**

TABLE A.3: Hydrostatic pressures of bottom elements

A.1.2 Calculation of Material Density for FE-Model A

To attain a state of static equilibrium for a floating object (Archimedes' principle) the buoyancy force must be equal to the weight of the water displaced (=weight of pontoon), as expressed in equation (A.5):

$$\text{Buoyancy force} \quad (F_b) \quad + \quad \text{Weight force} \quad (F_g) = 0 \tag{A.5}$$

$$F_{(g)} = \nabla \cdot g \cdot \rho_{sea} = \Delta \cdot g \tag{A.6}$$

To comply with the formulas above the volume of all solid elements in the FE-Model A multiplied by their density must be equal to the displacement of the pontoon. Hence, the material density is calculated as stated in equation (A.8).

$$\Delta = \nabla \cdot \rho_{sea} = V_{Mat} \cdot \rho_{Mat} \tag{A.7}$$

$$\rho_{Mat} = \frac{\Delta}{V_{Mat}} \tag{A.8}$$

The material volume V_{Mat} is calculated with equation (A.9). To maintain a uniform weight distribution the bulkheads on both ends of the pontoon are neglected.

$$V_{Mat} = L \cdot B \cdot D - (L \cdot (B - 2 \cdot t_s) \cdot (D - 2 \cdot t_s)) \tag{A.9}$$

V_{Mat} $[mm^3]$	Δ [t]	ρ_{Mat} $[t/mm^3]$
2.84E+11	578	2.035E-09

TABLE A.4: Material density of solid elements

A.1.3 Calculation of Section Loads for FE-Model B and C

The pontoon is divided into 12 sections along its whole length. Due to the symmetry condition sections listed in table 3.6 with the master points 0, 5a, 5b, and 10 are half the size of sections 1,2,3,4,6,7,8 and 9. Thus, the pontoon is divided in 10 equal sections. The transverse symmetry plane lies between sections 5a and 5b. As only half of the pontoon is modelled in the finite element space only the loads of master points 0-5a are applied. The volumes V of each section are derived from the 3D-Model in *Rhinoceros*.

The buoyancy force $Fb_{(s)}$ of each section is calculated by the following equation:

$$Fb_{(s)} = -V \cdot g \cdot \rho_{sea} \tag{A.10}$$

Since the equation of Archimedes (equation (A.5)) has to be fulfilled, the weight force $Fg_{(s)}$ of each full section is calculated by the following equation:

$$Fg_{(s)} = \frac{\Sigma Fb_{(s)}}{10} \tag{A.11}$$

For each half section equation (A.12) needs to be applied:

$$Fg_{(s)} = \frac{\Sigma Fb_{(s)}/10}{2} \tag{A.12}$$

The resulting section loads are the addition of weight and buoyancy forces:

$$Fz_{(s)} = Fb_{(s)} + Fg_{(s)} \tag{A.13}$$

As displayed in table A.2 the summation of all section loads $Fz_{(s)}$ is zero since the equation of Archimedes (equation (A.5)) is fulfilled.

Master - points	**x-pos.** [mm]	**V** [m3]	$Fb_{(s)}$ [N]	$Fg_{(s)}$ [N]	$Fz_{(s)}$ [N]
0	0	-2.82	-28348	283387	255040
1	4270	-22.55	-226719	566774	340055
2	8540	-45.09	-453425	566774	113349
3	12810	-67.64	-680121	566774	-113346
4	17080	-90.18	-906826	566774	-340052
5a	21350	-53.55	-538432	283387	-255045
5b	21350	-53.55	-538432	283387	-255045
6	25620	-90.18	-906826	566774	-340052
7	29890	-67.64	-680121	566774	-113346
8	34160	-45.09	-453425	566774	113349
9	38430	-22.55	-226719	566774	340055
10	42700	-2.82	-28348	283387	255040
Summation:		**-564**	**-5667742**	**5667742**	**0**

Table A.5: Section loads for FE-Model B & C

A.2 Validation of FE-Model A

To validate the results of the finite element simulation in section 3.4 principles of the beam theory are applied to estimate the global deflection of the pontoon in a triangular wave. Since the pontoon is exposed to loads derived from its own weight and its buoyancy distribution two load cases are superimposed: one with a uniform and another with a triangular load distribution. The pontoon structure itself is approximated as a beam, simply supported on both ends.

Table A.6 shows all necessary data for the following manual calculations:

Length	L	42700	[mm]
Breadth	B	8800	[mm]
Depth	D	5000	[mm]
Maximum wave height	H_W	3000	[mm]
Skin thickness	t_s	250	[mm]
Young's modulus	E	10000	$[N/mm^2]$
Displacement	Δ	578	[t]
Density of sea water	ρ_{sea}	1025	$[kg/m^3]$
Gravity	g	9.81	$[m/s^2]$

TABLE A.6: Main particulars of pontoon

The area moment of inertia of the pontoon's cross section about the neutral axis is calculated by equation (A.14). This formula is valid for hollow rectangular cross sections with a specific skin/wall thickness.

$$I_{y_0} = \frac{B \cdot D^3}{12} - \frac{(B - 2 \cdot t_s) \cdot (D - 2 \cdot t_s)^3}{12} \tag{A.14}$$

$$I_{y_0} = \frac{8800\,\text{mm} \cdot 5000\,\text{mm}^3}{12} - \frac{(8800\,\text{mm} - 2 \cdot 250\,\text{mm}) \cdot (5000\,\text{mm} - 2 \cdot 250\,\text{mm})^3}{12}$$

$$= 2.864 \times 10^{13}\,\text{mm}^4 \tag{A.15}$$

A.2.1 Load Case: Weight Force

Equation (A.16) [14] defines the maximum deflection of a beam under a uniform load distribution as shown in figure A.2.

$$w_{w_{max}} = \frac{5 \cdot q_w \cdot L^4}{384 \cdot E \cdot I_{y_0}} \quad \text{at} \quad \frac{L}{2} \tag{A.16}$$

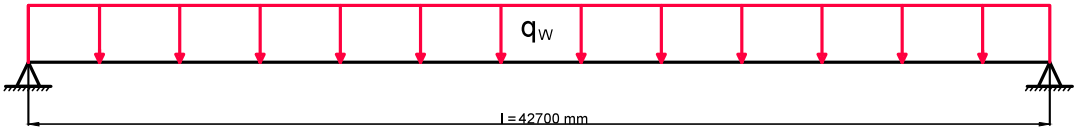

FIGURE A.2: Load case: weight force

A homogeneous weight distribution over the pontoon deck is assumed:

$$q_w = P_w \cdot B \tag{A.17}$$

$$P_w = \frac{F_w}{A} = \frac{\Delta \cdot g}{L \cdot B} \tag{A.18}$$

$$q_w = \frac{\Delta \cdot g}{L} = \frac{578\,000\,\mathrm{kg} \cdot 9.81\,\mathrm{N/s^2}}{42\,700\,\mathrm{mm}} = 133\,\mathrm{N/mm} \tag{A.19}$$

$$w_{w_{max}} = \frac{5 \cdot 133\,\mathrm{N/mm} \cdot (42\,700\,\mathrm{mm})^4}{384 \cdot 10\,000\,\mathrm{N/mm^2} \cdot 2.864 \times 10^{13}\,\mathrm{mm^4}} = 20\,\mathrm{mm} \tag{A.20}$$

A.2.2 Load Case: Buoyancy Force

The maximum deflection of a beam with a triangular load distribution, as shown in figure A.3, can be calculated by equation (A.21) [14].

$$w_{b_{max}} = -\frac{q_b \cdot L^4}{120 \cdot E \cdot I_{y_0}} \quad \text{at} \quad \frac{L}{2} \tag{A.21}$$

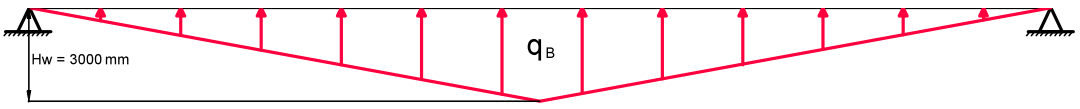

FIGURE A.3: Load case: buoyancy force

For calculating the line load q_b the load peak has to be taken into account [14]. Thus, the hydrostatic pressure P_h at the wave crest is determined.

$$q_b = P_h \cdot B \tag{A.22}$$

$$P_h = \rho \cdot g \cdot H_w \tag{A.23}$$

$$P_h = 1025\,\mathrm{kg/m3} \cdot 9.81\,\mathrm{m/s2} \cdot 3\,\mathrm{m} = 30\,166\,\mathrm{N/m^2} \tag{A.24}$$

$$q_b = 0.0302\,\mathrm{N/mm^2} \cdot 8800\,\mathrm{mm} = 265\,\mathrm{N/mm} \tag{A.25}$$

$$w_{w_{max}} = -\frac{265\,\mathrm{N/mm} \cdot (42\,700\,\mathrm{mm})^4}{120 \cdot 10\,000\,\mathrm{N/mm^2} \cdot 2.864 \times 10^{13}\,\mathrm{mm^4}} = -26\,\mathrm{mm} \tag{A.26}$$

A.2.3 Superposition of Load Cases

The global deflection of the pontoon in a triangle wave derives from superimposing both load cases shown in figures A.2 & A.3 and by adding up results of equations (A.16) & (A.21):

$$w_{max} = w_{w_{max}} + w_{b_{max}} \tag{A.27}$$

$$w_{max} = 20\,\mathrm{mm} + (-26\,\mathrm{mm}) = -6\,\mathrm{mm} \tag{A.28}$$

B Quasi-Static Load Case - 46m Sailing Yacht

B.1 Main Particulars

The main particulars of the 46m sailing yacht "EXO" are listed in the table below and are fundamental for the following load calculations. In figure B.1 the dimensions are partially visualized.

Length over all	L_{oa}	=	46000	[mm]
Length waterline	L_{Wl}	=	42725	[mm]
Draft of canoe body	T_c	=	1600	[mm]
Draft max	T_{max}	=	6500	[mm]
Breadth max	B_{max}	=	8880	[mm]
Depth	D	=	4740	[mm]
Displacement	Δ	=	250000	[kg]
	∇	=	243.902	$[m^3]$
Longitudinal center of gravity	LCG	=	23176	[mm]
Vertical center of gravity	VCG	=	0	[mm]
Displacement Design	Δ_D	=	240000	[kg]
Ballast displacement ratio	G_K/Δ_D	=	21%	
Keel weight	G_K	=	50400	[kg]
LCG of keel	LCG_K	=	21261	[mm]
VCG of keel	VCG_K	=	-5158	[mm]
Light ship displacement	LDT	=	199600	[kg]
	VCG_{LDT}	=	1302	[mm]
Density of sea water	$\rho = \rho_{sea}$	=	1025	$[kg/m^3]$
Gravity	g	=	9.81	$[m/s^2]$

TABLE B.1: Main particulars (HASC) of 46m sailing yacht "EXO"

Because the load calculations should reflect as much as possible a realistic sailing condition, all values in table B.1 are according to the "*Half-Average-Sailing Condition*" (HASC = tanks 50% filled) with a displacement of $\Delta = 250$ tons, slightly bigger than the design displacement of $\Delta_D = 240$ tons.

The yacht's actual vertical center of gravity VCG is slightly above the waterline, to simplify calculations it is aligned with the height of the waterline VCG=0 in this load model, as shown in figure B.1. This simplification certainly leads to a slightly greater righting moment, but is reasonable from a conservative point of view and in terms of a worst-case loading condition (section 2.1).

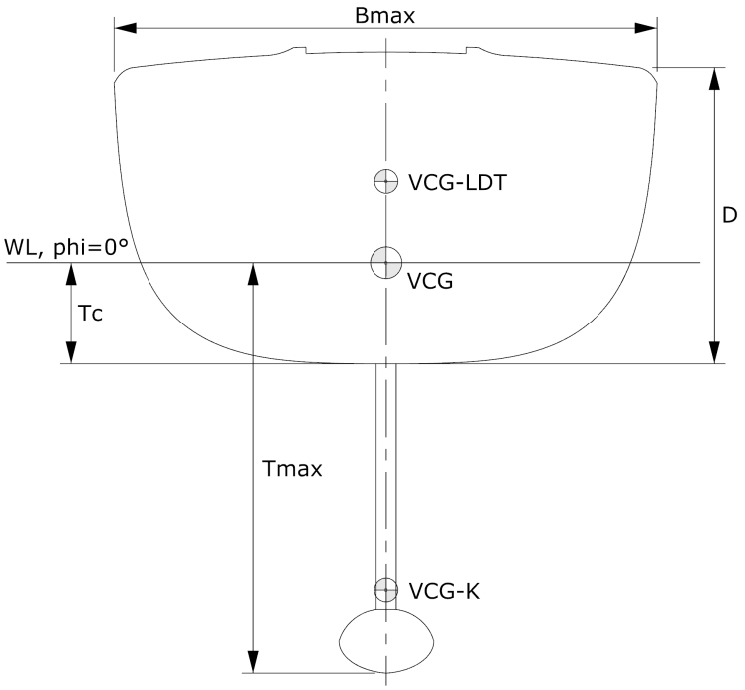

FIGURE B.1: Vertical centers of gravity

The bulb keel's vertical center of gravity is located at VCG_K = -5158 mm below the waterline with a weight equal to 21% of the design displacement Δ_D. Thus, the vertical center of gravity of the light ship displacement (= Hull without bulb keel) VCG_{LDT}, as stated in table B.6, can be calculated by equilibrium of moments:

$$VCG_{LDT} = \frac{\Delta \cdot VCG - G_K \cdot VCG_K}{LDT} = 1302\,[\text{mm}] \tag{B.1}$$

B.2 Hydrostatic Data

According to the load case description in section 3.2.1 the hydrostatic data of the yacht is evaluated for a sagging condition in a sinusoidal wave with a wave length λ equal to the yacht's waterline length L_{Wl} and a maximum wave height of $H_{1/100}$=3.427 [m]. In this quasi-static sailing condition the yacht is due to its sail forces heeled up to $\phi = 30$ degrees and a trim angle of zero is assumed.

Displacement	Δ	=	250000	[kg]
Longitudinal CoG	LCG	=	23.176	[m]
Wave length	λ	=	42.725	[m]
Significant wave height	Hs	=	2.052	[m]
Maximum wave height	$H_{1/100}$	=	3.427	[m]
Heeling	ϕ	=	30	[°]
Trim	β	=	0	[°]

TABLE B.2: Input data for hydrostatic calculations

Since this load case should reflect a sailing condition as close as possible to reality, the maximum wave height $H_{1/100}$, as stated in table B.2, is calculated by the following method based on actual physics of irregular waves. This method takes a maximum wave steepness (height to period ratio) for irregular seas (Jonswap spectrum) into account, because steeper waves immediately break and therefore fade away [13]. The wave breaking limit is expressed in the relation below:

$$\frac{H_s}{{T_p}^2} < 0.075 \tag{B.2}$$

where the wave's peak period T_p is determined by equation (B.3) [13]:

$$T_p = \sqrt{\frac{2\pi\lambda}{g}} \quad [s] \tag{B.3}$$

Thus, a given wave length λ in meters leads to significant wave height H_s (in meters) and to an approximated maximum attainable wave height $H_{1/100}$ by 1.67 times H_s before wave breaking occurs [15].

B.2.1 Hydrostatic Data - CatiaV5 Model

With regard to the design tool hydrostatic data and buoyancy distribution is evaluated at 20 sections. In the CatiaV5 Export-file below each section's buoyancy and its corresponding center of buoyancy in longitudinal, transverse and vertical position is listed.

Produkt : MultiSelectio n
Datum : Montag, 13 O ktober 2014 10:42:02
Autor : dleidenf
"Only main bodies" opti on : Unchecked

Component	Sub-Component	Volumen[m3]	Gx[mm]	Gy[mm]	Gz[mm]
1		3,3634	-1489,541	-21,948	761,086
2		9,6010	-3578,17	-73,549	714,538
3		15,6300	-5816,372	-158,185	586,169
4		19,8990	-8078,653	-283,714	381,308
5		21,3210	-10348,556	-467,716	122,490
6		19,6910	-12620,935	-733,541	-154,505
7		15,8240	-14895,119	-1096,761	-408,387
8		11,2550	-17175,125	-1536,006	-609,060
9		7,44759	-19469,351	-1973,622	-752,378
10		5,0560	-21786,939	-2328,526	-837,548
11		4,0610	-24133,506	-2565,923	-850,303
12		4,3230	-26488,751	-2668,868	-780,790
13		5,82879	-28820,569	-2633,906	-628,990
14		8,6150	-31125,86	-2475,444	-402,578
15		12,5310	-33416,521	-2225,199	-112,917
16		17,0030	-35699,835	-1931,742	227,525
17		20,3920	-37969,003	-1593,061	542,501
18		19,5100	-40193,291	-1158,578	716,033
19		14,33766	-42497,49	-742,995	750,506
20		8,21300	-44577,457	-449,866	904,025
MultiSelection		243,902	-23175,657	-1161,243	140,60

B.3 Wave Load Calculations

All global load calculations are performed in an Excel-Spreadsheet *"Quasi-static load case" - Yacht/Wave loads* (on CD-ROM). The listed tables in section B.3 are exported from this spreadsheet and brief explanations were added. All calculations and results are according to the coordinate system presented below:

Description	Axis	Positive direction	Origin
Longitudinal	x	Aft	Frame 0 (Bow nose)
Transverse	y	Starboard	Centerplane
Vertical	z	Up	Waterline $\phi = 0°$ (VCG)

TABLE B.3: Coordinate system for calculations and results

According to the description of the design tool in section 3 the hull is divided into 20 equal sections along its length and thus global loads acting on the hull structure are calculated at 20 master points, each defining the longitudinal center of each section. All master points are in transverse and vertical alignment with the origin and thus with the vertical center of gravity of the yacht VCG. In all following tables the longitudinal center (x-position) of each master point is listed in the first column C1.

An exception is the 9a labelled row, since it is not part of the 20 hull sections but represents the master point of the bulb keel complying with its longitudinal center of gravity LCG_K as stated in table B.1. Yet, this master point has its vertical alignment with the origin. Hence, all calculations in row 9a are only referring to loads derived from the bulb keel!

Furthermore it is very important to note that for an easier data exchange and a reasonable FE-Model setup the yacht, although 30 degrees heeled, is modelled throughout the whole project in upright position with a 30 degrees rotated water surface. Hence, all following load calculations are according to the previously described model orientation, so that horizontal and vertical force components of weight and buoyancy are in alignment with transverse and vertical directions of the coordinate system as stated in table B.3 and visualized in figure B.2.

B.3.1 Calculations of Weight Forces

For the given weight distribution of the yacht, listed in column C2, the heel angle dependent transverse and vertical weight force components are calculated for each section in column C4 and C5. The whole weight of the bulb keel is assigned to master point 9a and its force components calculated respectively. This highly concentrated load is later distributed to a designated area in the FE-Model, where the keel is actually attached to the hull (section 3.7). In column C6 and C7 each section's center of gravity is listed; all in transverse and vertical alignment with the origin. An exception is row 9a complying with the vertical center of gravity of the bulb keel far below the waterline.

Force components and their centers of gravity are illustrated in the schematic figure B.2.

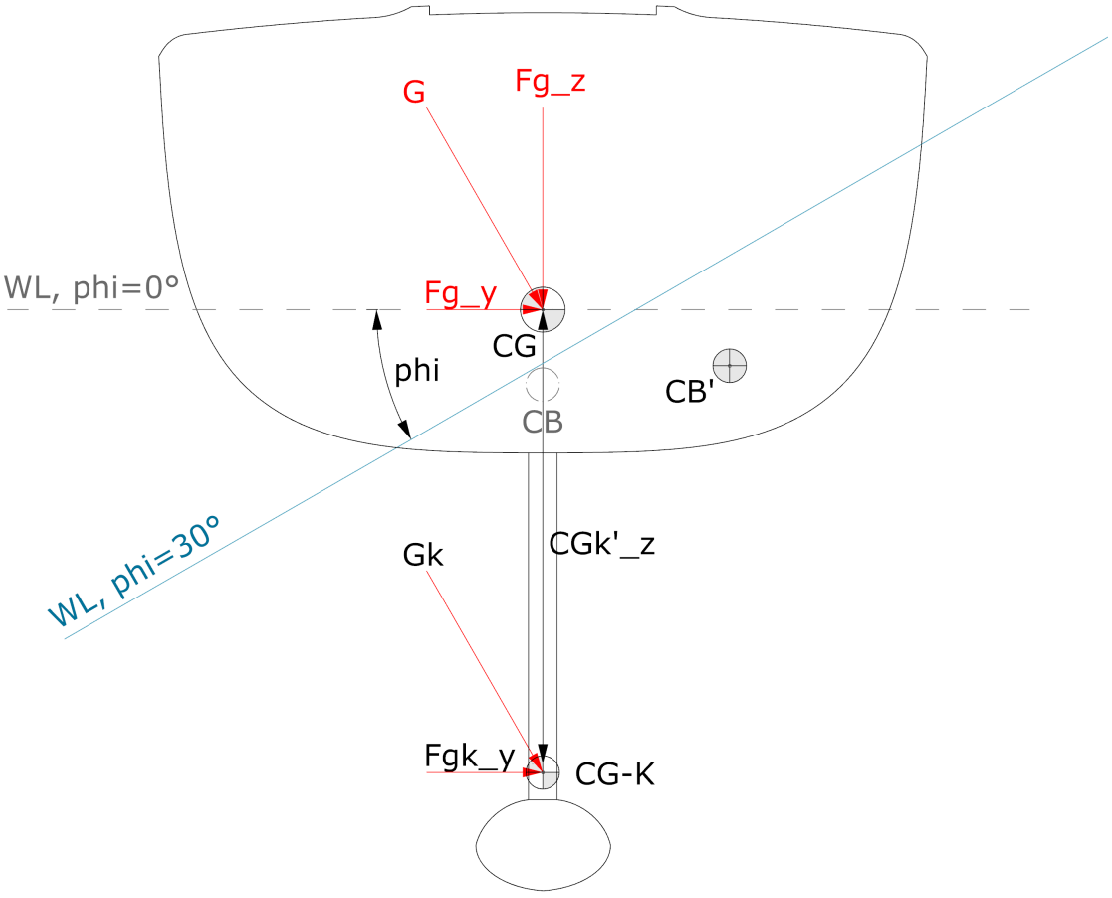

FIGURE B.2: Diagram of weight force components

		Weight					
Column	**C1**	**C2**	**C3**	**C4**	**C5**	**C6**	**C7**
Equation			$C1 \cdot C2 \cdot g$	$C2 \cdot \sin(\phi) \cdot g$	$C2 \cdot \cos(\phi) \cdot g$		
Section	**x-pos.** [mm]	$\mathbf{G}_{(x)}$ [kg]	$\mathbf{My}_{(x)}$ [Nmm]	$\mathbf{Fg\_y}_{(x)}$ [N]	$\mathbf{Fg\_z}_{(x)}$ [N]	$\mathbf{CG\_y}_{(x)}$ [mm]	$\mathbf{CG\_z}_{(x)}$ [mm]
1	1150	5719	6.45E+07	28051	48586	0	0
2	3450	6775	2.29E+08	33232	57560	0	0
3	5750	7740	4.37E+08	37967	65760	0	0
4	8050	8622	6.81E+08	42292	73253	0	0
5	10350	9421	9.57E+08	46210	80038	0	0
6	12650	10120	1.26E+09	49638	85976	0	0
7	14950	10719	1.57E+09	52576	91064	0	0
8	17250	11234	1.90E+09	55105	95444	0	0
9	19550	11667	2.24E+09	57225	99117	0	0
9a	21261	50400	1.05E+10	247212	428184	0	-5158
10	21850	12016	2.58E+09	58938	102083	0	0
11	24150	12249	2.90E+09	60080	104062	0	0
12	26450	12398	3.22E+09	60813	105331	0	0
13	28750	12464	3.52E+09	61137	105892	0	0
14	31050	12373	3.77E+09	60692	105121	0	0
15	33350	12013	3.93E+09	58923	102057	0	0
16	35650	11324	3.96E+09	55544	96205	0	0
17	37950	10366	3.86E+09	50845	88066	0	0
18	40250	9108	3.60E+09	44677	77382	0	0
19	42550	7552	3.15E+09	37043	64161	0	0
20	44850	5719	2.52E+09	28051	48586	0	0
Summation		**250000**	**5.684E+10**	**1226250**	**2123927**		

TABLE B.4: Weight force calculations

With regard to to the load case the sailing yacht should have zero trim. Hence, the longitudinal center of buoyancy and gravity must be in alignment. Through an equilibrium of moments the longitudinal center of gravity LCG can be determined:

$$LCG = \frac{\Sigma(G_{(x)} \cdot x)}{\Delta} = \frac{\Sigma My_{(x)}}{\Sigma G_{(x)}} \tag{B.4}$$

$$LCG = \frac{5.684 \times 10^{10}\,\mathrm{Nmm}}{250\,000\,\mathrm{kg} \cdot 9.81\,\mathrm{m/s^2}} = 23\,176\,\mathrm{mm} \tag{B.5}$$

B.3.2 Calculations of Buoyancy Forces

The hydrostatic data of the sailing yacht attached in section B.2.1 in a sinusoidal wave at a heeling angle of $\phi = 30$ degrees is linked to the Excel-spreadsheet. In column C8 of table B.5 the previously determined buoyancy distribution is linked. The heel angle dependent transverse and vertical buoyancy force components are calculated for each section in column C10 and C11. Due to heeling and hull shape characteristics the buoyancy center of the hull moves outward and generates a transverse and vertical lever arm towards its origin (CB'_y & CB'_z), listed in column C12 and C13. The lever arms vary along the 20 sections according to the shape of the underwater hull.

The force components and their centers of buoyancy are illustrated in schematic figure B.3.

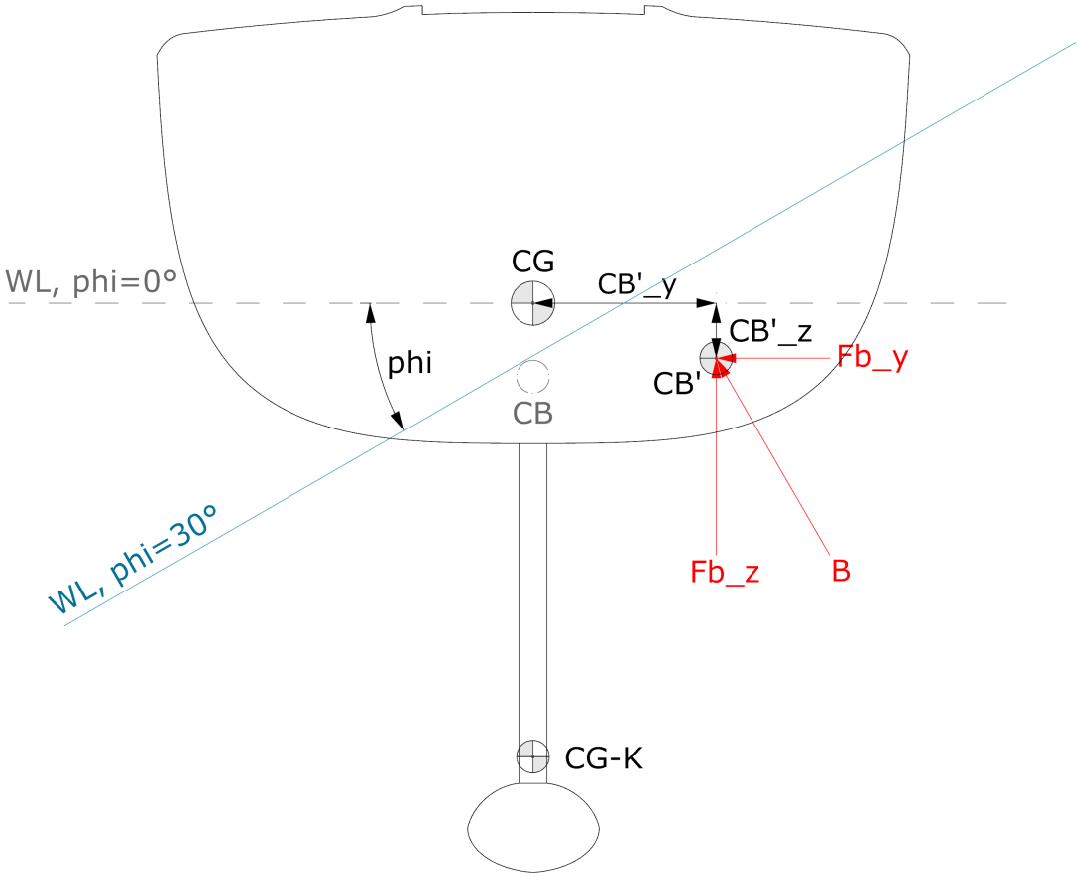

FIGURE B.3: Diagram of buoyancy force components

		Buoyancy					
Column	**C1**	**C8**	**C9**	**C10**	**C11**	**C12**	**C13**
Equation			$C1 \cdot C8 \cdot g \cdot \rho$	$-C8 \cdot \sin(\phi) \cdot g \cdot \rho$	$-C8 \cdot \cos(\phi) \cdot g \cdot \rho$		
Section	**x-pos.** [mm]	$\mathbf{B}_{(x)}$ [m3]	$\mathbf{My}_{(x)}$ [Nmm]	$\mathbf{Fb\_y}_{(x)}$ [N]	$\mathbf{Fb\_z}_{(x)}$ [N]	$\mathbf{CB'\_y}_{(x)}$ [mm]	$\mathbf{CB'\_z}_{(x)}$ [mm]
1	1150	3.363	3.89E+07	-16910	-29289	21.948	761.086
2	3450	9.601	3.33E+08	-48270	-83606	73.549	714.538
3	5750	15.630	9.04E+08	-78582	-136108	158.185	586.169
4	8050	19.899	1.61E+09	-100045	-173283	283.714	381.308
5	10350	21.321	2.22E+09	-107194	-185665	467.716	122.490
6	12650	19.691	2.50E+09	-98999	-171471	733.541	-154.505
7	14950	15.824	2.38E+09	-79557	-137797	1096.761	-408.387
8	17250	11.255	1.95E+09	-56586	-98010	1536.006	-609.060
9	19550	7.448	1.46E+09	-37444	-64854	1973.622	-752.378
9a	21261						
10	21850	5.056	1.11E+09	-25420	-44028	2328.526	-837.548
11	24150	4.061	9.86E+08	-20417	-35364	2565.923	-850.303
12	26450	4.323	1.15E+09	-21734	-37645	2668.868	-780.790
13	28750	5.829	1.69E+09	-29305	-50758	2633.906	-628.990
14	31050	8.615	2.69E+09	-43313	-75020	2475.444	-402.578
15	33350	12.531	4.20E+09	-63001	-109121	2225.199	-112.917
16	35650	17.003	6.10E+09	-85485	-148064	1931.742	227.525
17	37950	20.392	7.78E+09	-102523	-177576	1593.061	542.501
18	40250	19.510	7.90E+09	-98089	-169895	1158.578	716.033
19	42550	14.338	6.13E+09	-72084	-124854	742.995	750.506
20	44850	8.213	3.70E+09	-41292	-71520	449.866	904.025
Summation		**243.902**	**5.684E+10**	**-1226250**	**-2123927**		

TABLE B.5: Buoyancy force calculations

Through an equilibrium of moments the longitudinal center of buoyancy LCB can be determined:

$$LCB = \frac{\Sigma(B_{(x)} \cdot x)}{\nabla} = \frac{\Sigma My_{(x)}}{\Sigma B_{(x)}} \tag{B.6}$$

$$LCB = \frac{5.684 \times 10^{10}\,\mathrm{Nmm}}{243.902\,\mathrm{m}^3 \cdot 9.81\,\mathrm{m/s}^2 \cdot 1025\,\mathrm{kg/m}^3} = 23\,176\,\mathrm{mm} \tag{B.7}$$

In case of the evaluated quasi-static load case the sailing yacht has a trim of zero since the longitudinal center of buoyancy LCB is equal to the longitudinal center of gravity LCG (B.5).

B.3.3 Determination of Righting Moment RM

The righting moment of a heeled yacht (as explained in section 2.1), is depending on the distance d between the force lines of the center of gravity *CG* and the center of buoyancy *CB'* as shown in figure B.4 ($RM = d \cdot \Delta$).

Since the yacht's vertical center of gravity VCG is zero and in alignment with the origin of the coordinate system, only the righting arm d measured from the buoyancy force line to the origin is needed to determine the righting moment, as shown in diagram B.4. This distance d is unknown, but the transverse and vertical lever arms (CB'_y & CB'_z) for each section are available from the hydrostatic analysis and their corresponding buoyancy force components from the spreadsheet calculations. Hence, in table B.6 in column C14 the righting moment RM_T is calculated. Due to each section's outward moving center of buoyancy, every single hull section contributes its specific amount to the total righting moment, summed up at the bottom of column C14.

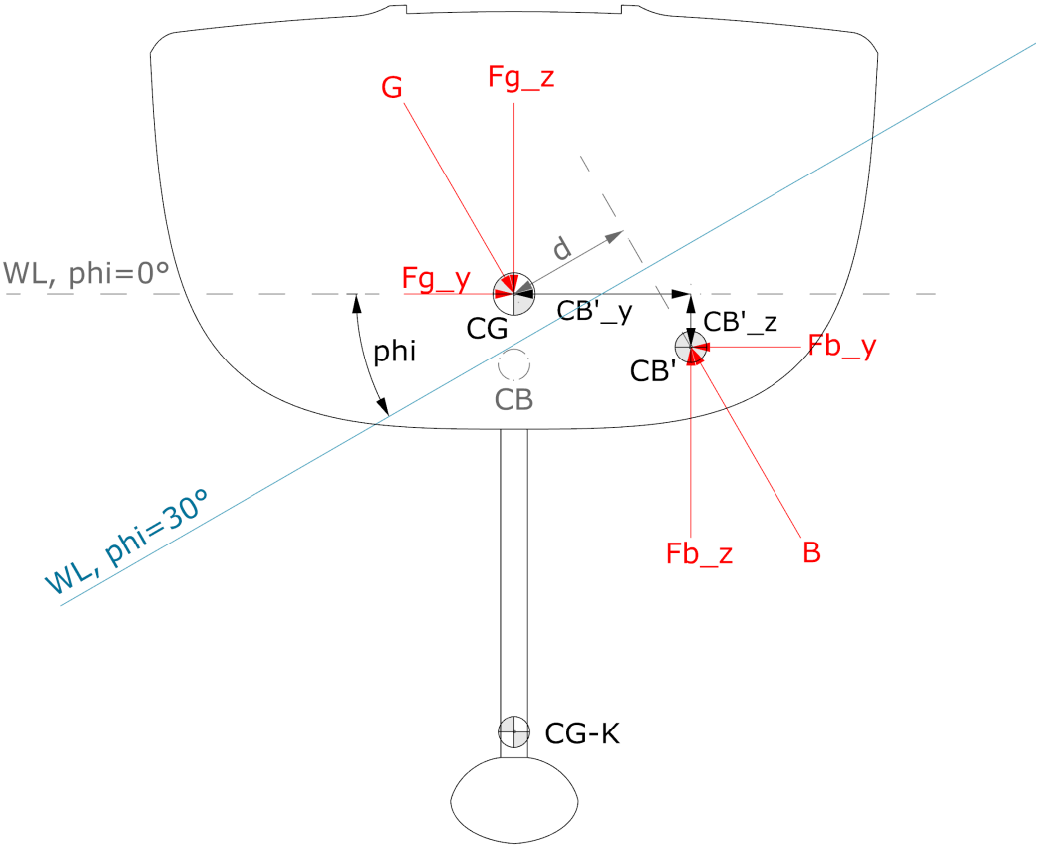

FIGURE B.4: Diagram of righting arms and force components

		Righting moment			
Column	**C1**	**C14**	**C15**	**C16**	**C17**
Equation		$C10 \cdot C13 + C11 \cdot C12$	$C4 \cdot C7$	$C14 \cdot \{(\Sigma C14 - \Sigma C15)/\Sigma C14\}$	$C15 + C16$
Section	**x-pos.** [mm]	**RM_T**$_{(x)}$ [Nmm]	**RM_K**$_{(x)}$ [Nmm]	**RM_H**$_{(x)}$ [Nmm]	**RM**$_{(x)}$ [Nmm]
1	1150	-1.35E+07		-6.98E+06	-6.98E+06
2	3450	-4.06E+07		-2.10E+07	-2.10E+07
3	5750	-6.76E+07		-3.49E+07	-3.49E+07
4	8050	-8.73E+07		-4.51E+07	-4.51E+07
5	10350	-1.00E+08		-5.17E+07	-5.17E+07
6	12650	-1.10E+08		-5.71E+07	-5.71E+07
7	14950	-1.19E+08		-6.13E+07	-6.13E+07
8	17250	-1.16E+08		-6.00E+07	-6.00E+07
9	19550	-9.98E+07		-5.16E+07	-5.16E+07
9a	21261		-1.28E+09		-1.28E+09
10	21850	-8.12E+07		-4.20E+07	-4.20E+07
11	24150	-7.34E+07		-3.79E+07	-3.79E+07
12	26450	-8.35E+07		-4.32E+07	-4.32E+07
13	28750	-1.15E+08		-5.96E+07	-5.96E+07
14	31050	-1.68E+08		-8.70E+07	-8.70E+07
15	33350	-2.36E+08		-1.22E+08	-1.22E+08
16	35650	-3.05E+08		-1.58E+08	-1.58E+08
17	37950	-3.39E+08		-1.75E+08	-1.75E+08
18	40250	-2.67E+08		-1.38E+08	-1.38E+08
19	42550	-1.47E+08		-7.59E+07	-7.59E+07
20	44850	-6.95E+07		-3.59E+07	-3.59E+07
Summation		**-2.64E+09**	**-1.28E+09**	**-1.36E+09**	**-2.64E+09**

TABLE B.6: Righting moment calculations

Taking figure B.1 into consideration each component generates actually its own righting moment (weight stability + form stability) and leads to the total righting moment of the yacht: the bulb keel with its very low center of gravity VCG_K and the hull without the bulb keel (LDT) with its VCG_{LDT} above the waterline but with an outward moving buoyancy center. Hence, a very high righting moment is actually generated by the bulb keel, but this information is lacking in column C14 since the hydrostatic data is analysed for the yacht's total displacement with its vertical center of gravity at zero. Therefore the distribution of righting moments along the whole hull length needs to be corrected.

In column C15 the righting moment of the bulb keel RM_K is calculated by multiplying its transverse force component Fg_y with its vertical lever arm CG_Z as illustrated in figure B.5.

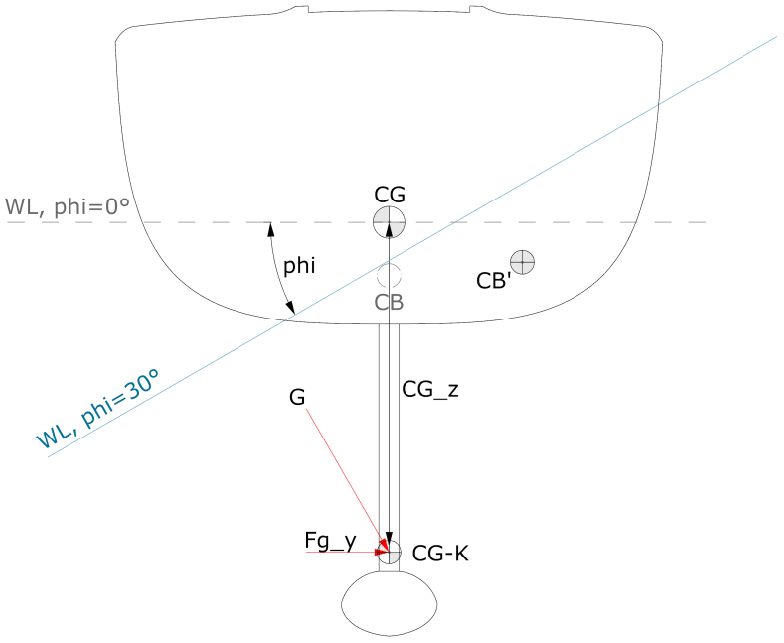

FIGURE B.5: Force components and righting arm of bulb keel

In column C16 the righting moment of the hull without the bulb keel RM_H is calculated by subtracting the righting moment of the keel RM_K proportionally from the righting moment distribution in column C14 to maintain the characteristic hydrostatics of the hull along its length. As can be seen in column C17 the adjusted righting moments add up to the original value in column C14, but with a correct distribution along the hull length (see also figure B.6).

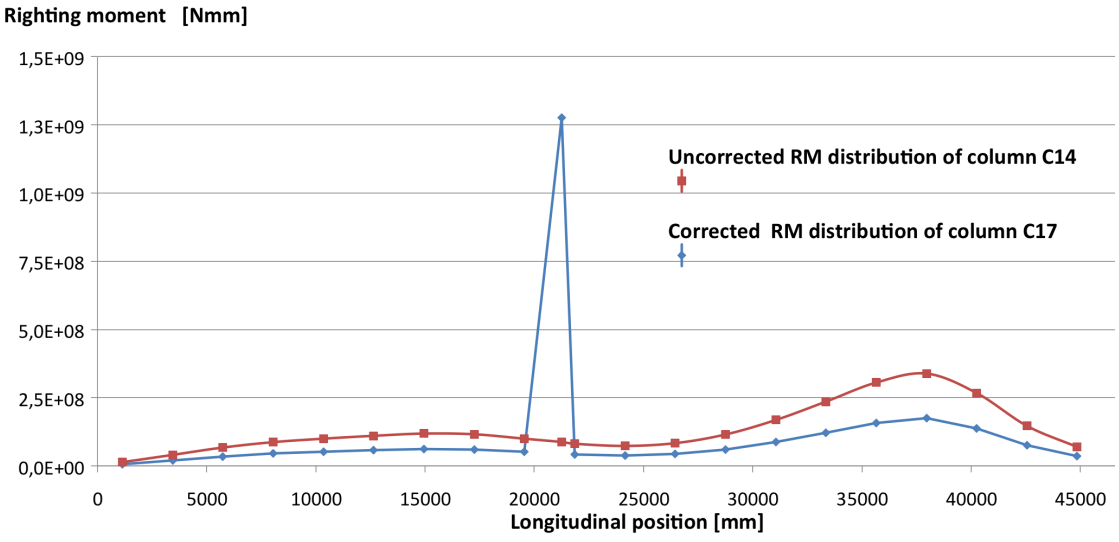

FIGURE B.6: Righting moment distribution along hull length

B.3.4 Equilibrium of Forces and Moments

Since the quasi-static load case reflects a steady-state sailing condition, where all moments and forces are in equilibrium, calculated weight and buoyancy forces must be in balance and are evaluated accordingly.

Column C17 shows the moments around the longitudinal axis calculated in table B.7. In column C18 the vertical force components of weight and buoyancy are summed up and multiplied by their lever arms C1 resulting in the moments around the transverse axis (C19). Likewise the transverse force components of weight and buoyancy (C20) multiplied by their lever arms resulting in the moments around the vertical axis (C21).

		Equilibrium				
Column	**C1**	**C17**	**C18**	**C19**	**C20**	**C21**
Equation			$C5 + C11$	$C1 \cdot C18$	$C4 + C10$	$C1 \cdot C20$
Section	**x-pos.** [mm]	$\mathbf{Mx}_{(x)} = \mathbf{RM}_{(x)}$ [Nmm]	$\mathbf{Fz}_{(x)}$ [N]	$\mathbf{My}_{(x)}$ [Nmm]	$\mathbf{Fy}_{(x)}$ [N]	$\mathbf{Mz}_{(x)}$ [Nmm]
1	1150	-6.98E+06	19297	2.22E+07	11141	1.28E+07
2	3450	-2.10E+07	-26046	-8.99E+07	-15038	-5.19E+07
3	5750	-3.49E+07	-70348	-4.04E+08	-40615	-2.34E+08
4	8050	-4.51E+07	-100030	-8.05E+08	-57752	-4.65E+08
5	10350	-5.17E+07	-105628	-1.09E+09	-60984	-6.31E+08
6	12650	-5.71E+07	-85495	-1.08E+09	-49361	-6.24E+08
7	14950	-6.13E+07	-46733	-6.99E+08	-26982	-4.03E+08
8	17250	-6.00E+07	-2566	-4.43E+07	-1481	-2.56E+07
9	19550	-5.16E+07	34263	6.70E+08	19782	3.87E+08
9a	21261	-1.28E+09	428184	9.10E+09	247212	5.26E+09
10	21850	-4.20E+07	58055	1.27E+09	33518	7.32E+08
11	24150	-3.79E+07	68699	1.66E+09	39663	9.58E+08
12	26450	-4.32E+07	67686	1.79E+09	39078	1.03E+09
13	28750	-5.96E+07	55134	1.59E+09	31832	9.15E+08
14	31050	-8.70E+07	30101	9.35E+08	17379	5.40E+08
15	33350	-1.22E+08	-7064	-2.36E+08	-4078	-1.36E+08
16	35650	-1.58E+08	-51859	-1.85E+09	-29941	-1.07E+09
17	37950	-1.75E+08	-89510	-3.40E+09	-51679	-1.96E+09
18	40250	-1.38E+08	-92513	-3.72E+09	-53412	-2.15E+09
19	42550	-7.59E+07	-60693	-2.58E+09	-35041	-1.49E+09
20	44850	-3.59E+07	-22934	-1.03E+09	-13241	-5.94E+08
Summation		**-2.64E+09**	**0**	**0**	**0**	**0**

TABLE B.7: Equilibrium of global forces and moments

According to table B.7 the summation of all forces in transverse and vertical direction is zero and so are the moments around the transverse and vertical axes.

Obviously the summation of moments around the longitudinal axis add up to the righting moment RM, which is in balance with the heeling moment induced by the sail forces listed in table B.10 in section B.4.

B.4 Rig Load Calculations

All rig load calculations are performed in an Excel-Spreadsheet *"Quasi-static load case" - Yacht/Rig loads* (on CD-ROM).

The rig load calculations are according to the **GL - Rules for Classification & Construction Part 4**, *Chapter 2 - Design and Construction of Large Modern Yacht Rigs* [12].

B.4.1 Input Data and Sail Plan

According to *Gl-Rules* Category II (Mid displacement, Offshore, short handed) is applicable for the 46m sailing yacht *"EXO"*.

Righting moment at 30 heel	$RM_{30°}$	=	**2638817**	[Nm]
Mainsail hoist	P	=	54.163	[m]
Height of foresail	I	=	52.136	[m]
Foot of mainsail	E	=	16.364	[m]
Length of headstay	lo	=	57.603	[m]
Main sheet attachment aft of gooseneck	x_{ms}	=	12.574	[m]
Angle of headstay	α_{hs}	=	71.58	[°]
Inward angle of backstay's	β_{bs}	=	86	[°]
Distance shroud chain plate to mast base	d	=	3.553	[m]
Mainsail area, projected laterally	A_m	=	546.92	[m^2]
Foresail area, projected laterally	A_f	=	466.27	[m^2]
Side force coefficient mainsail	SFC_m	=	0.9	[-]
Side force coefficient foresail	SFC_f	=	1.1	[-]
Center of effort of mainsail = 0,39 P	CoE_m	=	21.124	[m]
Center of effort of foresail = 0,39 I	CoE_f	=	20.333	[m]
Center of lateral resistance below waterline	CLR	=	1.644	[m]
Distance CoEm to CLR	$\overline{CoE_mCLR}$	=	28.455	[m]
Distance CoEf to CLR	$\overline{CoE_fCLR}$	=	25.671	[m]

TABLE B.8: Input data for rig load calculations

The rig specific abbreviations in the table above are displayed on the sail plan in figure B.7.

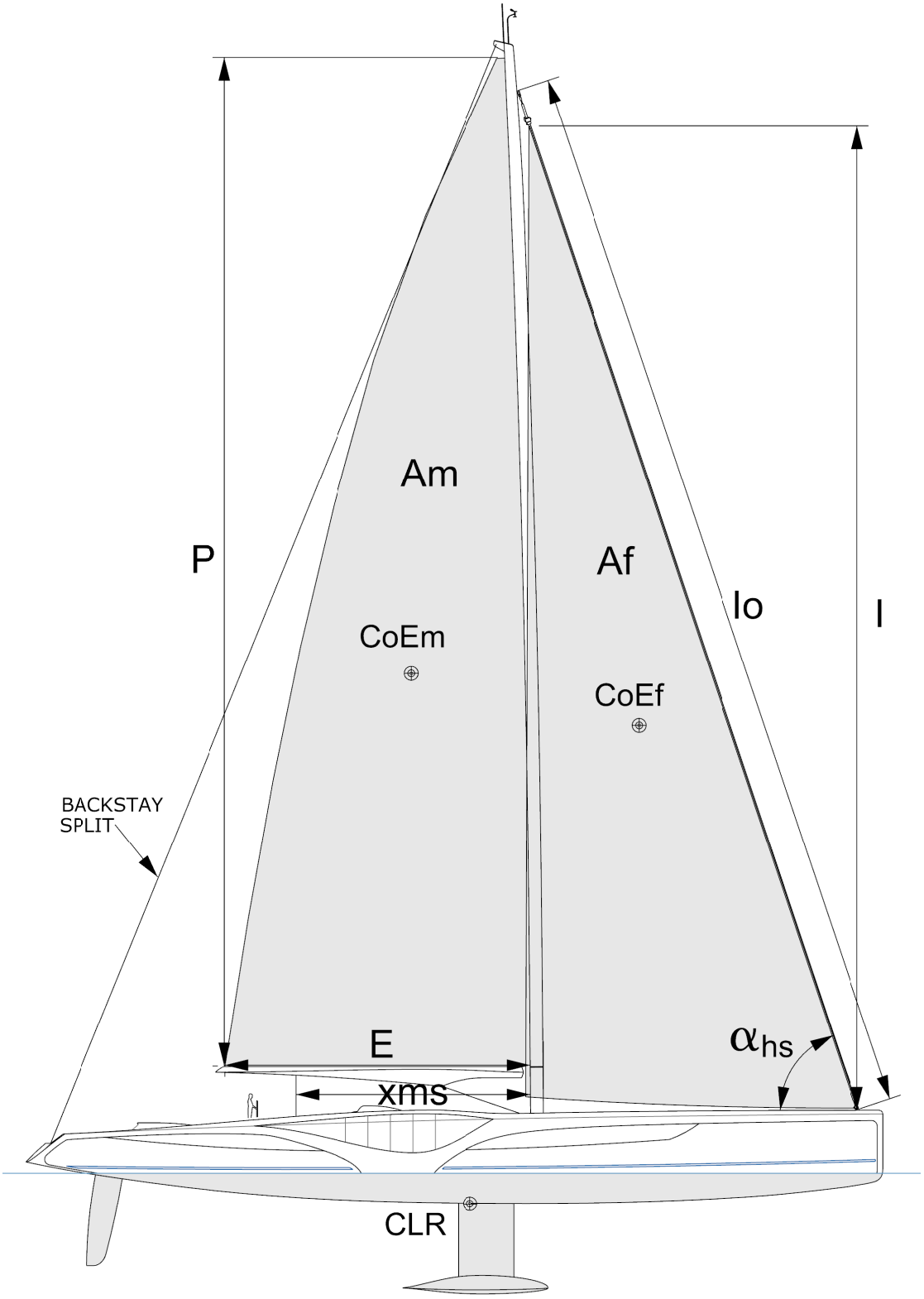

FIGURE B.7: Sail plan of 46m sailing yacht "EXO"

B.4.2 Transverse Sail Forces

According to section 3.2.1:

Basis for all rig loads are the transverse sailing forces. These forces are determined through the righting moment of the yacht at 30 degrees of heel RM30°, since the hull's righting moment and the heeling moment induced by the sail forces are in balance in a steady sailing condition. Each sail's contribution to the resulting heeling moment HM is assumed to be proportional to the sail's area and the distance of its centre of effort above the underwater body's centre of lateral resistance [12].

Transverse force from mainsail:

$$F_{tm} = \frac{RM_{30°}}{\overline{CoE_mCLR} + \frac{A_f \cdot SFC_f}{A_m \cdot SFC_m} \cdot \overline{CoE_fCLR}} = 47\,801\,[\mathrm{N}] \tag{B.8}$$

Transverse force from foresail:

$$F_{tf} = \frac{A_f \cdot SFC_f}{A_m \cdot SFC_m} \cdot F_{tm} = 49\,808\,[\mathrm{N}] \tag{B.9}$$

B.4.3 Main Sheet Load

According to section 4.1.3:

The vertical main sheet load is based on the tension force occurring in the mainsail leech. The tension force in the leech can be estimated with the *catenary formula* (B.11), where the transverse mainsail force is distributed over the mainsail leech and a leech sag is taken into account. As can be seen in figure B.8 the resulting leech tension force is highly dependent on the amount of sag, defining the sail profile.

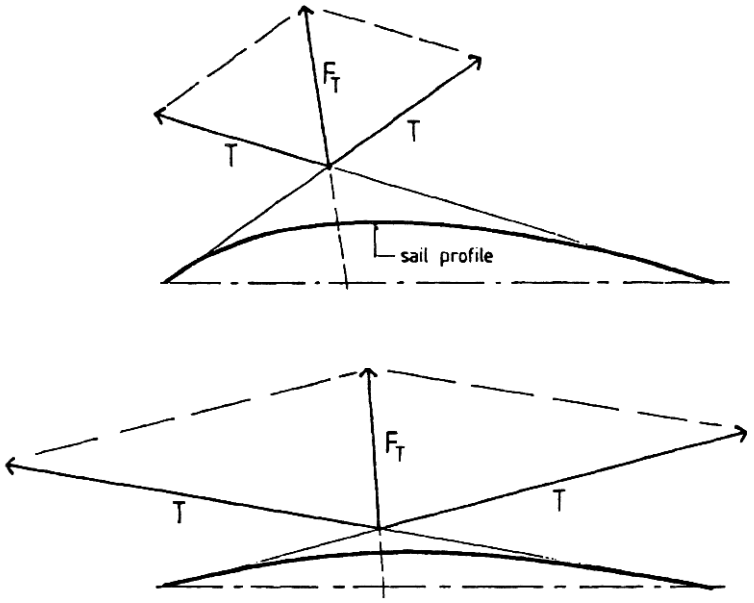

FIGURE B.8: Correlation of leech tension forces and sag [6]

The mainsail leech load is estimated with equation (B.11), considering a sag fraction of $\mathbf{s = 0{,}065}$ (6,5% of leech length for all categories) and a roach factor determined with equation (B.10):

$$f_r = \frac{A_m}{0,5 \cdot P \cdot E} = 1.234\,[-] \tag{B.10}$$

$$F_{ml} = \frac{F_{tm}}{8 \cdot s} \cdot f_r = 113\,448\,[\mathrm{N}] \tag{B.11}$$

The vertical main sheet load is derived from the equilibrium of moments about the gooseneck (boom-mast connection).

Vertical main sheet load:

$$F_{ms(z)} = \frac{E}{x_{ms}} \cdot F_{ml} = 147\,643\,[\mathrm{N}] \tag{B.12}$$

B.4.4 Headstay Load

According to section 4.2.2:

By applying the *catenary formula* the headstay load can be determined. For category II a headstay sag of s=0,015 (1,5% of headstay length) is applied and the transverse foresail force is distributed along the length of the sail-carrying headstay.

$$F_{hs} = \frac{F_{tf}}{8 \cdot s} \cdot f_r = 415\,070\,[\mathrm{N}] \tag{B.13}$$

The horizontal and vertical force components of the headstay load depend on the headstay angle α_{hs} measured to the horizontal water surface.

Horizontal headstay load:

$$F_{hs(x)} = F_{hs} \cdot \cos(\alpha_{hs}) = 131\,154\,[\mathrm{N}] \tag{B.14}$$

Vertical headstay load:

$$F_{hs(z)} = F_{hs} \cdot \sin(\alpha_{hs}) = 393\,805\,[\mathrm{N}] \tag{B.15}$$

B.4.5 Shroud Load V1

According to section 4.2:

With regard to the rules loads of standing rigging have to be determined with a geometric non-linear finite element analysis. However, in the framework of this concept study the shroud load V1 is determined by the classical *Skene's Method* [7]. *Skene's Method* is based on an equilibrium of moments, where the hydrostatic righting moment of the yacht is balanced to the heeling moment due to sail forces. In this steady-sailing condition the mast is in compression and the windward shrouds are in tension. Hence, the heeling moment can be approximated to equal the vertical chain plate load times the horizontal distance between mast base center and chain plate for the shrouds, as illustrated below:

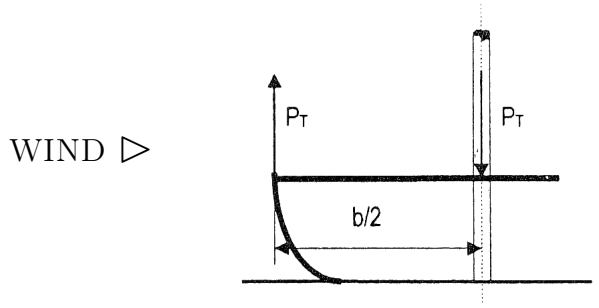

FIGURE B.9: Skene's Method for determination of shroud and mast loads [7]

Skene's Method is mainly used to dimension rig components and thus the coefficient 1.5 RM acts as a safety factor to take heels greater than 30 degrees into account. Since global and rig loads have to be in balance, the coefficient 1.5 will be neglected.

Vertical shroud load V1:

$$F_{V1(z)} = \frac{RM_{30°}}{d} = 742\,701\,[\text{N}] \tag{B.16}$$

The horizontal distance (d = 3553 mm) between chain plate of the V1 shroud and mast is illustrated in figure B.10.

B.4.6 Backstay Load

According to section 4.2.3:

The vertical force component of the backstay is obtained by opposing the forestay and mainsheet loads under equilibrium of moments about the mast base. The horizontal force component of the backstay is assumed to be equal to the headstay's horizontal force component. Furthermore the chain plates of the shrouds are in transverse alignment with the mast base, so no additional longitudinal moment is caused.

Horizontal backstay load:

$$F_{bs(x)} = F_{hs(x)} = 131\,153\,[\text{N}] \tag{B.17}$$

The lever arms in table B.9 are measured to the mast base. The measurements are displayed in figure B.10 in section B.4.8.

Rig force		Unit	Lever arm		Unit
$F_{hs(z)}$ =	393805	[N]	x_{hs}=	17.212	[m]
$F_{hs(x)}$ =	131154	[N]	z_{hs}=	0	[m]
			x_{bs} =	26.103	[m]
$F_{bs(x)}$ =	131154	[N]	z_{bs}=	-1.767	[m]
$F_{ms(z)}$ =	147643	[N]	x_{ms}=	12.931	[m]

TABLE B.9: Lever arms of rig force

Vertical backstay load:

$$F_{bs(z)} = \frac{F_{hs(x)} \cdot z_{hs} + F_{hs(z)} \cdot x_{hs} - F_{ms(z)} \cdot x_{ms} - F_{bs(x)} \cdot z_{bs}}{x_{bs}} = 195\,406\,[\mathrm{N}] \quad \text{(B.18)}$$

To take the backstay split (figure A.2) into account, the horizontal and vertical force components are divided into two equal loads: one located on portside and the other on starboard. Due to the backstay split the inward backstay angle of β_{bs} causes a transverse force component on each side.

Horizontal backstay load - portside & starboard:

$$F_{bsp(x)} = F_{bss(x)} = \frac{F_{bs(x)}}{2} = 65\,577\,[\mathrm{N}] \quad \text{(B.19)}$$

Vertical backstay load - portside & starboard:

$$F_{bsp(z)} = F_{bss(z)} = \frac{F_{bs(z)}}{2} = 97\,703\,[\mathrm{N}] \quad \text{(B.20)}$$

Transverse backstay load - portside:

$$F_{bsp(y)} = F_{bs(z)} \cdot \cos(\beta_{bs}) = 6815\,[\mathrm{N}] \quad \text{(B.21)}$$

Transverse backstay load - starboard:

$$F_{bss(y)} = -F_{bsp(y)} = -6815\,[\mathrm{N}] \tag{B.22}$$

B.4.7 Mast Compression Load

Since backstays, headstays, shrouds and even the mainsheet (via the boom and mainsail) are attached to the mast at a certain point, their vertical load components are transferred to the mast and add up as the compression force at it's base. In reality the distribution of rig loads is much more complex due to the flexibility of the rig, its interactions and interferences with attached sails and standing and running rig components. Nevertheless, from a conservative point of view the mast compression force is - in this simplified load model - approximated by the following equation:

$$F_{m(z)} = -\Sigma F_{(z)} \tag{B.23}$$

Vertical mast compression load:

$$F_{m(z)} = -\{F_{hs(z)} + F_{bsp(z)} + F_{bss(z)} + F_{ms(z)} + F_{V1(z)}\} = -1\,479\,555\,[\mathrm{N}] \tag{B.24}$$

B.4.8 Equilibrium of Forces and Moments

With regard to the quasi-static load case, reflecting a steady-state sailing condition where all moments and forces are in equilibrium the calculated rig forces must be in balance and are in consequence evaluated. In column C1-C3 of table B.10 the coordinates/lever arms of each rig force component are listed. Their measurements can be tracked in figure B.10. In column C4-C6 all rig loads are displayed and in column C7-C9 the resulting moments about the mast base are calculated and listed.

	Coord. to mast base			**Rig loads**			**Moments**		
Column	C1	C2	C3	C4	C5	C6	C7	C8	C9
Equation							$C6 \cdot C2 + C5 \cdot C3$	$C4 \cdot C3 + C6 \cdot C1$	$C4 \cdot C2 + C5 \cdot C1$
Component	**x** [mm]	**y** [mm]	**z** [mm]	**Fx** [N]	**Fy** [N]	**Fz** [N]	**Mx** [Nmm]	**My** [Nmm]	**Mz** [Nmm]
Main sheet	-12931	0	-975			147643	0.00E+00	-1.91E+09	0.00E+00
Headstay	17212	0	0	131154		393805	0.00E+00	6.78E+09	0.00E+00
Shroud V1	0	3553	0			742701	2.64E+09	0.00E+00	0.00E+00
Backstay Ps	-26103	-2317	-1767	-65577	6815	97703	-2.38E+08	-2.43E+09	-2.60E+07
Backstay Sb	-26103	2317	-1767	-65577	-6815	97703	2.38E+08	-2.43E+09	2.60E+07
Mast comp.	0	0	0			-1479555	0.00E+00	0.00E+00	0.00E+00
Summation:				**0**	**0**	**0**	**2.64E+09**	**0**	**0**

TABLE B.10: Equilibrium of rig forces and moments

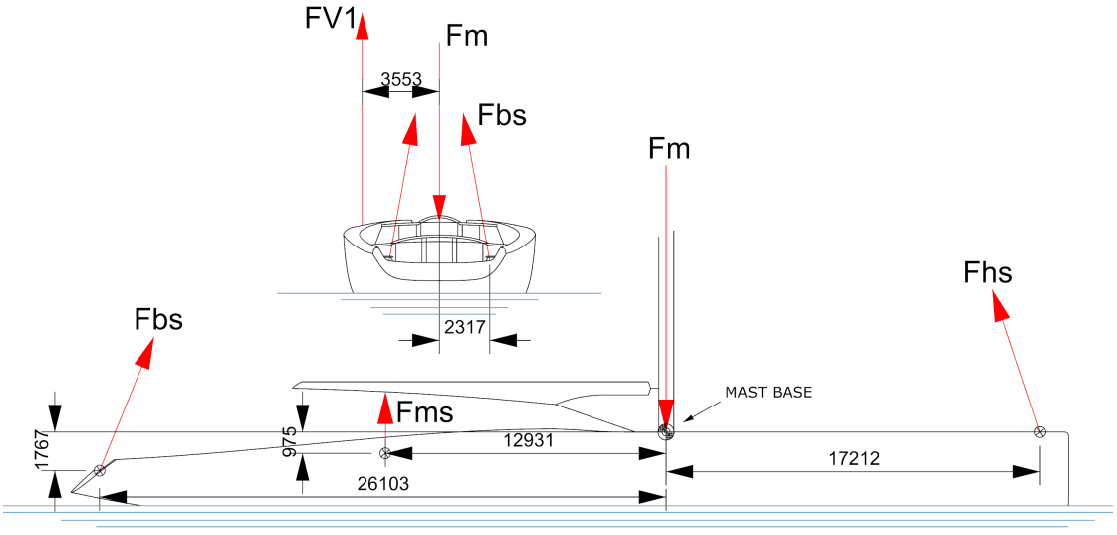

FIGURE B.10: Lever arms of rig forces, measured to mast base

According to table B.10 the sum of all forces in longitudinal, transverse and vertical direction is zero and so are the moments about the transverse and vertical axes. Obviously the moments about the longitudinal axis add up to the heeling moment HM, which is in balance with the hydrostatic righting moment calculated in table B.7 in section B.3.

C Dimensioning of Hull Structure

Due to the fact that the present developed hull structure is not similar to any conventional hull constructions, application of rules and standards from classifications societies is limited to fast preliminary dimensioning. Hence, dimensions are mostly based on first principle calculations and standard engineering methods. Occasionally, rules and standards from classifications societies are applied in parts and act solely as first indications.

C.1 Composite Materials and Design Stresses

The yacht's hull structure is build from carbon fibre based composite materials. Preliminary values for carbon fabrics and core materials and design stresses for sandwich panels and truss members are derived from the **ISO 12215-5 Small craft - Hull construction and scantling** - *Part 5: Design pressures for monohulls, design stresses, scantlings determination* [8].

All laminates consist out of balanced quadraxial carbon fabrics, as listed in table C.1. Only quadraxial fabrics are used since they approach quasi-isotropic mechanical properties due to their balanced fibre distribution (0/45/90/-45). Their application is inevitable for preliminary concept evaluations, because actually highly anisotropic mechanical properties of composite materials are simplified in the final FE-Simulation as isotropic.

Carbon fabric - balanced quadraxial 0/45/90/-45				
Ψ	σ_{ut} $[N/mm^2]$	σ_{uc} $[N/mm^2]$	τ_u $[N/mm^2]$	E $[N/mm^2]$
0.5	243	150	128	28700

TABLE C.1: Mechanical properties of carbon fabric ([8], table C5)

The core material for sandwich panels and truss members is listed below:

Rigid PVC I				
ρ $[kg/m^3]$	τ_u $[N/mm^2]$	G_c $[N/mm^2]$	σ_{uc} $[N/mm^2]$	E_c $[N/mm^2]$
100	1.12	31	1.32	90
150	1.92	48	2.41	162

TABLE C.2: Mechanical properties of core material ([8], table D2)

In table C.3 the design stresses are stated representing a **reserve factor of 2**:

Laminate design stress - tension σ_{dt}	$0,5 \cdot \sigma_{ut} = 121,5$	$[N/mm^2]$
Laminate design stress - compression σ_{dc}	lesser of $0,5 \cdot \sigma_{uc} = 75$ $0,3 \cdot \sqrt{E \cdot E_c \cdot G_c} = 182$	$[N/mm^2]$
Core design shear stress τ_d	$0,55 \cdot \tau_u = 1,1$	$[N/mm^2]$

TABLE C.3: Design stresses ([8], table 10&11)

C.2 Dimensions of Sandwich Panels

Owing to the fact that in the framework of this concept study dynamic loads (slamming) are neglected, bottom panels are dimensioned with respect to their hydrostatic pressure loads. The required moment of inertia is only calculated for one bottom panel (highlighted grey in figure C.1), which has the largest unsupported span b of the entire hull structure. Its dimension are defining for all other sandwich panel dimensions of the yacht structure.

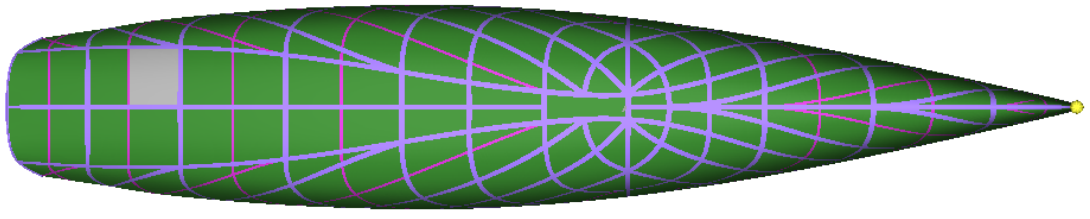

FIGURE C.1: Bottom panel with largest unsupported span (grey)

The required moment of inertia for sandwich panels is roughly estimated by the equation below according to ISO 12215-5, section 10.5.3.

$$I_{req}/cm = \frac{b^3 \cdot k_c^3 \cdot P \cdot k_3}{12 \cdot 10^6 \cdot k_1 \cdot E} \quad cm^4/cm \tag{C.1}$$

Since ISO standard is applicable for crafts up to 24 meters of length the bottom pressure P is estimated according to the **Rules for Classification of Pleasure Yachts** - *Part B Hull and Stability* [16].

Design pressures for the bottom of displacement sailing yachts ([16], section 5.3.2) are defined as follows:

$$P = 0,24 \cdot L^{0,5} \cdot (1 - \frac{h_0}{2T}) + 10 \cdot (h_0 + a \cdot L) \quad \text{but not} < 10 \cdot D \quad kN/m^2 \tag{C.2}$$

with:

Length of waterline	L	=	42,73	[m]
Depth	D	=	4,74	[m]
Draft	T	=	1.60	[m]
Vertical distance lower edge of plate to WL	h_0	=	0,61	[m]
Coefficient for pdr, aft of L/2	a	=	0.036	[-]

According to equation (A.8) the bottom pressure for the selected hull panel (grey highlighted in figure C.1) derives to P = 47,4 kN/m^2.

Hence, the required moment of inertia for the bottom panel is calculated by equation (C.1) with the following data:

Panel length	l	=	2377	[mm]
Panel's shorter dimension	b	=	2060	[mm]
Plate curvature	c	=	133	[mm]
Curvature correction	$k_c = 1,1 - \frac{3,33 \cdot c}{b}$	=	0.885	[-]
Deflection factor	k_1	=	0.017	[-]
Bending stiffness factor	$k_3 = \frac{0,027 \cdot (l/b)^2 - 0,029 \cdot (l/b) + 0,011}{(l/b)^2 - 1,463 \cdot (l/b) + 1,108}$	=	0,018	[-]
Bottom pressure	P	=	47.4	$[kN/m^2]$
E-Modulus of carbon laminate	E	=	28700	$[N/mm^2]$

$$I_{req}/cm = \frac{b^3 \cdot k_c^3 \cdot P \cdot k_3}{12 \cdot 10^6 \cdot k_1 \cdot E} = 0.883\,\mathrm{cm}^4/\mathrm{cm} \tag{C.3}$$

The moment of inertia for a sandwich panel where outer and inner skin are of the same material can be approximated by following equation:

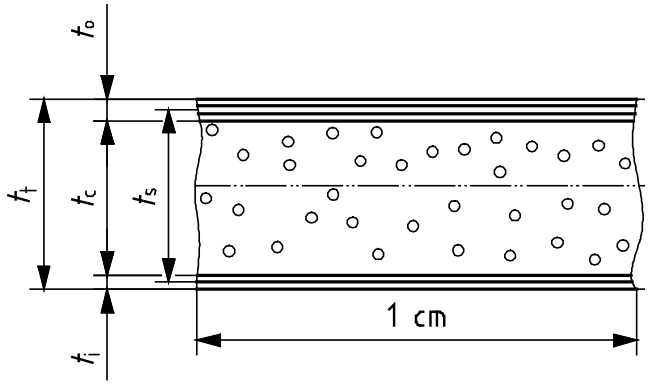

$$I_{att}/cm = \frac{t_o \cdot t_i \cdot t_s^2}{1000(t_o + t_i)}$$

FIGURE C.2: Moment of inertia formula for a sandwich stripe ([8], section D.2)

In table C.4 the selected sandwich panels of all components are listed; detailed dimensions with mechanical properties can be found in section C.6.

Dimensions of sandwich panels		**Hull**	**Deck, bulkheads , mast&keel foundation**	
Outer laminate thickness	t_o	3	2	[mm]
Core thickness	t_c	35	35	[mm]
Inner laminate thickenss	t_i	2	2	[mm]
Distance between centorids of skins	t_s	37.5	37	[mm]
Attained momen of intertia	I_{att}/cm	1.69	1.37	$[cm^4/cm]$

TABLE C.4: Dimensions of sandwich panels

C.3 Dimensions of Truss Members

In view of the objective to create a hull with load carrying and stiffness increasing truss members; this structural network network needs to be adequately dimensioned. The hull panels are solely dimensioned to withstand hydrostatic pressures, any additional stiffness to cope with global loads derives from the truss members.

With a simplified model the required hull-girder section modulus (or moment of inertia) can be estimated. The yacht is simplified as a beam freely supported at its ends with the maximal force trying to bend it [2]. In case of the 46m sailing yacht "EXO" the maximum longitudinal bending moment of 9500 kNm occurs in the mast/keel area as shown in figure 3.20 in section 3.7.

The following two equations [14] define the maximum bending moment and deflection of a beam under a point force at half length, as shown in figure C.3.

$$w_{max} = \frac{F \cdot l^3}{48 \cdot E \cdot Iy_0} \quad \text{at} \quad \frac{L}{2} \tag{C.4}$$

$$M_{max} = \frac{F \cdot l}{4} \quad \text{at} \quad \frac{L}{2} \tag{C.5}$$

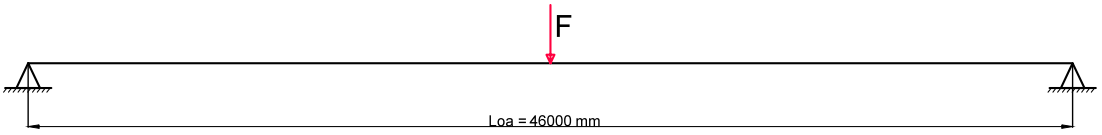

FIGURE C.3: Yacht simplified as beam, both ends freely supported

As dimensions of truss members depend on the claimed longitudinal stiffness of the yacht, a design constraint needs to be defined. For preliminary evaluation a maximum allowable deflection of L/200 is claimed, referring to a common engineering rule of thumb. The core of sandwich panels and truss members is considered ineffective in carrying any bending moment and is only transmitting shear forces; merely the Young's modulus of the outer and inner sandwich laminates is taken into account [8]. Hence, by claiming a maximum deflection of $w_{max} = L/200$ and by substituting the force in equation (C.4) with equation (C.5) the required moment of inertia of the yacht's main cross section can be estimated:

$$I_{req} = \frac{M_{max} \cdot l^2}{12 \cdot E \cdot w_{max}} = 2.54 \times 10^{11}\,\text{mm}^4 \tag{C.6}$$

with:

Length over all	l	=	46000	[mm]
Maximum long. bending moment	M_{max}	=	9,5E09	[Nmm]
Maximum allowable deflection	w_{max} = L/200	=	230	[mm]
E-Modulus of sandwich laminate	E	=	28700	$[N/mm^2]$

To stay below the smallest design stress of $\sigma_{uc} = 75N/mm^2$ a minimum section modulus is required, calculated as stated below:

$$SM_{req} = \frac{M_{max}}{\sigma_{uc}} = 1.27 \times 10^8 \,\mathrm{mm}^3 \tag{C.7}$$

The yacht's cross section at half length (equals approx. main section) with its previously calculated hull and deck panel dimensions (C.4) defines the start value. In several iterations truss member dimensions and their laminate thicknesses are varied until the cross section of the yacht complies with the required section modulus and the moment of inertia. In the following the truss members with their final dimensions are presented.

For the sake of simplicity all truss members are assumed to be *"Square"* top hat stiffeners and only their top laminate is taken into account, as illustrated below. Four different sizes are defined with their dimensions listed in table C.5; detailed dimensions with mechanical properties can be found in section C.6.

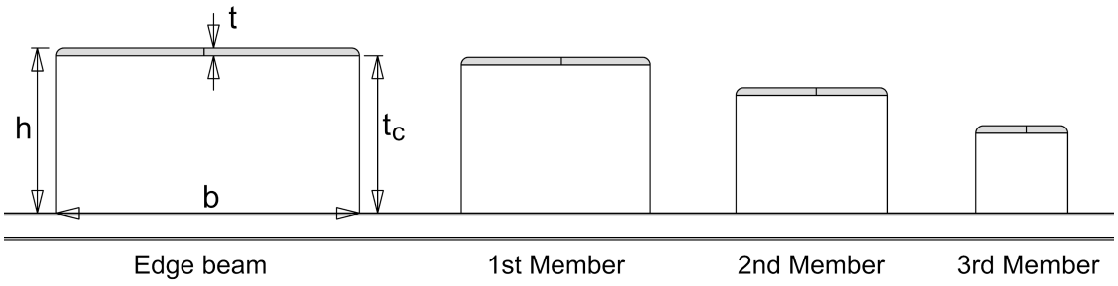

FIGURE C.4: Top hat stiffeners

Dimensions in [mm]		**Edge beam**	**1st Member**	**2nd Member**	**3rd Member**
Laminate	t	8	6	6	6
Core thickness	tc	210	200	160	110
Total height	h	218	206	166	116
Maximum breadth	b	400	250	200	120
Tapered breadth	bt	160	150	-	-
Structure components		Edge beam	Hull, main bulkhead	Deck, bulkheads	Deck, bullheads, mast&keel foundation

TABLE C.5: Dimensions of top hat stiffeners

With these sandwich panel and truss member dimensions (table C.4&C.5) the yacht's cross section is analysed in *Rhinoceros* and illustrated in figure C.5.

Attained moment of inertia:

$$I_{att} = Iy_o = 4.957 \times 10^{11} \,\mathrm{mm}^4 \quad \longrightarrow \mathrm{OK} \tag{C.8}$$

With these sandwich panel and truss member dimensions (table C.4&C.5) the yacht's cross section has an attained moment of inertia of $I_{att} = 4,957e11\ mm^4$, as illustrated in C.5.

FIGURE C.5: Yacht's cross section at L/2, carbon laminate only

Considering the neutral axis is approx. at half depth height, the attained section modulus is estimated by the following equation:

$$SM_{att} = \frac{I_{att}}{D/2} = 2.09 \times 10^8\,\mathrm{mm}^3 \quad \longrightarrow \mathrm{OK} \tag{C.9}$$

C.4 Isotropic Analysis of E-Moduli

In the final FE-Model the developed hull structure is defined as a surface model. Although each truss member is actually located on top of sandwich panels, they are integrated into the surfaces of the model and divide them into small panels, as visualized in figure C.6.

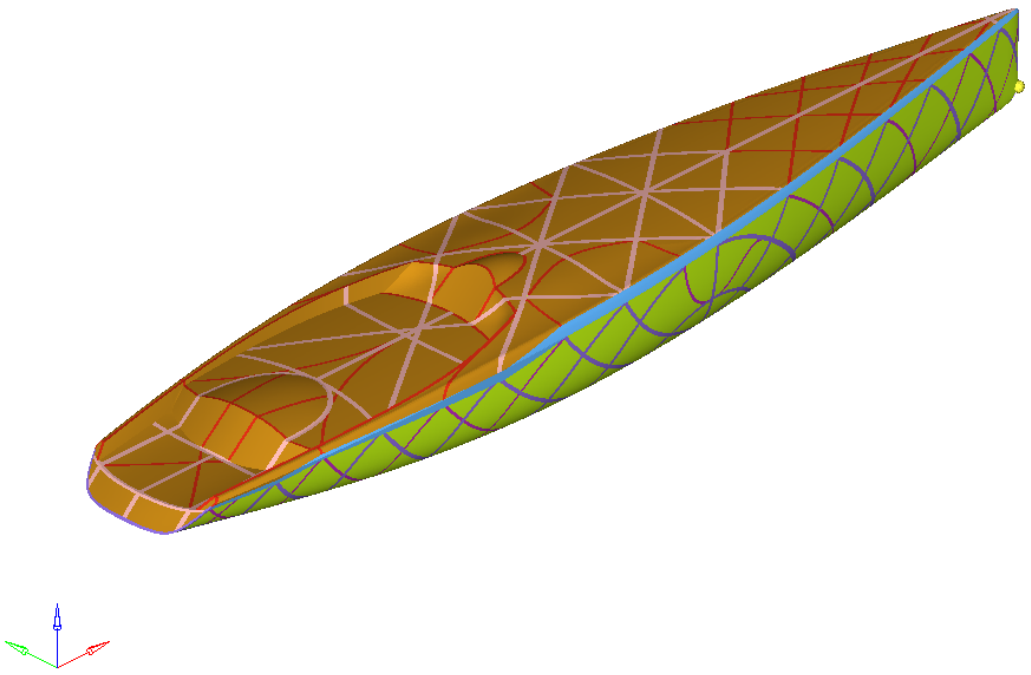

FIGURE C.6: FE-Model - surfaces define truss members and panels

Thus, the thickness applied to any surface with a truss member must also include the thickness of the corresponding sandwich panel. Likewise, the implemented isotropic E-Modulus must represent properties of truss member and sandwich panel. This is why the structural properties of the sandwich panels and truss members are substituted by a homogeneous plate with an isotropic E-Modulus.

The calculations for corresponding isotopic E-Moduli of each structure component group are based on a spreadsheet by *Dykstra Naval Architects* and are listed in section C.6.

In the following paragraph the principles of these spreadsheets for calculating the isotropic E-Moduli is presented.

In case of the present sailing yacht the truss members and hull and deck panels are mainly subjected to tension and compressions forces and are hardly exposed to excessive deflections along the hull length. Due to this fact isotropic E-moduli are approximated by claiming that the axial stiffness (EA) for sandwich and homogeneous plate are the same. Bending stiffness (EI) is neglected. This leads to satisfying results as the validation in section C.5 shows.

Table C.6 presents exemplary, how the isotropic Young's modulus of deck sandwich panels (listed in section C.6) are calculated.

Sandwich panels - deck	**b**	**t**	**A = b x t**	**Area centroid z-pos.**	$Iy_{own} = (b \cdot t^3)/12$	**E**	**EA**
	[mm]	[mm]	$[mm^2]$	[mm]	$[mm^4]$	$[N/mm^2]$	[N]
Outer laminate	100	2	200	18.5	6.667E+01	28700	5.740E+06
Core	100	35	3500	0.0	3.573E+05	90	3.150E+05
Inner laminate	100	2	200	-18.5	6.667E+01	28700	5.740E+06
		$\Sigma(A)$	**3900**			$\Sigma(EA)$	**1.180E+07**

$$E_{iso} = \frac{\Sigma(EA)}{\Sigma(A)} = 3024\,\mathrm{N/mm^2} \quad \text{for homogeneous plate, t = 39mm} \tag{C.10}$$

TABLE C.6: Isotropic E-Modulus of homogeneous substitution plate

C.5 Validation of Isotropic E-Moduli and Finale FE-Simulation

Figure C.7 displays the yacht's main cross section in two perspectives. One side presents the homogenized plates with their corresponding isotropic E-Moduli; this shows at the same time how the FE-Model is set up. In the other half the cross section is presented just with actual sandwich laminates and their corresponding E-Moduli.

In table C.7 the area analysed in *Rhinoceros* (A), vertical position of area centroid and the own moment of inertia (Iy_{own}) of each structure component group are listed. A structure group includes components of same dimensions and composite lay-up and thus equal isotropic E-Moduli. The calculations for corresponding isotropic E-Moduli of each structure component group are listed in section C.6. With these isotropic E-Moduli the cross section's total stiffness about the neutral axis (EIy_o) is calculated in table C.7.

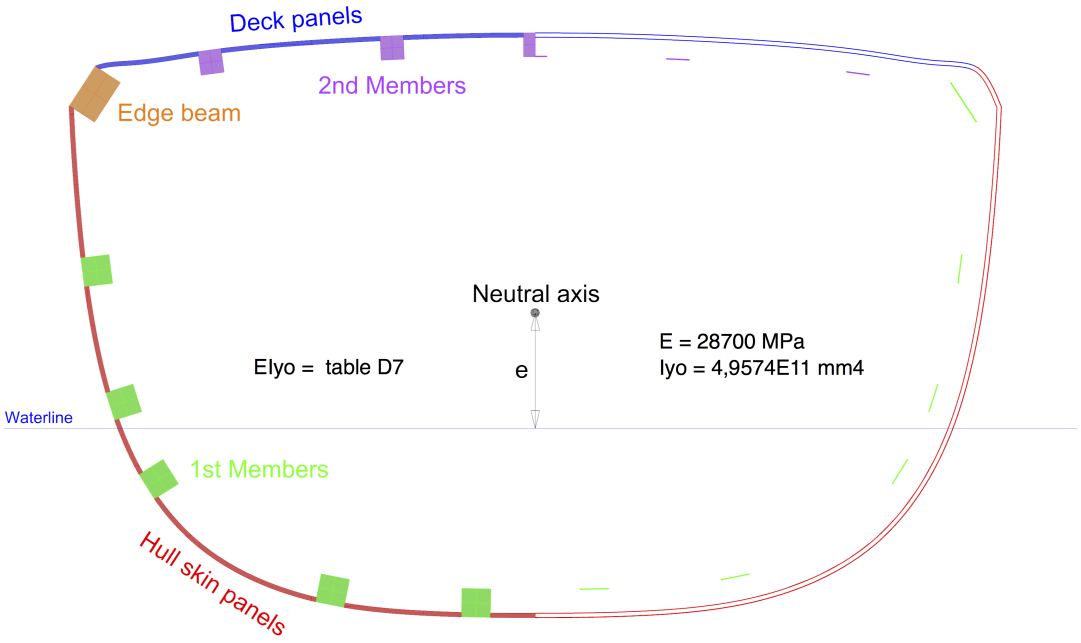

FIGURE C.7: Main cross section - homogenized plates, E_{iso} (left), sandwich laminates (right)

Components	A	Area centroid z-pos.	Iy_{own}	E_{iso}	EA	z x EA	z^2 x EA	EI_{own}
	$[mm^2]$	$[mm]$	$[mm^4]$	$[N/mm^2]$	$[N]$	$[Nmm]$	$[Nmm^2]$	$[Nmm^2]$
Hull skin panels	461836	-121.637	9.693E+11	3729	1.722E+09	-2.095E+11	2.548E+13	3.615E+15
Deck panels	255155	3279	1.916E+09	3024	7.716E+08	2.530E+12	8.294E+15	5.794E+12
Hull skin - 1st members	615011	-350	6.956E+11	1380	8.487E+08	-2.972E+11	1.041E+14	9.599E+14
Deck - 2nd members	205018	3218	1.562E+09	1486	3.047E+08	9.805E+11	3.156E+15	2.321E+12
Edge beam	209633	2864	2.370E+09	1541	3.230E+08	9.251E+11	2.649E+15	3.652E+12
Summation:	**1746653**				**3.970E+09**	**3.929E+12**	**1.423E+16**	**4.586E+15**

Neutral axis above WL	$e = \Sigma(z \cdot EA)/\Sigma(EA)$	=	*990*	[mm]
Total stiffness about WL	$EIy = \Sigma(EIy_{own})/\Sigma(z^2 \cdot EA)$	=	*1.881E+16*	$[Nmm^2]$
Total stiffness about neutral axis	$EIy_0 = EIy - \{e^2 \cdot \Sigma(EA)\}$	=	*1.493E+16*	$[Nmm^2]$

TABLE C.7: Coss section's total stiffness based on isotropic E-Moduli

According to section C.3 the yacht's hull can be simplified as a beam - freely supported at both ends. Subjected to a force derived from the maximal longitudinal bending moment, the beam's deflection is calculated by the following equation:

$$w_{max} = \frac{M_{max} \cdot l^2}{12 \cdot EIy_0} \quad \text{at} \quad \frac{L}{2} \tag{C.11}$$

Attained deflection, cross section stiffness derived from sandwich laminates:

$$w_{max} = \frac{9.5 \times 10^9\,\mathrm{Nmm} \cdot (46\,000\,\mathrm{mm})^2}{12 \cdot 28\,700\,\mathrm{N/mm^2} \cdot 4.9574 \times 10^{11}\,\mathrm{mm^4}} = 117.7\,\mathrm{mm} \tag{C.12}$$

Attained deflection, cross section stiffness derived from homogenized plates with isotropic E-Moduli:

$$w_{max} = \frac{9.5 \times 10^9\,\mathrm{Nmm} \cdot (46\,000\,\mathrm{mm})^2}{12 \cdot \cdot 1.493 \times 10^{16}\,\mathrm{mm^4}} = 112.2\,\mathrm{mm} \tag{C.13}$$

As shown in the table below, the assumptions stated at the beginning of this chapter lead to acceptable results.

Comparison	**Global deflection of hull girder**	
	Deflection at L/2	Deviation
Homogenized plates **Sandwich laminates**	112.2 [mm] 117.7 [mm]	4.7%

C.6 Composite Laminate Properties of Panels and Truss Members

Composite laminate properties

Structure components: Panels of deck, bulkheads and mast&keel foundation

	Ply	Description	Material	Fabric or core weight [g/m2] or [kg/m3]	Fibre fraction ψ [-]	Ply thickness [mm]	Core thickness [mm]	Width [mm]	Cured ply weight [kg/m2]	E [Gpa]
Outside	1	Balanced quadraxial	Carbon	720	0,5	1,0		1000	1,44	28,70
	2	Balanced quadraxial	Carbon	720	0,5	1,0		1000	1,44	28,70
	3	Core	Rigid PVC	100			35,0	1000	3,5	0,09
	4	Balanced quadraxial	Carbon	720	0,5	1,0		1000	1,44	28,70
	5	Balanced quadraxial	Carbon	720	0,5	1,0		1000	1,44	28,70
	6									
	7									
	8									
	9									
	10									
	11									
	12									
	13									
	14									
	15									
	16									
	17									
	18									
	19									
Inside	20									
					Total thickness	39		Total weight	9,26	

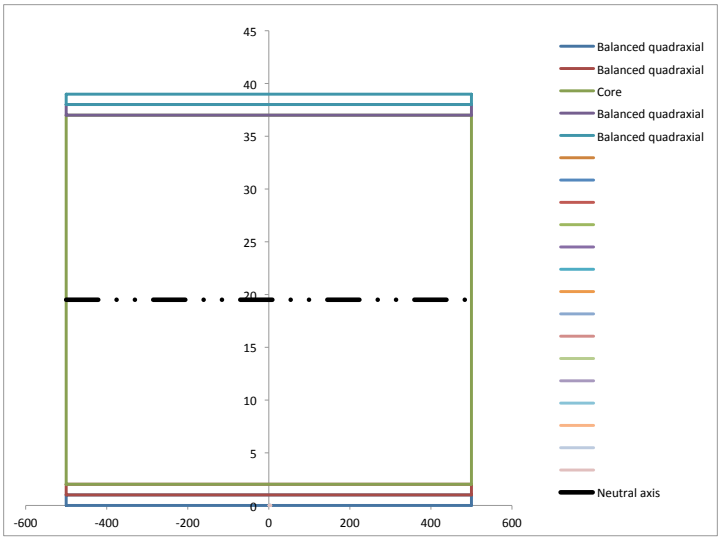

Laminate properties in tens / compr

A total	39000	[mm2]
Neutral axis	19,50	[mm]
EA	117950	[kN]
E iso tens/cor	3,024	[Gpa]

Composite laminate properties

Structure components: Panels of hull skin

Ply thickness $t = \frac{1}{2,16} \cdot (\frac{1,8}{\Psi} - 0,6) \cdot w$ mm w in kg/m^2

	Ply	Description	Material	Fabric or core weight w [g/m2] or [kg/m3]	Fibre fraction ψ [-]	Ply thickness t [mm]	Core thickness [mm]	Width [mm]	Cured ply weight [kg/m2]	E [Gpa]
Outside	1	Balanced quadraxial	Carbon	720	0,5	1,0		1000	1,44	28,70
	2	Balanced quadraxial	Carbon	720	0,5	1,0		1000	1,44	28,70
	3	Balanced quadraxial	Carbon	720	0,5	1,0		1000	1,44	28,70
	4	Core	Rigid PVC	150			35,0	1000	5,25	0,16
	5	Balanced quadraxial	Carbon	720	0,5	1,0		1000	1,44	28,70
	6	Balanced quadraxial	Carbon	720	0,5	1,0		1000	1,44	28,70
	7									
	8									
	9									
	10									
	11									
	12									
	13									
	14									
	15									
	16									
	17									
	18									
	19									
Inside	20									
					Total thickness	40		Total weight	12,45	

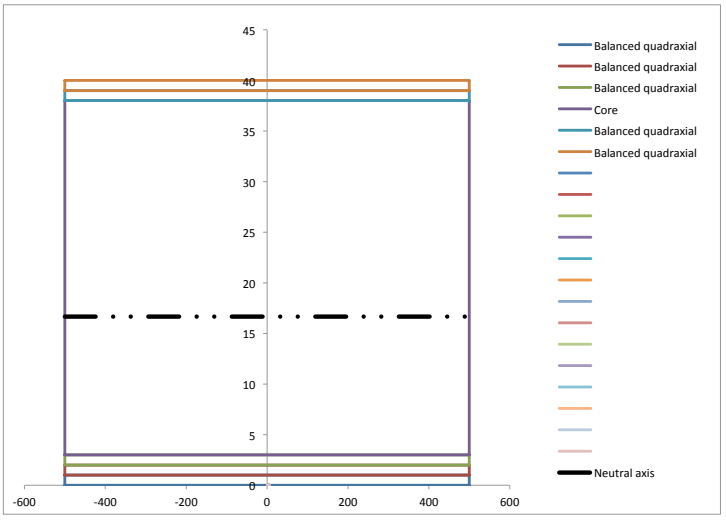

Laminate properties in tens / compr

A total	40000	[mm2]
Neutral axis	16,65	[mm]
EA	149170	[kN]
E iso tens/compr	3,729	[Gpa]

Composite laminate properties

Structure components: 1st members of hull

	Ply	Description	Material	Fabric or core weight [g/m2] or [kg/m3]	Fibre fraction ψ [-]	Ply thickness [mm]	Core thickness [mm]	Width [mm]	Cured ply weight [kg/m2]	E [Gpa]
Outside	1	Balanced quadraxial	Carbon	720	0,5	1		1000	1,44	28,70
	2	Balanced quadraxial	Carbon	720	0,5	1		1000	1,44	28,70
	3	Balanced quadraxial	Carbon	720	0,5	1		1000	1,44	28,70
	4	Core	Rigid PVC	150			35	1000	5,25	0,16
	5	Balanced quadraxial	Carbon	720	0,5	1		1000	1,44	28,70
	6	Balanced quadraxial	Carbon	720	0,5	1		1000	1,44	28,70
	7	Core	Rigid PVC	100			200	1000	20	0,09
	8	Balanced quadraxial	Carbon	720	0,5	1		1000	1,44	28,70
	9	Balanced quadraxial	Carbon	720	0,5	1		1000	1,44	28,70
	10	Balanced quadraxial	Carbon	720	0,5	1		1000	1,44	28,70
	11	Balanced quadraxial	Carbon	720	0,5	1		1000	1,44	28,70
	12	Balanced quadraxial	Carbon	720	0,5	1		1000	1,44	28,70
	13	Balanced quadraxial	Carbon	720	0,5	1		1000	1,44	28,70
	14									
	15									
	16									
	17									
	18									
	19									
Inside	20									
					Total thickness	246		Total weight	41,09	

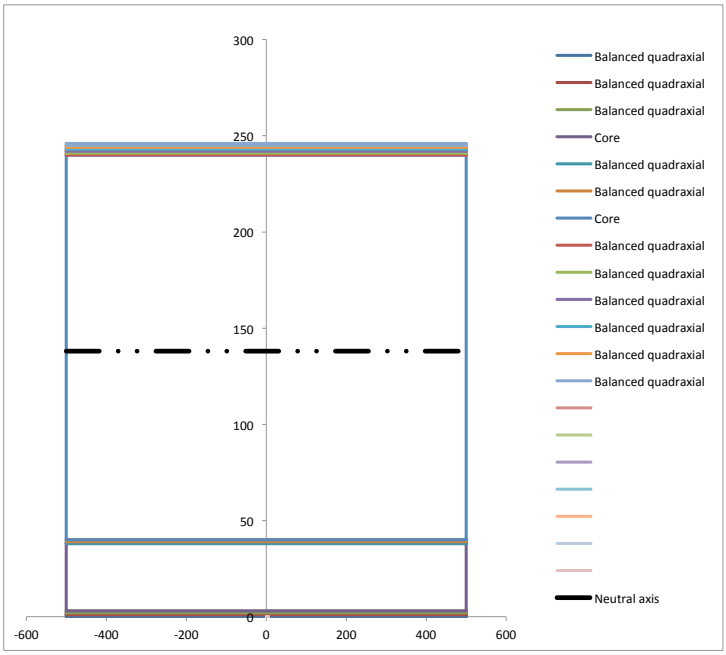

Laminate properties in tens / compr

A total	246000	[mm2]
Neutral axis	138,05	[mm]
EA	339370	[kN]
E iso tens/cor	1,380	[Gpa]

Composite laminate properties

Structure components: 3rd members of hull

	Ply	Description	Material	Fabric or core weight [g/m2] or [kg/m3]	Fibre fraction ψ [-]	Ply thickness [mm]	Core thickness [mm]	Width [mm]	Cured ply weight [kg/m2]	E [Gpa]
Outside	1	Balanced quadraxial	Carbon	720	0,5	1		1000	1,44	28,70
	2	Balanced quadraxial	Carbon	720	0,5	1		1000	1,44	28,70
	3	Balanced quadraxial	Carbon	720	0,5	1		1000	1,44	28,70
	4	Core	Rigid PVC	150			35	1000	5,25	0,16
	5	Balanced quadraxial	Carbon	720	0,5	1		1000	1,44	28,70
	6	Balanced quadraxial	Carbon	720	0,5	1		1000	1,44	28,70
	7	Core	Rigid PVC	100			110	1000	11	0,09
	8	Balanced quadraxial	Carbon	720	0,5	1		1000	1,44	28,70
	9	Balanced quadraxial	Carbon	720	0,5	1		1000	1,44	28,70
	10	Balanced quadraxial	Carbon	720	0,5	1		1000	1,44	28,70
	11	Balanced quadraxial	Carbon	720	0,5	1		1000	1,44	28,70
	12	Balanced quadraxial	Carbon	720	0,5	1		1000	1,44	28,70
	13	Balanced quadraxial	Carbon	720	0,5	1		1000	1,44	28,70
	14									
	15									
	16									
	17									
	18									
	19									
Inside	20									
					Total thickness	156		Total weight	32,09	

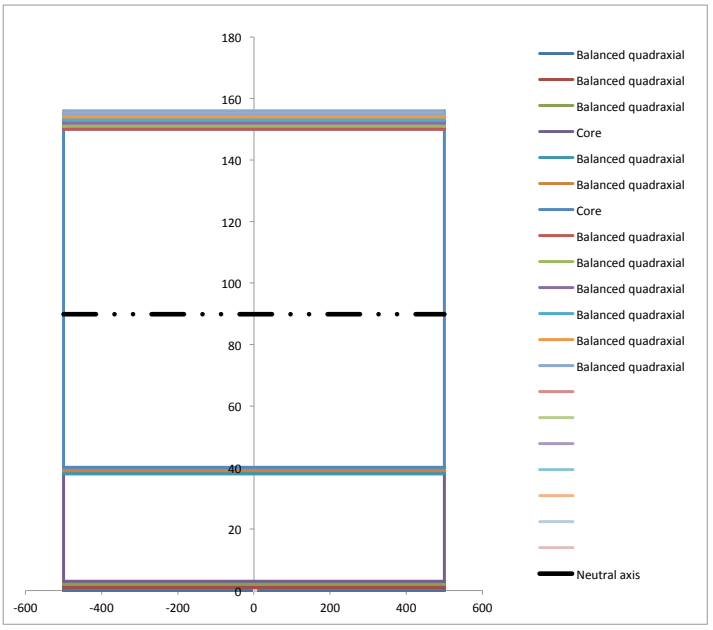

Laminate properties in tens / compr

A total	156000	[mm2]
Neutral axis	89,87	[mm]
EA	331270	[kN]
E iso tens/cor	2,124	[Gpa]

Composite laminate properties

Structure components: 1st members of main bulkheads

	Ply	Description	Material	Fabric or core weight [g/m2] or [kg/m3]	Fibre fraction ψ [-]	Ply thickness [mm]	Core thickness [mm]	Width [mm]	Cured ply weight [kg/m2]	E [Gpa]
Outside	1	Balanced quadraxial	Carbon	720	0,5	1		1000	1,44	28,70
	2	Balanced quadraxial	Carbon	720	0,5	1		1000	1,44	28,70
	3	Core	Rigid PVC	100			35	1000	3,5	0,09
	4	Balanced quadraxial	Carbon	720	0,5	1		1000	1,44	28,70
	5	Balanced quadraxial	Carbon	720	0,5	1		1000	1,44	28,70
	6	Core	Rigid PVC	100			200	1000	20	0,09
	7	Balanced quadraxial	Carbon	720	0,5	1		1000	1,44	28,70
	8	Balanced quadraxial	Carbon	720	0,5	1		1000	1,44	28,70
	9	Balanced quadraxial	Carbon	720	0,5	1		1000	1,44	28,70
	10	Balanced quadraxial	Carbon	720	0,5	1		1000	1,44	28,70
	11	Balanced quadraxial	Carbon	720	0,5	1		1000	1,44	28,70
	12	Balanced quadraxial	Carbon	720	0,5	1		1000	1,44	28,70
	13									
	14									
	15									
	16									
	17									
	18									
	19									
Inside	20									
					Total thickness	245		Total weight	37,9	

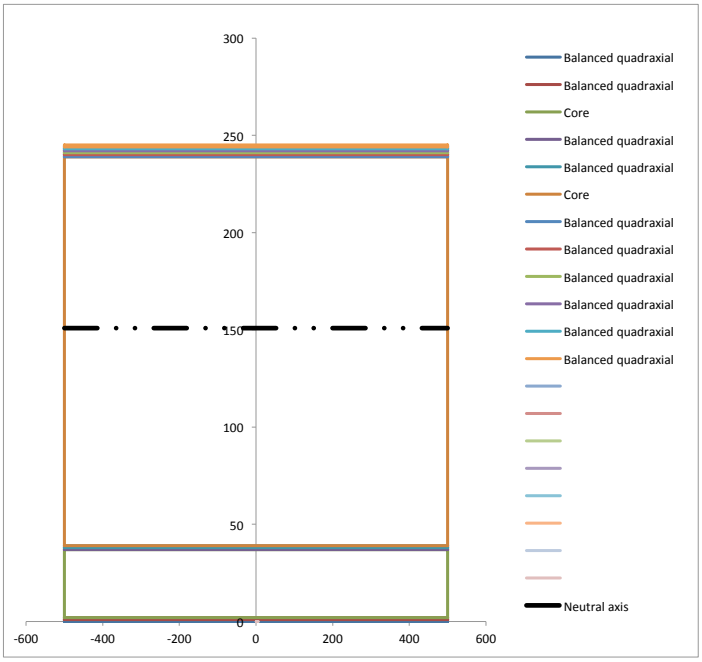

Laminate properties in tens / compr

A total	245000	[mm2]
Neutral axis	150,82	[mm]
EA	308150	[kN]
E iso tens/cor	1,258	[Gpa]

Composite laminate properties

Structure components: 2nd members of deck and bulkheads

	Ply	Description	Material	Fabric or core weight [g/m2] or [kg/m3]	Fibre fraction ψ [-]	Ply thickness [mm]	Core thickness [mm]	Width [mm]	Cured ply weight [kg/m2]	E [Gpa]
Outside	1	Balanced quadraxial	Carbon	720	0,5	1		1000	1,44	28,70
	2	Balanced quadraxial	Carbon	720	0,5	1		1000	1,44	28,70
	3	Core	Rigid PVC	100			35	1000	3,5	0,09
	4	Balanced quadraxial	Carbon	720	0,5	1		1000	1,44	28,70
	5	Balanced quadraxial	Carbon	720	0,5	1		1000	1,44	28,70
	6	Core	Rigid PVC	100			160	1000	16	0,09
	7	Balanced quadraxial	Carbon	720	0,5	1		1000	1,44	28,70
	8	Balanced quadraxial	Carbon	720	0,5	1		1000	1,44	28,70
	9	Balanced quadraxial	Carbon	720	0,5	1		1000	1,44	28,70
	10	Balanced quadraxial	Carbon	720	0,5	1		1000	1,44	28,70
	11	Balanced quadraxial	Carbon	720	0,5	1		1000	1,44	28,70
	12	Balanced quadraxial	Carbon	720	0,5	1		1000	1,44	28,70
	13									
	14									
	15									
	16									
	17									
	18									
	19									
Inside	20									
					Total thickness	205		Total weight	33,9	

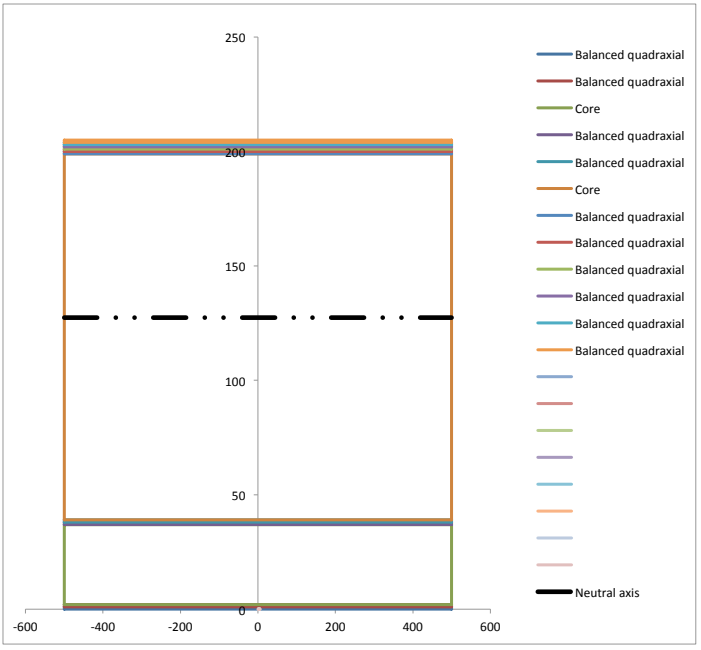

Laminate properties in tens / compr

A total	205000	[mm2]
Neutral axis	127,39	[mm]
EA	304550	[kN]
E iso tens/cor	1,486	[Gpa]

Composite laminate properties

Structure components: 3rd members of deck, bulkheads and mast & keel foundation

	Ply	Description	Material	Fabric or core weight [g/m2] or [kg/m3]	Fibre fraction ψ [-]	Ply thickness [mm]	Core thickness [mm]	Width [mm]	Cured ply weight [kg/m2]	E [Gpa]
Outside	1	Balanced quadraxial	Carbon	720	0,5	1		1000	1,44	28,70
	2	Balanced quadraxial	Carbon	720	0,5	1		1000	1,44	28,70
	3	Core	Rigid PVC	100			35	1000	3,5	0,09
	4	Balanced quadraxial	Carbon	720	0,5	1		1000	1,44	28,70
	5	Balanced quadraxial	Carbon	720	0,5	1		1000	1,44	28,70
	6	Core	Rigid PVC	100			110	1000	11	0,09
	7	Balanced quadraxial	Carbon	720	0,5	1		1000	1,44	28,70
	8	Balanced quadraxial	Carbon	720	0,5	1		1000	1,44	28,70
	9	Balanced quadraxial	Carbon	720	0,5	1		1000	1,44	28,70
	10	Balanced quadraxial	Carbon	720	0,5	1		1000	1,44	28,70
	11	Balanced quadraxial	Carbon	720	0,5	1		1000	1,44	28,70
	12	Balanced quadraxial	Carbon	720	0,5	1		1000	1,44	28,70
	13									
	14									
	15									
	16									
	17									
	18									
	19									
Inside	20									
					Total thickness	155		Total weight	28,9	

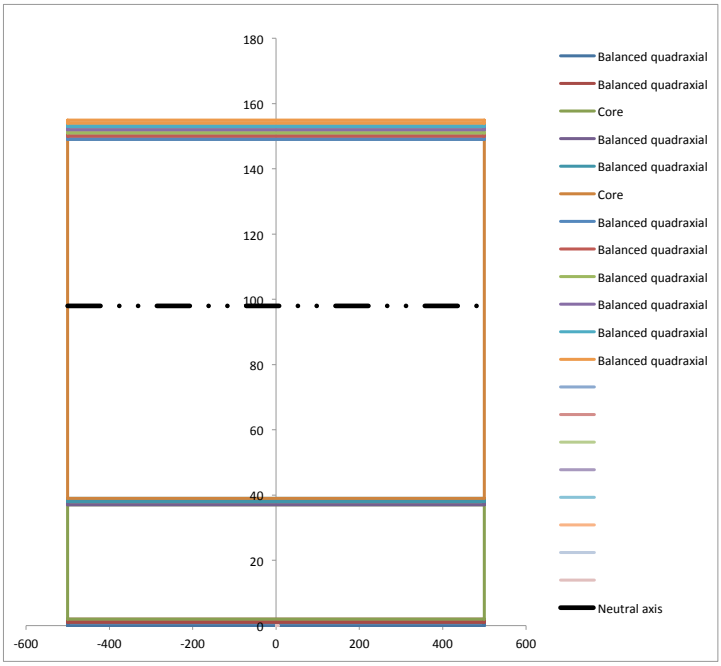

Laminate properties in tens / compr

A total	155000	[mm2]
Neutral axis	98,00	[mm]
EA	300050	[kN]
E iso tens/cor	1,936	[Gpa]

Composite laminate properties

Structure components: Edge beam

	Ply	Description	Material	Fabric or core weight [g/m2] or [kg/m3]	Fibre fraction ψ [-]	Ply thickness [mm]	Core thickness [mm]	Width [mm]	Cured ply weight [kg/m2]	E [Gpa]
Outside	1	Balanced quadraxial	Carbon	720	0,5	1		1000	1,44	28,70
	2	Balanced quadraxial	Carbon	720	0,5	1		1000	1,44	28,70
	3	Balanced quadraxial	Carbon	720	0,5	1		1000	1,44	28,70
	4	Core	Rigid PVC	150			35	1000	5,25	0,16
	5	Balanced quadraxial	Carbon	720	0,5	1		1000	1,44	28,70
	6	Balanced quadraxial	Carbon	720	0,5	1		1000	1,44	28,70
	7	Core	Rigid PVC	100			210	1000	21	0,09
	8	Balanced quadraxial	Carbon	720	0,5	1		1000	1,44	28,70
	9	Balanced quadraxial	Carbon	720	0,5	1		1000	1,44	28,70
	10	Balanced quadraxial	Carbon	720	0,5	1		1000	1,44	28,70
	11	Balanced quadraxial	Carbon	720	0,5	1		1000	1,44	28,70
	12	Balanced quadraxial	Carbon	720	0,5	1		1000	1,44	28,70
	13	Balanced quadraxial	Carbon	720	0,5	1		1000	1,44	28,70
	14	balanced quadraxial	Carbon	720	0,5	1		1000	1,44	28,70
	15	balanced quadraxial	Carbon	720	0,5	1		1000	1,44	28,70
	16									
	17									
	18									
	19									
Inside	20									
					Total thickness	258		Total weight	44,97	

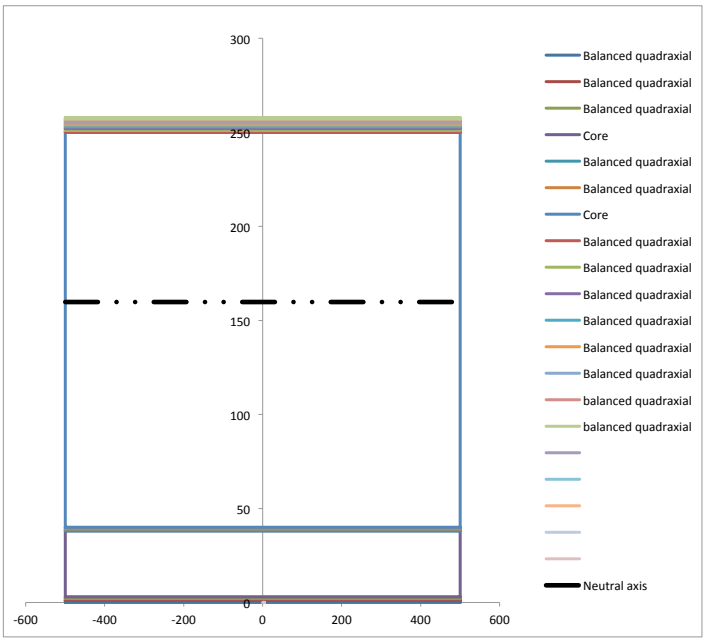

Laminate properties in tens / compr

A total	258000	[mm2]
Neutral axis	159,79	[mm]
EA	397670	[kN]
E iso tens/cor	1,541	[Gpa]

Data of structure components & approx. structure weight

Part	Description	Area [m2]	Thickness [mm]	E [Mpa]	Laminate weight [kg/m2]	Area weight [kg]
Hull	panels	428,4	40	3729	12,45	5334
Large truss members	1st members	86,3	246	1380	41,09	3547
Small truss members	3rd members	18,2	156	2124	32,09	583
Edge beam		30,8	258	1541	44,97	1384
Deck	panels	270,0	39	3024	9,26	2501
Medium truss members	2nd members	38,1	205	1486	33,9	1292
Small truss members	3rd members	19,7	155	1936	28,9	569
Bulkheads	panels	155,3	39	3024	9,26	1438
Large truss members	1st members	8,6	245	1258	37,9	326
Medium truss members	2nd members	8,3	205	1486	33,9	282
Small truss members	3rd members	12,1	155	1936	28,9	351
Mast&keel foundation	panels	12,5	39	3024	9,26	116
Small truss members	3rd members	4,3	155	1936	28,9	124
	Total area	**1093**			**Total weight**	**17847**

Bibliography

[1] F. Fossati. *Aero-Hydrodynamics and the Performance of Sailing Yachts.* International Marine / McGraw-Hill, New York, 2009. ISBN: 0071629106.

[2] E.R. Eliasson L. Larsson. *Principles of Yacht Design.* Adlard Coles Nautical, London, 2007. ISBN 0713678550.

[3] R. Fogg M. Meunier. *Challanges Associated with Design and Build of Composite Sailing Super Yachts.* Design, Construction & Operation of Super and Mega Yachts Conference, Genoa, 2009.

[4] O. Sigmund M.P. Bendsoe. *Topology Optimization: Theory, Methods and Applications.* Springer Verlag, Berlin, Heidelberg, New York, 2003. 978-3642076985.

[5] C.A. Brebbia S. Hernandez. *Design and Nature VI: Comparing Design in Nature With Science and Engineering.* WIT Press, Southampton, 2012. ISBN: 1845645928.

[6] R. Garrett. *The Symmetry of Sailing: The Physics of Sailing for Yachtsmen.* Adlard Coles Nautical, London, 1996. ISBN: 1574090003.

[7] A.R. Claughton R.A. Shenoi, J.F. Wellicome. *Sailing Yacht Design, Theory.* University of Southampton, Southampton, 1998. ISBN: 0582368561.

[8] ISO-NORM. *ISO 12215-5: Small craft - Hull construction and scantling - Part 5: Design pressures for monohulls, design stresses, scantlings determination.* International Organization for Standardization, 2009.

[9] K. Hochkirch, H. Brandt. Segelleistungsprognose aus Messungen im OriginalmaÃ§stab. `http://www.futureship.net/downloads/20001104_Yachtbau_Symposium_HH.pdf`, 2000. Accessed: 2012-01-15.

[10] Altair. *User manual AltairHyperworks*. Butterworth Heinemann, Oxford, 2000. ISBN 0-7506-4851-1.

[11] R. Cazacu, L. Grama. Overview of structural topology optimization methods for plane and solid structures. `http://imtuoradea.ro/auo.fmte/files-2014-v3/Cazacu%20Razvan(Mechanics)-OVERVIEW%20OF%20STRUCTURAL%20TOPOLOGY%20OPTIMIZATION%20METHODS%20FOR%20PLANE%20AND%20SOLID%20STRUCTURES.pdf`, 2014. Accessed: 2014-11-07.

[12] GL. *Design and Construction of Large Modern Yacht Rigs*. Germanischer Lloyd, Germany, Hamburg, 2009.

[13] H. ten Have. *Bugamena - 36m. classic sloop: Longitudinal strength analysis*. Dykstra Naval Architects, Amsterdam, 2008.

[14] Prof. O. Springer. *Lastfallsammlung für Einzelträger*. University of Applied Sciences, Bremen, 2008.

[15] T. Ainsworth. Significant Wave Height. `http://www.mxak.org/weather/pdfs/waves.pdf`, 2008. Accessed: 2014-09-25.

[16] RINA. *Rules for the Classification of Pleasure Yachts - Part B: Hull and Stability*. Registro Italiano Navale, Genova - Italy, 2011.